Smithsonian

Contributions to Astrophysics

VOLUME 1, NUMBER 2

PAPERS ON REDUCTION METHODS FOR PHOTOGRAPHIC METEORS

SMITHSONIAN INSTITUTION

Washington, D. C.

1957

Publications of the Astrophysical Observatory

This series, *Smithsonian Contributions to Astrophysics*, was inaugurated in 1956 to provide a proper communication for the results of research conducted at the Astrophysical Observatory of the Smithsonian Institution. Its purpose is the "increase and diffusion of knowledge" in the field of astrophysics, with particular emphasis on problems of the sun, the earth, and the solar system. Its pages are open to a limited number of papers by other investigators with whom we have common interests.

Another series is *Annals of the Astrophysical Observatory*. It was started in 1900 by the Observatory's first director, Samuel P. Langley, and has been published about every 10 years since that date. These quarto volumes, some of which are still available, record the history of the Observatory's researches and activities.

Many technical papers and volumes emanating from the Astrophysical Observatory have appeared in the *Smithsonian Miscellaneous Collections*. Among these are *Smithsonian Physical Tables*, *Smithsonian Meteorological Tables*, and *World Weather Records*.

Additional information concerning these publications may be secured from the Editorial and Publications Division, Smithsonian Institution, Washington, D. C.

FRED L. WHIPPLE, *Director*,
Astrophysical Observatory,
Smithsonian Institution.

Cambridge, Mass.

For sale by the Superintendent of Documents, U. S. Government Printing Office
Washington 25, D. C. - Price 70 cents

Contents

Reduction Methods for Photographic Meteor Trails[1]

By Fred L. Whipple[2] and Luigi G. Jacchia[3]

Methods for determining the space trajectories of meteors observed simultaneously from two stations have been developed by various investigators including Bessel (1839), Schaeberle (1895), Turner (1907), Olmsted (1931), and others. The present photographic techniques of observing meteors simultaneously from two stations (Whipple, 1938) require a precise reduction technique suitable for mechanical rather than for tabular methods of calculation. The use of rotating shutters in the determination of meteoric velocities further complicates the reduction, as does the necessity, in many cases, of solving for the instant of the meteor from the photographic trails. The solution now includes the determination of meteoric deceleration as well as the velocity and usual geometric circumstances of the phenomenon. Hence the reduction process has become relatively complex.

In the methods of reduction presented here we borrow freely from established techniques. Rectangular coordinates and direction cosines enter extensively, as they are most adaptable to efficient mechanical computation. The choice of notation has presented a difficult problem because of the multiplicity of symbols required. By the generous use of subscripts we have avoided duplication as much as possible.

Measurement of a meteor trail and comparison stars

At each station the meteor trail and the field stars are photographed simultaneously on an emulsion. We shall assume that the star images are untrailed, or that some point or points along the trailed images of the stars can be identified in time and are measurable. The optical projection will be assumed approximately gnomonic, as though points on the celestial sphere were projected through its center onto a plane surface. Graphical corrections in reduction can make allowance for rather large deviations from perfect projection. In case the projection itself deviates markedly from the gnomonic, as in fast Schmidt camera systems with curved focal surfaces, the negatives should be copied on flat glass plates by means of a lens system approximately to a gnomonic projection (see pl. 1). Measurements are then made on the positives.

The gnomonic projection is very closely approximated by current astronomical lens systems, even those of rapid focal ratio and wide field. This projection has the advantage that great circles project into straight lines in the plane; meteor trails lie so nearly on great circles that careful measurement and reduction usually are required to demonstrate deviations.

Preparation of the photographic material. Stars

[1] Carried out in part under research contracts with the U. S. Naval Bureau of Ordnance (Re3d), the U. S. Office of Naval Research, Contract No. N5ori-07647, and the U. S. Army Office of Ordnance Research, Contract No. DA-19-020-ORD-2556. Reproduction in whole or in part is permitted for any purposes of the U. S. Government.

[2] Smithsonian Astrophysical Observatory.

[3] Harvard College Observatory.

to be measured can be identified directly by marking with ink on the glass side of the photographic plates (see pl. 2). If film is to be measured, it should be placed between two good-quality pieces of glass fastened firmly at the edges to prevent slippage of the film. Identification marks can then be made on the glass surface.

Choice of comparison stars. For all good-quality cameras of focal length greater than about 3 inches, the precision of measurement and reduction is greater than that of the star positions in the Bonner Durchmusterung catalog (BD). Astrographic catalog positions are suitable where right ascension and declination are tabulated directly, but identification problems are difficult because meteor trails usually extend over two or more zones. Where only rectangular coordinates are tabulated the reduction of adjacent zone coordinates to a common system is added to the problem of identification. Hence the astrographic catalog positions are rarely useful in the reduction of meteor trails, with the exception of the Helsingfors Zone (+39° to +47°) and the Catania Zone (+46° to +55°) which give right ascension and declination of all stars.

Normally, star positions should be selected from the Astronomische Gesellschaft catalogs (AG) or from the Yale catalog. The meteor trail should be sketched lightly in pencil on a BD chart and the AG stars identified in its neighborhood. Stars for measurement should be selected at uniform intervals along the trail (x-direction) and alternately on opposite sides of the trail (+ and $-y$) as close to the trail as is convenient or possible. The number of stars required increases with trail length and field distortion. For a focal length of 6 inches and a meteor trail 10° long, eight or ten stars are usually sufficient. No trail should be reduced with fewer than six comparison stars. With film, more comparison stars are usually necessary. No precise general rule can be given; the experimenter should determine the optimum number on the basis of his own experience. To minimize the centering errors in stars with images distorted by vignetting, it is recommended that the stars selected be as nearly of the same photographic magnitude, and as near the plate limit, as possible.

Measuring engine. The ideal measuring engine for our purpose has two mutually perpendicular precision screws to measure x and y coordinates simultaneously in a plane. Periodic errors should not exceed one micron, or should be calibrated and capable of correction. Precise perpendicularity of the ways is not important in meteor reductions. The ways must be straight within approximately one micron per centimeter. Large deviations from perpendicularity and some smooth curvature of the ways, as well as considerable systematic errors in the screws, can be allowed for precisely in the reductions.

Single-screw measuring engines in which the plate can be turned through 180° in its plane can also be used effectively, as can engines in which the y-screw is quite short compared to the x-screw. No accuracy is lost if y must be measured at a different time from x; in fact, this technique is recommended.

A relatively low-power microscope is advisable for the measurement of meteor trails. Mutually perpendicular crosswires, parallel to the ways of the engine, are required. One of the excellent measuring engines made by D. W. Mann and currently used in the Harvard Meteor Program appears in plate 3.

Measurements. The meteor trail should be carefully oriented parallel to one of the engine ways. The convenience in checking errors and in combining "direct" and "reverse" measures well repays a little effort to make the parallelism good to a few microns over the length of the trail. Measures in y, perpendicular to the trail, should be made for each comparison star, and at frequent uniform intervals along the trail, perhaps at every millimeter. Measures in x, along the trail, should be made for each star at the beginning and end of the trail, at the beginning, end, and middle of each shutter break, and at the beginning, end, and middle of each flare or noticeable irregularity in the trail. Measures in y along the trail need not be made at the same points as measures in x.

It is convenient to identify the shutter breaks by numbers in time sequence, and to identify the flares or irregularities in the trail by consecutive letters. When inspection shows that it is possible, it is also convenient to use

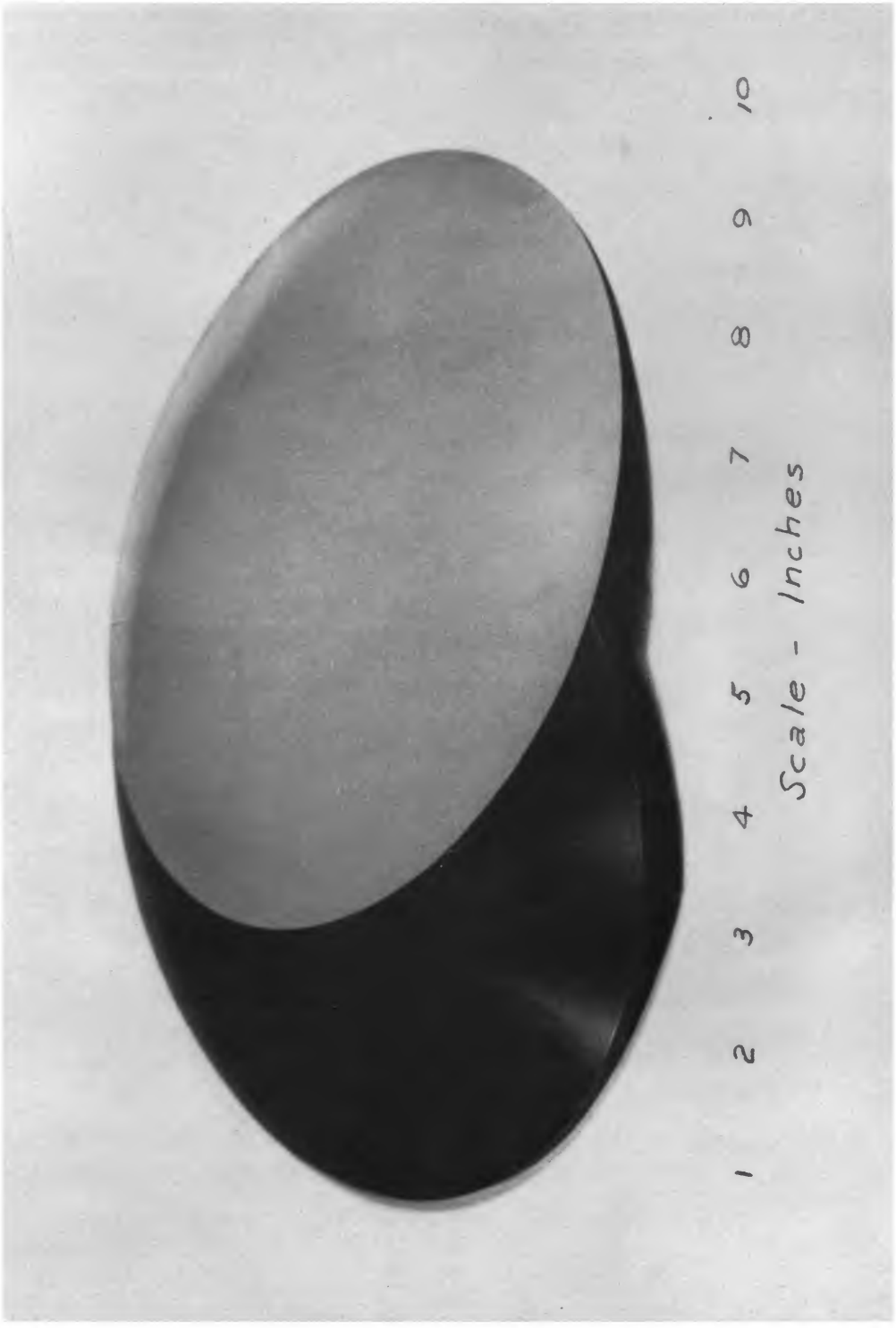

A curved film for the Baker Super-Schmidt meteor cameras.

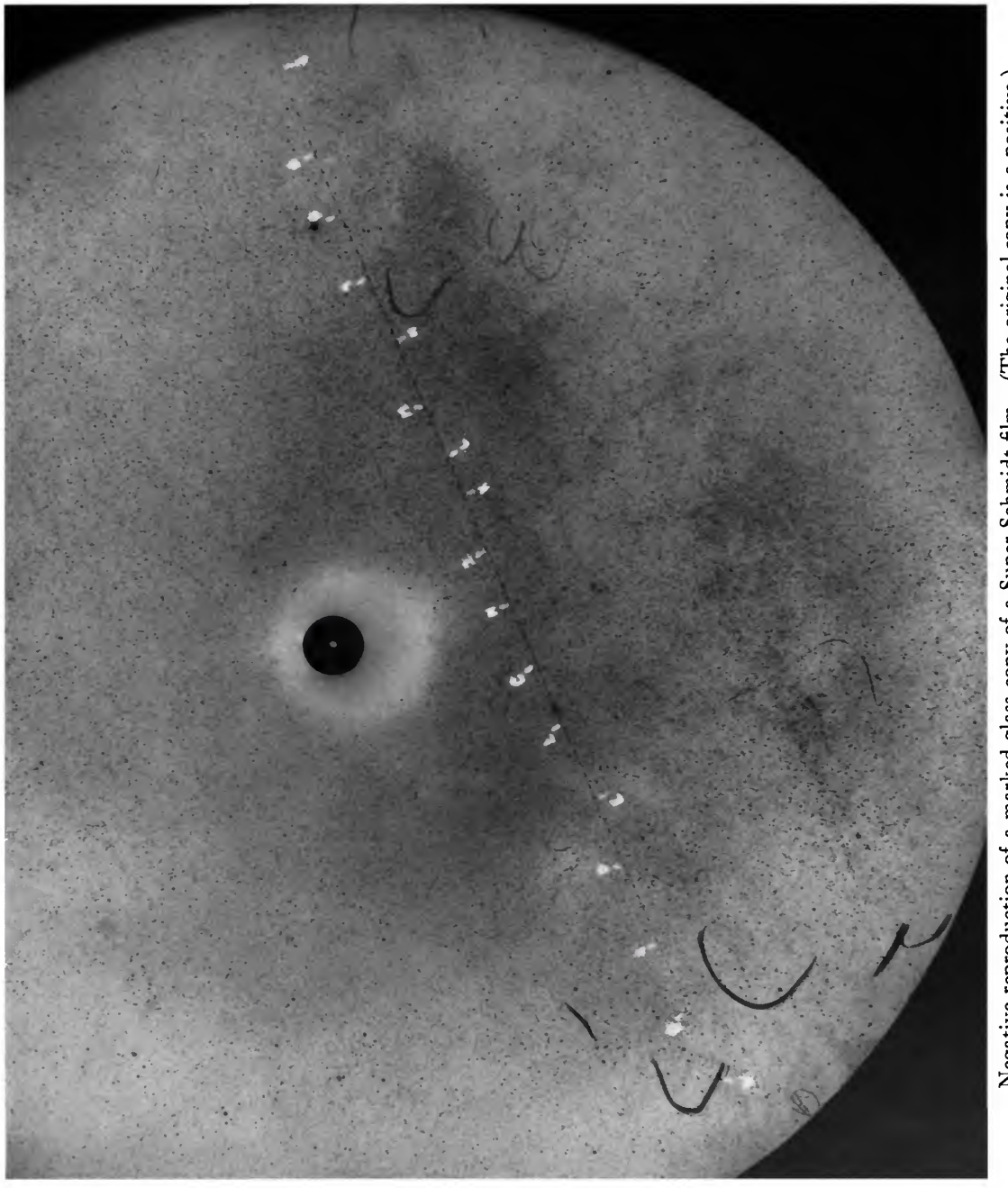

Negative reproduction of a marked glass copy of a Super-Schmidt film. (The original copy is a positive.)

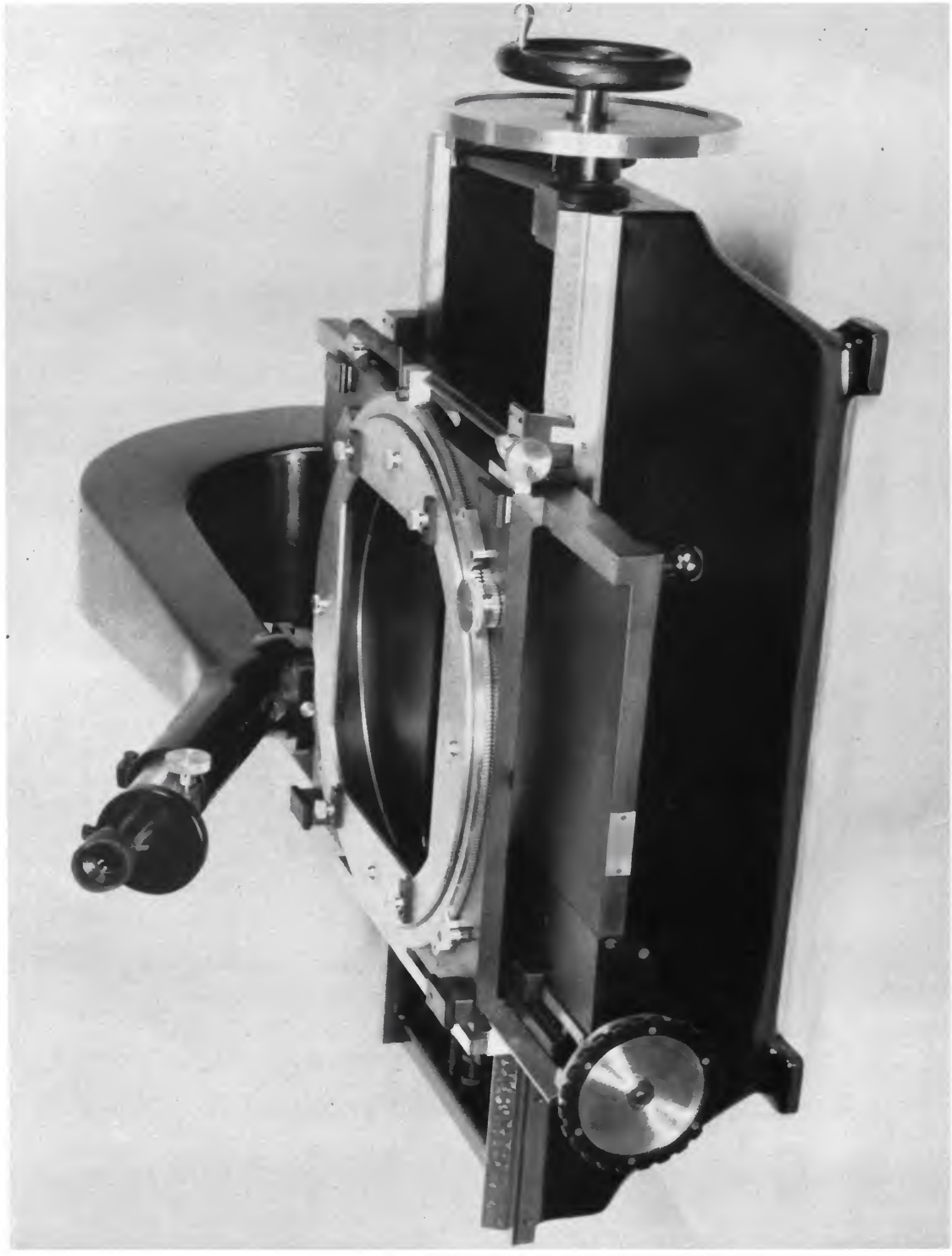

A 2-screw rotatable horizontal measuring engine built for the U. S. Naval Bureau of Ordnance by D. W. Mann, Lincoln, Mass.

the same letter to identify the flares on the trails on each of the paired photographs from the two stations.

The focus of the microscope should be set most carefully at the beginning, end, and middle of the trail to establish the best compromise in case the engine carriage is not precisely flat. Focus can be tested most accurately by the minimizing of parallax between the wires and star images when the eye is moved across the eyepiece.

On most measuring engines, because of possible backlash, it is advisable to make all measures with the screw turning in the direction of increasing scale readings. Measures on meteor trails are most advantageously made with the microscope crosswires respectively parallel and perpendicular to the meteor trail, to the accuracy within which the wires are straight. This necessitates measuring not at the intersection of the wires but at some definite position on each wire near the intersection. It is convenient and probably advisable to make all measures in one coordinate separately, and for all points consecutively in order of increasing x values. A remeasure of the first point at the end of such a run will indicate immediately whether the adjustment of the engine has been disturbed during the run or whether temperature changes have affected the settings systematically. Temperature changes should be eliminated as much as possible, but in a closed room their effect tends to stabilize during the course of an hour or two of measuring. Hence a repetition of earlier measures in the same sequence will often show a progressive decrease in the differences of the readings. Physical disturbance of the engine will usually show as a distinct break in the series of differences in readings. Where systematic temperature variations cannot be avoided, a few checks at representative points in a run should be made at the end; if the difference in readings changes smoothly from beginning to end, the original set can be accepted without correction.

All measures made "direct," with the plate in its original position, should be repeated "reverse" after the plate has been turned 180° in its own plane.

Each "measure" should be the mean of three or more fairly rapid settings.

Combination of the measures. The combination of direct and reverse measures not only eliminates systematic errors between the meteor trail and stars and between various parts of the meteor trail but also provides an almost foolproof method of checking for setting or reading errors. Usually it is most convenient to reduce the "reverse" set of measures to values nearly identical with those of the "direct" set by subtracting their values from an appropriate number. Then differences, direct measures minus reverse, can be taken easily and plotted for both x and y on a magnified (at least 100 times) ordinate scale against x as abscissa. The resulting points should lie on a curve that is smooth within the accuracy of the settings (a very few microns). Conspicuous deviations that are not correlated with abrupt changes in the brightness of the trail or in image quality should be rechecked on the measuring engine. When possible it is often time-saving to leave the plate in the measuring engine until the measures have been combined, so that errors can be checked quickly after they have been detected.

After gross errors have been eliminated, the mean of the direct measures and the constant minus the reverse measures should be obtained. These values constitute the measures to be used in the reductions.

Reductions for the apparent radiant

Corrections for stellar proper motion. The AG or other position of each star, s, should be corrected for proper motion in right ascension, α_s, and declination, δ_s, if values of the proper motion can be found in the appropriate catalogs. It should be noted that the proper motions should be applied for the interval from the epoch of the stellar observations in the AG or other catalog to the epoch of the meteor, fractions of years being taken into account. Also, attention should be given to the fact that some catalogs give proper motions as $\Delta\alpha$ and some as $\Delta\alpha \cos \delta$, per year or per century.

Stellar direction cosines and precession. The stellar coordinates, after correction for proper motion, are transformed into equatorial direc-

tion cosines λ_s, μ_s, ν_s, for the mean equinox of the catalog, by the formulae:

$$\begin{aligned}\lambda_s&=\cos\delta_s\cos\alpha_s\\ \mu_s&=\cos\delta_s\sin\alpha_s\\ \nu_s&=\sin\delta_s\end{aligned}\qquad(1)$$

Check:

$$\lambda_s^2+\mu_s^2+\nu_s^2=1.\qquad(1a)$$

Six significant figures in calculation are usually appropriate. The check formula is not adequate for direction cosines smaller than approximately 0.2, and will not check erroneous table entries in both functions. A repetition of this phase of the calculation is advisable to guard against errors.

Precession can be applied most easily to each star position by means of nine precessional direction-cosines, Xx, Xy, etc., applied to the direction cosines of the star position as follows:

$$\begin{aligned}\lambda_2&=X_x\lambda_1+X_y\mu_1+X_z\nu_1\\ \mu_2&=Y_x\lambda_1+Y_y\mu_1+Y_z\nu_1\\ \nu_2&=Z_x\lambda_1+Z_y\mu_1+Z_z\nu_1\end{aligned}\qquad(2)$$

where the precessional direction cosines apply to the transformation from Equinox 1 (λ_1, μ_1, ν_1) to Equinox 2 (λ_2, μ_2, ν_2). Tabulations of these direction cosines from 1850 to 1950 applying to the transformation to 1900 have been made by E. C. Bower (1932).

The Bower tabulations apply for transformations from the mean equinox at the beginning of the year to the mean equinox of 1900.0. The direction cosines to be applied in equations (2) may be obtained by the Cracovian calculation (Banachiewicz, 1925, 1929):

$$\begin{array}{ll}(X_xY_xZ_x)=(+X_x-Y_x-Z_x) & (X_xX_yX_z)\\ (X_yY_yZ_y)=(-X_y+Y_y+Z_y) & (Y_xY_yY_z)\\ (X_zY_zZ_z)=(-X_z+Y_z+Z_z) & (Z_xZ_yZ_z)\end{array}$$

Equinox 1 to 2.	Equinox 2 to 1900.0.	Equinox 1 to 1900.0.

This notation denotes a calculation convention more convenient than the usual matrix convention. All quantities on the left are the sums of three products of quantities in two vertical columns on the right. For example,

$$Y_x(1,2)=-Y_x(2)X_x(1)+Y_y(2)Y_x(1)+Y_z(2)Z_x(1),$$
$$Z_y(1,2)=-Z_x(2)X_y(1)+Z_y(2)Y_y(1)+Z_z(2)Z_y(1).$$

The tabulations by Bower may also be used less conveniently in two steps, Equinox 1 to 1900.0 and 1900.0 to Equinox 2.0

Similar quantities for reduction from the current year to 1950.0 are given in the British Nautical Almanac.

The direction cosines of the star positions are rotated from the mean equinox of the star catalog to the mean equinox at the beginning of the year nearest in time to the meteor (a September meteor of 1948 to the mean equinox of 1949, etc.).

A transfer to the true position at date would carry advantages too slight to offset the additional computation involved. The meteor positions are affected by aberration in the same fashion as the star positions, while light-time is negligible on any basis. The combined errors in aberration and precession-nutation over half a year enter the solution chiefly in terms of absolute time. They amount to a maximum error of 3^s of time in the absolute position of the meteor, or about 50 feet. Refraction of light in the atmosphere also affects the meteor positions and the star positions in almost the same fashion. Its minor differential effects can be taken into account accurately in the general reduction.

Standard coordinates of the star positions. Standard coordinates, ξ and $\overline{\eta}$, are rectangular coordinates in the plane of celestial-sphere projection (approximately that of the photographic plate) with origin at the center of projection. They are expressed in radian measure. The coordinate $\overline{\eta}$ increases northerly along the hour circle through the center fo projection, and ξ increases easterly along a tangent to the parallel of declination at the center.

The center of projection, α_c, δ_c, may be taken as the plate center and determined with sufficient precision by means of a ruler on the plate and a BD chart. Rough precession must be applied. The direction cosines of the origin of the new rectangular system and those of the poles of the two coordinate axes are computed from the following formulae to the same relative precision as the direction cosines of the star positions:

$$\text{Plate center}\begin{cases}\lambda_c=\cos\delta_c\cos\alpha_c\\ \mu_c=\cos\delta_c\sin\alpha_c\\ \nu_c=\sin\alpha_c\end{cases}$$

$$\bar{\eta}\text{ axis}\begin{cases}\lambda_\eta=-\sin\delta_c\cos\alpha_c\\ \mu_\eta=-\sin\delta_c\sin\alpha_c\\ \nu_\eta=+\cos\delta_c\end{cases}\qquad(3)$$

$$\bar{\xi}\text{ axis}\begin{cases}\lambda_\xi=-\sin\alpha_c\\ \mu_\xi=+\cos\alpha_c\\ \nu_\xi=0\end{cases}$$

Check:

$$\begin{aligned}&\lambda_c^2+\mu_c^2+\nu_c^2=1 \qquad &&\lambda_c\lambda_\eta+\mu_c\mu_\eta+\nu_c\nu_\eta=0\\ &\lambda_\eta^2+\mu_\eta^2+\nu_\eta^2=1 &&\lambda_c\lambda_\xi+\mu_c\mu_\xi=0\\ &\lambda_\xi^2+\mu_\xi^2=1 &&\lambda_\xi\lambda_\eta+\mu_\xi\mu_\eta=0.\end{aligned}\qquad(3a)$$

For each star the cosine of σ_s, the angle between the star position and the center, and the standard coordinates of the star position are computed as follows:

$$\begin{aligned}\cos\sigma_s&=\lambda_s\lambda_c+\mu_s\mu_c+\nu_s\nu_c\\ \bar{\eta}_s&=(\lambda_s\lambda_\eta+\mu_s\mu_\eta+\nu_s\nu_\eta)/\cos\sigma_s\\ \bar{\xi}_s&=(\lambda_s\lambda_\xi+\mu_s\mu_\xi)/\cos\sigma_s\end{aligned}\qquad(4)$$

Check:

$$\cos^2\sigma_s(1+\bar{\eta}_i^2+\bar{\xi}_i^2)=1.\qquad(4a)$$

Equation (4a) does not provide a satisfactory end-figure check for values of $\bar{\xi}$ or $\bar{\eta}$ less than 0.2. A second or a reverse calculation (equation 10) is generally required.

Standard coordinates along the meteor trail. SIX-CONSTANT METHOD: The measured positions can be expressed in terms of the standard coordinates by means of a least-squares solution of the following linear equations for all of the measured stars:

$$\begin{aligned}a_x\bar{\xi}_s+b_x\bar{\eta}_s+c_x&=x_s\\ a_y\bar{\xi}_s+b_y\bar{\eta}_s+c_y&=y_s\end{aligned}\qquad(5)$$

Here a_x, b_x, . . . , c_y are plate constants, the unknowns in the least squares solution. Residuals are more conveniently expressed in the reverse sense, *computed* minus *observed:*

$$\begin{aligned}\Delta x_s&=x_s(\text{Comp.})-x_s(\text{obs.})\\ \Delta y_s&=y_s(\text{Comp.})-y_s(\text{obs.})\end{aligned}\qquad(6)$$

Check:

$$\sum\Delta x_s=\sum\Delta y_s=0.\qquad(6a)$$

(In addition, all the three normal equations must be satisfied.)

At this stage of the calculation the accumulated small errors arising from optical distortion, large-scale emulsion distortion, misplacement of the plate center, differential aberration, differential refraction, systematic screw error, and systematic deviations of the engine ways from linearity can all be eliminated graphically. Deviations of the engine ways from perpendicularity are already allowed for precisely in the least-squares solution, as are all other linear effects along the emulsion.

The residuals, Δx_s and Δy_s, for each measured star position are plotted separately as ordinates against the measured x_s as abscissa. Smooth curves are drawn through the residual points on these graphs.

All the measures made on the meteor trail are corrected from these curves of residuals, the measured x being used as argument to provide the appropriate correction from either the Δx or Δy curve. The corrections are applied as follows:

$$\begin{aligned}x\text{ (corrected)}&=x\text{ (measured)}+\Delta x\text{ (curve)}\\ y\text{ (corrected)}&=y\text{ (measured)}+\Delta y\text{ (curve).}\end{aligned}\qquad(7)$$

These corrected measures are henceforth used in all calculations involving trail coordinate measures.

It will be seen that this graphical correction method has the merit of transferring all the measures from the actual photograph to the theoretically perfect plane of projection, and hence eliminates the various errors listed above. The remaining errors are those arising in the measurement, from optical or photographic image distortion, from small-scale errors in the emulsion or measuring engine, and from errors in the star positions.

After the measured x's and y's on the meteor trail have been corrected by the residual curves, the values of y along the trail should be plotted as ordinate expanded against x as abscissa. If the meteor trail is part of a great circle, the points will lie on a straight line within the accuracy of measurement. In this case, it is convenient to express y as a linear function of x and to use these rectified values of y in determining the great-circle motion. If the

trail shows clear evidence of curvature, the early straight-line portion *only* should be used in determining the great-circle motion for computing the radiant. For flare measures to be used in calculating the instant of the meteor, the originally corrected y values are best. For meteors of exceptionally long duration (>3 seconds), gravity may cause an observable curvature of the trail. To correct for this effect, see section on corrections for gravity (p. 199).

The standard coordinates of any measured point on the photograph, with corrected coordinates x and y, may be obtained by making use of inverse plate constants by the following formulae:

$$\begin{aligned} \bar{\xi} &= a_\xi x + b_\xi y + c_\xi \\ \bar{\eta} &= a_\eta x + b_\eta y + c_\eta \end{aligned} \tag{8}$$

where

$$\begin{aligned} a_\xi &= b_y/c_{xy} & a_\eta &= -a_y/c_{xy} \\ b_\xi &= -b_x/c_{xy} & b_\eta &= +a_x/c_{xy} \\ c_\xi &= (-b_y c_x + b_x c_y)/c_{xy} & c_\eta &= (+a_y c_x - a_x c_y)/c_{xy} \end{aligned} \tag{9}$$

and

$$c_{xy} = a_x b_y - a_y b_x.$$

Equation (9) may be checked by applying equation (8) to the measures of a single star (uncorrected). With proper arrangement of the computation the application of equation (8) may be checked on the summed values of x, y, $\bar{\xi}$, and $\bar{\eta}$.

The direction cosines of points on the meteor trail are computed from $\bar{\xi}$ and $\bar{\eta}$ as follows:

$$\begin{aligned} \lambda &= (\lambda_c + \lambda_\eta \bar{\eta} + \lambda_\xi \bar{\xi}) / + \sqrt{1 + \bar{\xi}^2 + \bar{\eta}^2} \\ \mu &= (\mu_c + \mu_\eta \bar{\eta} + \mu_\xi \bar{\xi}) / + \sqrt{1 + \bar{\xi}^2 + \bar{\eta}^2} \\ \nu &= (\nu_c + \nu_\eta \bar{\eta}) / + \sqrt{1 + \bar{\xi}^2 + \bar{\eta}^2} \end{aligned} \tag{10}$$

Check:

$$\lambda^2 + \mu^2 + \nu^2 = 1 \text{ (Recompute } \lambda, \mu, \text{ or } \nu < 0.2). \tag{10a}$$

Equations (8), (9), and (10) need be applied to only a few points on the meteor trail. Usually the following will suffice: beginning point, b; end point, e; first shutter break, a; last shutter break, j; middle point, o; and each flare or irregularity, f_i, that can be identified on both photographs.

FOUR-CONSTANT METHOD: While the six-constant method may offer some advantages when the strip within which the comparison stars are selected is rather wide, it becomes difficult or even impossible to handle when the stars selected are very close to the meteor trail. Six constants will operate a linear transformation from the orthogonal $(\bar{\xi}\,\bar{\eta})$ system to an oblique (xy) system; when, however, the range in y is very small, it becomes impossible to determine the angle between the oblique coordinate axes. This difficulty is reflected in an ill-conditioned system of equations for whose solution it becomes necessary to carry a very large number of digits in the computation. As a safety measure, 10 digits have to be carried even in ordinary cases, greatly limiting the possibilities of programming the computation on ordinary punched-card calculators.

An added disadvantage is that the six-constant method cannot be dissociated from the lengthy least-squares process, which requires an overhauling of the whole solution whenever a mistake is discovered in the input data after the solution has been computed.

A simple way of avoiding these difficulties consists in assuming that the (xy) coordinate system also is orthogonal. If the engine ways are not exactly perpendicular to each other, we must then expect that the residuals Δx_s and Δy_s will show some dependence on y. This effect, however, should be quite small if the range in y for the comparison stars is small. Moreover, even in a six-constant solution the residuals are not entirely independent of y, due to the effect of field distortion.

Instead of equation (5) we shall write, then:

$$\begin{aligned} a\bar{\xi}_s + b\bar{\eta}_s + c &= x_s \\ b\bar{\xi}_s - a\bar{\eta}_s + d &= y_s. \end{aligned} \tag{11}$$

There is no need to determine the four unknowns a, b, c, d by least squares; a solution using two stars at the extremes of the meteor trail is quite satisfactory. Residuals (C–O), taken according to equation (6) are plotted against x and the resulting smooth curves are used to correct the observed x's and y's exactly

as before. Since the computed residuals may show a dependence on y, it is advisable to write in the diagram the value of $y_s - y_{trail}$ next to each point, and then draw the curve for $y_s - y_{trail} = 0$, as one would draw an isobar on a pressure map.

Standard coordinates are computed from corrected x's and y's using inverse plate constants:

$$\begin{aligned} \bar{\xi}_s &= Ax_s + By_s + C \\ \bar{\eta}_s &= Bx_s - Ay_s + D \end{aligned} \tag{12}$$

where

$$A = \frac{a}{a^2+b^2};\ B = \frac{b}{a^2+b^2};\ C = -\frac{ac+bd}{a^2+b^2};\ D = \frac{ad-bc}{a^2+b^2}. \tag{13}$$

The observed radiant. If the meteor trail is straight in the corrected xy plane, the direction cosines of the beginning, b, and end, e, points and a middle point, o, should be used in calculating the great-circle motion. If the trail is curved, three points from the early straight-line portion should be used. The direction cosines of the pole of the great-circle motion, λ_{Ap}, μ_{Ap}, and ν_{Ap} for Station A or λ_{Bp}, μ_{Bp}, ν_{Bp} for Station B are given by the equations:

$$\begin{aligned} \lambda_{Ap} \sin l_A &= \mu_{Ab}\nu_{Ae} - \nu_{Ab}\mu_{Ae} \\ \mu_{Ap} \sin l_A &= \nu_{Ab}\lambda_{Ae} - \lambda_{Ab}\nu_{Ae} \\ \nu_{Ap} \sin l_A &= \lambda_{Ab}\mu_{Ae} - \mu_{Ab}\lambda_{Ae}. \end{aligned} \tag{14}$$

(l_A is the length of the trail as photographed at Station A).

Checks:

$$\begin{aligned} &\lambda_{Ap}^2 + \mu_{Ap}^2 + \nu_{Ap}^2 = 1 \\ &\lambda_{Ap}\lambda_{Ab} + \mu_{Ap}\mu_{Ab} + \nu_{Ap}\nu_{Ab} = 0 \\ &\lambda_{Ap}\lambda_{Ae} + \mu_{Ap}\mu_{Ae} + \nu_{Ap}\nu_{Ae} = 0 \\ &\lambda_{Ap}\lambda_{Ao} + \mu_{Ap}\mu_{Ao} + \nu_{Ap}\nu_{Ao} = 0 \end{aligned} \tag{14a}$$

and similarly for λ_B, μ_B, ν_B.

The direction cosines of the apparent radiant λ_R, μ_R, ν_R, are obtained similarly from the equations:

$$\begin{aligned} \lambda_R \sin Q &= \mu_{Ap}\nu_{Bp} - \nu_{Ap}\mu_{Bp} \\ \mu_R \sin Q &= \nu_{Ap}\lambda_{Bp} - \lambda_{Ap}\nu_{Bp} \\ \nu_R \sin Q &= \lambda_{Ap}\mu_{Bp} - \mu_{Ap}\lambda_{Bp} \end{aligned} \tag{15}$$

Checks:

$$\begin{aligned} &\lambda_R^2 + \mu^2 + \nu^2 = 1 \\ &\lambda_R\lambda_{Ap} + \mu_R\mu_{Ap} + \nu_R\nu_{Ap} = 0 \\ &\lambda_R\lambda_{Bp} + \mu_R\mu_{Bp} + \nu_R\nu_{Bp} = 0 \end{aligned} \tag{15a}$$

Q is the angle of intersection between the two meteor trails as seen in the sky from Stations A and B.

The sign of sin Q is chosen to orient the radiant above the horizon.

For both stations the standard coordinates of the radiant ($\bar{\xi}_{AR}$, η_{AR}; $\bar{\xi}_{BR}$, η_{BR}) and first shutter break ($\bar{\xi}_{Aa}$, $\bar{\eta}_{Aa}$; $\bar{\xi}_{Ba}$, $\bar{\eta}_{Ba}$) on the photographs are required in later calculations, as are the theoretical x and y measures of the radiant. These quantities may well be computed at this stage. The appropriate equations are indicated below for Station A only:

cos σ_{AR}, $\bar{\xi}_{AR}$ and $_A\bar{\eta}_R$ from equation (4),
x_{AR} from equation (5) or (11)

and

cos $\sigma_{Aa} = (1 + \bar{\eta}_{Aa}^2 + \bar{\xi}_{Aa}^2)^{-\frac{1}{2}}$ from equation (4a).

Ranges and heights

For the moment we shall assume that the instant of appearance of the meteor is known. If the time of the meteor was not recorded from visual observations, methods for determining it can be found in the section on page 194.

Fundamental values in the computation of ranges are the relative rectangular coordinates in the astronomical equatorial system of Station B with respect to Station A when the sidereal time is zero at Station A. These quantities can be computed once and for all from the geocentric coordinates of the stations as follows:

$$\begin{aligned} \xi_{ABo} &= R_B \cos \phi'_B \cos (L_B - L_A) - R_A \cos \phi'_A \\ \eta_{ABo} &= R_B \cos \phi'_B \sin (L_B - L_A) \\ \zeta_{ABo} &= R_B \sin \phi'_B - R_A \sin \phi'_A. \end{aligned} \tag{16}$$

Here L stands for the geographic longitude, positive to the west, φ' for the *geocentric* latitude, and R_A, R_B for the distance of the stations from the center of the earth; the subscripts A and B refer to Stations A and B, respectively. A convenient unit is 100 km.

The distance R_{AB} between the two stations is obviously given by the equation

$$R_{AB}^2 = \xi_{ABo}^2 + \eta_{ABo}^2 + \zeta_{ABo}^2. \tag{17}$$

Let θ_A be the sidereal time at Station A corresponding to the appearance of the meteor.

The relative coordinates of Station B with respect to Station A at this instant are

$$\begin{aligned}\xi_{AB}&=\xi_{AB_0}\cos\theta_A-\eta_{AB_0}\sin\theta_A\\ \eta_{AB}&=\eta_{AB_0}\cos\theta_A+\xi_{AB_0}\sin\theta_A\\ \zeta_{AB}&=\zeta_{AB_0}\end{aligned}\qquad(18)$$

Check:

$$\xi_{AB}^2+\eta_{AB}^2+\zeta_{AB}^2=R_{AB}^2.$$

Let us now consider the plane through the meteor and Station B. The intersection of this plane with the celestial sphere is the great circle of motion of the meteor, as seen from Station B, whose pole is $\mathbf{P}_B=(\lambda_{B_2},\ \mu_{B_2},\ \nu_{B_2})$. The distance S_A of Station A from this plane is given by $S_A=\mathbf{R}_{AB}\cdot\mathbf{P}_B$, i. e., by the equation

$$S_A=\xi_{AB}\lambda_{B_2}+\eta_{AB}\mu_{B_2}+\zeta_{AB}\nu_{B_2}.\qquad(19)$$

The range R_{Ai} (distance from Station A) of any point i on the plane is given by $R_{Ai}=S_A$ sec ϵ_i, where ϵ_i is the angle between $\mathbf{P}_B$ and the range vector $\mathbf{R}_{Ai}$. Points on the meteor $(\lambda_{Ai},\ \mu_{Ai},\ \nu_{Ai})$ are just particular points on the plane; for them we shall have the equations

$$S_{Ai}=\lambda_{Ai}\lambda_{B_2}+\mu_{Ai}\mu_{B_2}+\nu_{Ai}\nu_{B_2}(=\cos\epsilon_i)\qquad(20)$$

and

$$R_{Ai}=S_A/S_{Ai}.\qquad(21)$$

In general, it is convenient to compute ranges (and heights) for four or five meteor points, conveniently spaced.

Ranges from Station B can be obtained in the same fashion as those from Station A, starting from the relative coordinates $(\xi_{BA_0},\ \eta_{BA_0},\ \zeta_{BA_0})$ of Station A with respect to B at sidereal time $\theta_B=0$. This procedure, however, is unnecessary, since clearly $\mathbf{R}_{BA}=-\mathbf{R}_{BA}$. We can thus write

$$R_{Bi}=S_B/S_{Bi}\qquad(22)$$

where

$$S_B=-(\xi_{AB}\lambda_{A_2}+\eta_{AB}\mu_{A_2}+\zeta_{AB}\nu_{A_2})\qquad(23)$$

and

$$S_{Bi}=\lambda_{Bi}\lambda_{A_2}+\mu_{Bi}\mu_{A_2}+\nu_{Bi}\nu_{A_2}.\qquad(24)$$

In computing heights above sea level for points on the meteor, it is convenient to compute first the heights $(h_{Ai},\ h_{Bi})$ above a plane through the station, normal to the zenith direction.

The direction cosines of the zenithal point for Station A are:

$$\begin{aligned}\lambda_{ZA}&=\cos\phi_A\cos\theta_A\\ \mu_{ZA}&=\cos\phi_A\sin\theta_A\\ \nu_{ZA}&=\sin\phi_A,\end{aligned}\qquad(25)$$

where ϕ_A is the geographic latitude.

The zenith distance Z_{Ai} for points on the meteor is given by the equation

$$\cos Z_{Ai}=\lambda_{ZA}\lambda_{Ai}+\mu_{ZA}\mu_{Ai}+\nu_{ZA}\nu_{Ai}.\qquad(26)$$

The heights h_{Ai} above the plane normal to the zenith direction are then obtained from the equation

$$h_{Ai}=R_{Ai}\cos Z_{Ai}.\qquad(27)$$

To obtain the heights H_i above sea level, we have to add the elevation of the station H_A above the level and a correction δh_{Ai}:

$$H_i=h_{Ai}+H_A+\delta h_{Ai}.\qquad(28)$$

The rigorous form of δh_{Ai} is

$$\delta h_{Ai}=(\rho_A^2+R_{Ai}^2+2\rho_A h_{Ai})^{1/2}-(\rho_A+h_{Ai})\qquad(29)$$

where ρ_A is the distance of the station from the mean local center of curvature of the geoid (i. e., the mean local radius of curvature plus the elevation of the station).

The computation of δh_{Ai} by equation (29) is somewhat laborious because it is obtained as the difference of two large quantities, so that a large number of digits are required in the square root. It is therefore much more convenient to compute δh_{Ai} from the expansion of an approximate formula (in which the zenith of the station is assumed to be the same as the zenith of the meteor points):

$$\delta h_{Ai}\approx\rho_A\left(m-\frac{m^2}{2}+\frac{m^3}{2}-\frac{5}{8}m^4+\ldots.\right),$$

where

$$m=\frac{R_{Ai}^2-h_{Ai}^2}{2\rho_A^2}.\qquad(30)$$

The error resulting from the use of this approximate formula does not exceed 20 meters

for meteors photographed within 45° of the zenith and is less than 150 meters for meteors 70° from the zenith. In ordinary cases it is quite safe to stop at the first term of the expansion, so that δh_{Ai} becomes

$$\delta h_{Ai} \approx \frac{1}{2\rho_A}(R_{Ai}^2 - h_{Ai}^2). \tag{31}$$

If this formula is used, instead of (30), the difference in size of the error is negligible. At 70° from the zenith the errors differ by less than 4 percent.

It is convenient to plot δh_{Ai} against h_{Ai} and to keep the resulting curve for further use in computing heights above sea level of other points on the meteor trajectory.

Distances along the meteor trail

When ranges R_{Ai} have been computed for two points ($i=1$ and $i=2$) on the meteor trajectory, the spatial distance between them can easily be determined. We first compute for each point the components of the vector $\mathbf{R}_{Ai}$ in the direction of the coordinate axes of the astronomical equatorial system:

$$\begin{aligned} \xi_{Ai} &= R_{Ai}\lambda_{Ai} \\ \eta_{Ai} &= R_{Ai}\mu_{Ai} \\ \zeta_{Ai} &= R_{Ai}\nu_{Ai}. \end{aligned} \tag{32}$$

Let us now define a system of distances D_{Ai} along the trail, starting from an arbitrary point, such as the observed beginning of the trail. The distance between our two points is then given by the equation

$$(D_{A2}-D_{A1})^2 = (\xi_{A2}-\xi_{A1})^2 + (\eta_{A2}-\eta_{A1})^2 + (\zeta_{A2}-\zeta_{A1})^2. \tag{33}$$

To compute meteor velocities and decelerations, we must first compute D_{Ai} for all the observed shutter breaks. The use of equation (33) for this purpose would obviously be prohibitively laborious. Millman and Hoffleit (1936) have shown that D_{Ai} can be computed by a very simple formula, involving only the corrected values x_{Ai} corresponding to individual breaks, the coordinates of the radiant (x_{AR}) and of the beginning point (x_{Aa}), and a constant, K_A. The formula is

$$D_{Ai} = K_A \frac{x_{Ai}-x_{Aa}}{x_{Ai}-x_{AR}} = K_A D'_{Ai}, \tag{34}$$

with

$$K_A = R_{Aa}\frac{\cos\sigma_{Aa}}{\cos\sigma_{AR}}.$$

Here for convenience x_{Aa} has been identified with the beginning of the meteor trail. It is obvious, however, that any other point could have been taken as the origin of D_{Ai}. In equation (34) it is convenient to compute first D'_{Ai} for all shutter breaks, and then to multiply them by the constant K_A. This latter quantity is a function of the meteor instant, while the D'_{Ai}'s (which we shall call "relative distances") are clearly independent of time and can be computed even before the instant of the meteor has been determined.

When a long series of x_{Ai} has to be converted into D'_{Ai}, it is useful to re-write equation (34) in the following manner, which is more suitable for machine computation:

$$D'_{Ai} = 1 - \frac{1}{\alpha+\beta x_{Ai}}, \text{ where } \beta = \frac{1}{x_{Aa}-x_{AR}} \text{ and } \alpha = -\beta x_{AR}.$$

Equation (34) fails when σ_{AR} is close to 90°, a rather common occurrence. The difficulty can be avoided if we re-write equation (34) in the form

$$D_{Ai} = \frac{F_A(x_{Ai}-x_{Aa})}{1+G_A(x_{Ai}-x_{Aa})}. \tag{35}$$

F_A and G_A are constants for each meteor, since clearly $F_A = K_A/(x_{Aa}-x_{AR})$ and $G_A = F_A/K_A$; they can therefore be determined by using known values of D_{Ai}, as determined from equation (33), for any two points other than the beginning points (center and end point are recommended).

There is a simple relation between h_{Ai} and D_{Ai} which can be used as a check for the fundamental meteor points for which ranges and heights were computed, as well as to compute heights for any shutter break:

$$h_{Ai} = h_{Aa} - D_{Ai}\cos Z_{AR}. \tag{36}$$

To obtain heights above sea level use equation (28), with a graph of δh_{Ai} as function of h_{Ai}.

Equation (34), or (35), with the subscript A changed to B can be used to compute distances along the trail photographed from Station B.

By taking each individual beginning point as the origin of the distances D_{Ai} and D_{Bi}, we obtain two systems of D's on the spatial trajectory, differing by a constant. To simplify inter-comparisons between the two trails, it is convenient to use a single origin for both D_{Ai} and D_{Bi}. To avoid negative D's, the earlier (greater height above sea level) of the two observed beginning points can be taken as the common origin.

Our task, then, will be to transfer the beginning point on one plate to the (xy) coordinate system of the other plate. This is only a particular case of point transfer, so what is said for the beginning point is valid for any other point on the trail. To stress the generality of the formulae, which can be useful for other purposes, we shall use the subscript "i" for the point to be transferred, instead of the "a" used for the beginning point.

We shall suppose that the transfer is to be made from plate A (Station A) to plate B (Station B). Let us first compute the three components ξ_{Ai}, η_{Ai}, ζ_{Ai} of $\mathbf{R}_{Ai}$ according to equation (32). The corresponding components of the range vector $\mathbf{R}_{Bi}$ from Station B are:

$$\begin{aligned} \xi_{Bi}&=\xi_{Ai}-\xi_{AB} \\ \eta_{Bi}&=\eta_{Ai}-\eta_{AB} \\ \zeta_{Bi}&=\zeta_{Ai}-\zeta_{AB}; \end{aligned} \tag{37}$$

and

$$R_{Bi}^2=\xi_{Bi}^2+\eta_{Bi}^2+\zeta_{Bi}^2. \tag{38}$$

The direction cosines of the transferred point are:

$$\begin{aligned} \lambda_{Bi}&=\xi_{Bi}/R_{Bi} \\ \mu_{Bi}&=\eta_{Bi}/R_{Bi} \\ \nu_{Bi}&=\zeta_{Bi}/R_{Bi} \end{aligned} \tag{39}$$

Checks:

$$\lambda_{Bi}\lambda_{Bp}+\mu_{Bi}\mu_{Bp}+\nu_{Bi}\nu_{Bp}=0 \tag{39a}$$

$$H_{Ai}=H_{Bi}. \tag{39b}$$

Standard coordinates $(\bar{\xi}_{Bi}, \bar{\eta}_{Bi})$ and trail coordinates (x_{Bi}, y_{Bi}) are then computed from equations (4) and (5). *In computing K_B for a transferred beginning point it must be remembered that σ_{Ba} and σ_{BR} must be computed for the transferred, not for the observed, beginning point.*

The equations for the transfer from plate B to plate A are entirely similar when subscripts are changed. It is perhaps worth mentioning that in equation (37) we would have to replace ξ_{AB} with ξ_{BA}, which is equal to $-\xi_{AB}$, and similarly for η_{AB} and ζ_{AB}.

If ranges R_{Ai} are desired for points (such as shutter breaks) for which D_{Ai} is available, the following procedure is very useful. Compute first the value of D_{Ai} for the point of minimum range on the meteor trail and let it be D_{Ae}:

$$D_{Ae}=\xi_{Aa}\lambda_{AR}+\eta_{Aa}\mu_{AR}+\zeta_{Aa}\nu_{AR}. \tag{40}$$

Here ξ_{Aa}, η_{Aa}, ζ_{Aa} are the range components of the beginning point (origin of D_{Ai}).

The minimum range itself, R_{Ae}, is computed from the equation

$$R_{Ae}^2=R_{Aa}^2-D_{Ae}^2 \tag{41}$$

Check:

$$R_{Ae}=S_A/\sin Q. \tag{41a}$$

Equation (41a) could be used directly to determine R_{Ae}. We have preferred to use it only as a check, since both S_A and sin Q may become very small in certain cases.

For any D_{Ai} we shall then have the equation

$$R_{Ai}^2=R_{Ae}^2+(D_{Ai}-D_{Ae})^2. \tag{42}$$

Times corresponding to shutter breaks

If P is the period of revolution of the rotating shutter and N the number of occultations, all equally spaced, in one revolution, the instant t_i corresponding to the i-th break can be written as

$$t_i=\frac{P}{N}i+\Delta t_i, \tag{43}$$

where Δt_i is a function of the position of the meteor relative to the center of rotation of the shutter. For frontal shutters ordinarily used with small cameras, Δt_i can be minimized by making the distance between the shutter plane and the first principal point of the objective lens as small as possible. If it is felt that Δt_i cannot be neglected altogether, the correction can be determined empirically by visual or photographic observations in the focal plane of the camera.

For Super-Schmidt cameras provided with focal, radial-edge shutters the correction is large, but can be rigorously determined from the observed (x, y) trail coordinates on the glass copy of the original curved film.

Let x_q, y_q be the observed coordinates of the center of rotation of the shutter, and x_c, y_c the coordinates of the projection center—either observed, or taken from the plate constants (equation (11); $x_c=c$; $y_c=d$), and let f be the focal length of the camera. Let us write:

$$\begin{matrix} d_x=x_q-x_c \\ d_y=y_q-y_c \end{matrix}; \quad u=d_y/d_x \quad ; \quad z=1+\frac{d^2}{f^2}$$
$$d^2=d_x^2+d_y^2$$

We have then

$$\Delta t_i=\pm\frac{\omega_i-\omega_o}{2\pi}P, \tag{44}$$

where

$$\tan\omega_i=z\frac{u(x_i-x_q)-(y_i-y_q)}{u(y_i-y_q)+(x_i-x_q)}. \tag{45}$$

Here ω_o designates the value of ω corresponding to the origin of t_i (usually the first break); x_i and y_i are the observed values of x and y of the i-th break. The sign of Δt_i is positive when the shutter edge chases the meteor, negative when it runs toward the meteor.

When the shutter center coincides with the projection center ($d_x=d_y=0$), equation (45) reduces to

$$\tan\omega=\frac{x_i-x_q}{y_i-y_q}. \tag{45a}$$

This formula can be safely used whenever $d<1$ cm.

When a meteor is photographed close to the shutter center, the variation of Δt_i with x_i becomes large and a smoothing of Δt_i as computed from x_i is in order.

Velocities and decelerations

When distances D_{Ai} have been computed and tabularly listed as a function of time t_{Ai}, they must be critically appraised before they can be used to compute velocities and decelerations.

First of all, a weight must be assigned to each value of D_{Ai} on the basis of the recorded quality of the basic x_{Ai} observations. Strictly speaking, the scale of weights should be computed from the relative inner scatter found for each quality class. If no such analysis is available, the following scale is recommended: 1=very poor, doubtful; 2=poor; 4=fair; 6=good; 8=excellent.

In the second place, the D_{Ai} must be inspected for inner consistency and to detect any possible instrumental effect (such as shutter or camera vibrations) that may be amenable to empirical correction. A simple and useful device is the construction of an approximate "retardation diagram." Take only the first third of the D_{Ai}'s and from them compute an approximate value V_{Ao} of the initial velocity of the meteor. For all shutter breaks compute $\Delta_{Ai}=D_{Ai}-V_{Ao}t_{Ai}$ and plot Δ_{Ai} against time t_{Ai}. The range Δ_{Ai} is only a small fraction of the range of D_{Ai}, so a large scale can be used in the plot. The scale should be such that the normal observational scatter is clearly apparent. Any large deviation from the mean curve should be checked to detect possible mistakes in the computation; if the computation is verified, one should consider whether the observed discrepancy is large enough to warrant rejection of the point. In a series of good observed points, there is no reason to retain a small number of doubtful or bad points, whose inclusion would lower the quality of the results. If periodic oscillations due to instrumental causes are present, they should be corrected as far as possible before any analysis is started. (See section on shutter and camera vibrations, p. 199.)

A direct numerical differentiation of the observed D_{Ai} with respect to t_{Ai} is not recommended, even if D_{Ai} were tabulated at equal time intervals (which is not the case with the Super-Schmidt meteors), because observational errors are magnified in the process of numerical differentiation and also because in this process it would be impossible to account correctly for the weight of each single observation.

Experience has shown that a very expedient and accurate way to compute velocities and decelerations is to fit to the observed values of D_{Ai}, by least squares, an equation of the type

$$D_{Ai}=a_A+b_At_{Ai}+c_Ae^{kt_{Ai}}, \tag{46}$$

where a_A, b_A and c_A are unknowns, and k is determined beforehand. A simple way to compute k is to read off four equidistant values of Δ_{Ai} (Δ_1, Δ_2, Δ_3, Δ_4) from a smooth curve drawn with the help of a French curve through the points of the retardation diagram. Let the time interval between two successive values of

the selected Δ_{Ai} be T. We have then the value:

$$k=\frac{1}{T}\,ln\,\frac{\Delta_4-2\Delta_3+\Delta_2}{\Delta_3-2\Delta_2+\Delta_1}. \tag{47}$$

When a_A, b_A, c_A have been determined, velocities and accelerations are easily obtained by differentiation:

$$\begin{aligned} V_{Ai}&=\frac{dD_{Ai}}{dt}=b_A+kc_A\,e^{kt_{Ai}};\\ \dot{V}_{Ai}&=\frac{dV_{Ai}}{dt}=k^2\,c_A\,e^{kt_{Ai}}. \end{aligned} \tag{48}$$

Since equation (46) is at best only an empirical approximation of the true form of D_{Ai} (t_{Ai}), we cannot expect it to hold good for the whole of the observed trail. When dealing with a long meteor, we shall find it convenient to break up the trail into sections (either independent, or overlapping) and to compute separate least-squares solutions for each of them. An ideal goal is to obtain individual values of c_A which exceed their computed probable errors by a factor of 20 or 30; and with a little experience one can judge how long each section should be to yield such a margin of safety. In any case, only the values of V_{Ai} and $\dot{V}_{Ai}$ computed for the center of each section should be taken as having full significance.

From equation (48) it is easy to see that b_A is the extrapolated value of V_{Ai} for $t_{Ai}=-\infty$. Thus the least-squares solution provides us automatically with an important quantity, the velocity V_∞ of the meteor before it was decelerated by the earth's atmosphere. If several values of b_A have been obtained for a meteor, from several sections, the value from the first section will be the best value of V_∞.

Determining the instant of the meteor

Instant from measures of flares. When flares in the meteor trails can be identified and measured from both stations, the instant of the meteor can be determined independently from each flare. This method, when possible, is more satisfactory than the method of equalizing the observed velocities from the two stations (described in the next section).

The flare method depends upon the fact that the line joining the two observing stations must lie in a plane determined by the directions of the flare as observed at the two stations. It will be apparent that the method fails in certain geometrical configurations. At middle latitudes the solution is usually precise within a few seconds of time if the stations are located along a diagonal to the cardinal directions and if the flare is sufficiently defined for accurate measures.

Let us select a flare (or any other clear-cut feature) which can be recognized on both plates. From the measured x's and y's we shall compute its celestial coordinates as seen from Station A $(\lambda_{Af}, \mu_{Af}, \nu_{Af})$ and from Station B $(\lambda_{Bf}, \mu_{Bf}, \nu_{Bf})$, respectively.

The quantities

$$\begin{aligned} l_f&=\mu_{Af}\nu_{Bf}-\nu_{Af}\mu_{Bf}\\ m_f&=\nu_{Af}\lambda_{Bf}-\lambda_{Af}\nu_{Bf}\\ n_f&=\lambda_{Af}\mu_{Bf}-\mu_{Af}\lambda_{Bf} \end{aligned} \tag{49}$$

Check:

$$l_f\lambda_{Af}+m_f\mu_{Af}+n_f\nu_{Af}=l_f\lambda_{Bf}+m_f\mu_{Bf}+n_f\nu_{Bf}=0 \tag{49a}$$

are the direction cosines of the pole of the great circle through the two projections of the flare on the celestial sphere multiplied by the sine of their distance in arc. For these projections to lie in a plane with the two stations, we must clearly have the condition

$$l_f\xi_{AB}+m_f\eta_{AB}+n_f\zeta_{AB}=0. \tag{50}$$

Replacing ξ_{AB}, η_{AB}, ζ_{AB} by the expressions given in equation (18) and writing

$$\begin{aligned} l_f\xi_{ABo}+m_f\eta_{ABo}&=A_f\\ m_f\xi_{ABo}-l_f\eta_{ABo}&=B_f\\ n_f\zeta_{ABo}&=C_f, \end{aligned} \tag{51}$$

we obtain the equation

$$A_f\cos\theta_A+B_f\sin\theta_A+C_f=0, \tag{52}$$

which, when solved, yields θ_A. As the equation is quadratic in either $\sin\theta_A$ or $\cos\theta_A$, it has two solutions, of which only one, obviously, is significant. When the two solutions fall close together, the accuracy of the time determination by this method must be considered to be

poor. The sidereal time, of course, must lie within the interval common to the two photographs.

Instant from equalization of velocities. This method is based on the fact that "relative" velocities $v_A=\frac{d}{dt}(D'_{Ai})$ and $v_B=\frac{d}{dt}(D'_{Bi})$ can be determined before the instant of the meteor is known. For any given point on the meteor trajectory we must clearly have

$$K_A v_A = K_B v_B. \tag{53}$$

Since K_A and K_B are functions of the meteor instant, the latter can be determined when equation (53) is rewritten to contain θ_A in explicit form. The method is not very sensitive and is recommended only when the flare method cannot be used for lack of reliable common points.

Let us suppose for a moment that v_A and v_B have been determined. We shall then write

$$M_A=\frac{v_A}{S_A}\frac{\cos\sigma_{Aa}}{\cos\sigma_{AR}};\quad M_B=\frac{v_B}{S_B}\frac{\cos\sigma_{Ba}}{\cos\sigma_{BR}} \tag{54}$$

$$P_A=\xi_{ABo}\lambda_{Bp}+\eta_{ABo}\mu_{Bp} \qquad P_B=\xi_{ABo}\lambda_{Ap}+\eta_{ABo}\mu_{Ap}$$

$$Q_A=\xi_{ABo}\mu_{Bp}-\eta_{ABo}\lambda_{Bp} \qquad Q_B=\xi_{ABo}\mu_{Ap}-\eta_{ABo}\lambda_{Ap} \tag{55}$$

$$A_s=M_A P_A+M_B P_B$$

$$B_s=M_A Q_A+M_B Q_B$$

$$C_s=(M_A v_B+M_B v_A)\zeta_{ABo}. \tag{56}$$

We then find θ_A by solving the equation

$$A_s\cos\theta_A+B_s\sin\theta_A+C_s=0. \tag{57}$$

To determine v_A and v_B it is best to proceed by successive approximations. First find the asymptotic velocities $v_{A\infty}(=b_A)$ and $v_{B\infty}(=b_B)$ by least squares, fitting to the observed values D'_{Ai} and D'_{Bi} an equation of the same type as equation (46). These asymptotic velocities can be used instead of v_A and v_B in equation (57) to obtain a first approximation to θ_A. Using this first approximation, we can transfer the center of the trajectory on plate A onto plate B and compute relative velocities for these two points. Since these are central points, the relative velocities pertaining to them will be more reliable than the extrapolated asymptotic velocities and will yield a better approximation to θ_A. The process may be repeated if the possible results seem to be justified by the labor.

Instant from an undriven monitoring plate. We shall suppose that the monitoring camera is placed close enough to the meteor camera that the parallax between the two cameras is negligible. Let us assume that the cameras are situated at Station A and that a time break is impressed on the star trails, centered around the instant θ_{AS} of local sidereal time.

For simplicity we shall consider only a short, central portion of the meteor trail, and select a few (four or five) time breaks on star trails in the region surrounding this portion. Measure x and y coordinates for the star breaks and for the meteor portion, and determine the coordinates (α, δ) of the plate center at the time of the star breaks. Compute standard coordinates of star breaks and plate constants (six-constant method preferable). If the area covered by the star breaks is not too wide, the field distortion within the area, as revealed by the individual residuals Δx and Δy, will be small; it must be made small because we shall be forced to neglect it.

Plot y against x for the measured points on the meteor trail, and derive a smoothed value y_M of y for a given value x_M of y near the center. For this point, compute standard coordinates, direction cosines, and finally right ascension and declination (α'_M, δ_M), all in the system of star breaks. The correct right ascension α_M corresponding to δ_M can be computed from the equation of the great circle of motion of the meteor:

$$\cos(\alpha_M-\alpha_P)=-\tan\delta_M\tan\delta_P. \tag{58}$$

Here α_P and δ_P are the right ascension and declination of the pole of the trail, both known from the driven meteor plate. The difference $\Delta\theta=\alpha_M-\alpha'_M$ is equal to the sidereal time elapsed between the instant of the star breaks and the instant of the meteor; i. e., we have the equation

$$\theta_A=\theta_{AS}+\Delta\theta. \tag{59}$$

This method fails when the meteor runs approximately along a parallel of declination. In that case, the difference $\Delta\theta$ can be computed from $\alpha_P - \alpha'_P$, where α'_P is the right ascension of the pole of the meteor trail, referred to the star breaks. If the meteor runs approximately along the celestial equator, the method fails completely unless some use can be made of identifiable common points.

Space trajectory by direct triangulation

When the angle of intersection Q between the great circles of motion of the meteor as seen from the two stations is very small, the method described in the section on ranges and heights (p. 189) fails. In such cases direct triangulation can be used.

The instant of the meteor must be known from visual observations or from a monitoring plate, and a good common point m (x_{Am}, y_{Am} on plate A; x_{Bm}, y_{Bm} on plate B) must be available. A second common point n, as remote as possible from m, is established by making use of the shutter breaks. Select a break (x_{An}, y_{An}) on plate A and evaluate the time interval t_{mn} between this break and the first point m; on plate B find the point (x_{Bn}, y_{Bn}) for which the time interval from point m is exactly equal to t_{mn}. Be sure to eliminate the effect of observational errors by first smoothing x_{Ai} and x_{Bi} (smoothing by differences is not recommended; comparison with a close-fitting polynomial is preferable).

We shall have two separate triangulations to compute R_{Am}, R_{Bm} and R_{An}, R_{Bn}; in the following formulae i stands for either m or n. R_{AB} is the spatial distance between the two stations.

The base angles α_i and β_i and the vertex angle γ_i are first computed from the equations

$$\begin{aligned} R_{AB}\cos\alpha_i &= \xi_{AB}\lambda_{Ai}+\eta_{AB}\mu_{Ai}+\zeta_{AB}\nu_{Ai} \quad (0<\alpha<\pi) \\ R_{AB}\cos\beta_i &= -(\xi_{AB}\lambda_{Bi}+\eta_{AB}\mu_{Bi}+\zeta_{AB}\nu_{Bi}) \quad (0<\alpha<\pi) \end{aligned} \tag{60}$$

$$\sin\gamma_i = \sin\alpha_i\cos\beta_i + \cos\alpha_i\sin\beta_i \tag{60a}$$

after which the ranges become

$$R_{Ai} = R_{AB}\frac{\sin\beta_i}{\sin\gamma_i};\quad R_{Bi} = R_{AB}\frac{\sin\alpha_i}{\sin\gamma_i}. \tag{61}$$

At this stage, we must decide whether we want to use the trail on plate A or the trail on plate B for the computation of the radiant, or a compromise between the two. Since the radiant is no longer defined as the intersection of the great circles corresponding to the trails, but rather as the vanishing point of the space trajectory of the meteor, we must expect to find a slight discrepancy between the two determinations. Suppose we have selected the trail on plate A as the most reliable. Then:

$$\begin{aligned} &\xi_{Ai}=R_{Ai}\lambda_{Ai} \quad \xi_{mn}=\xi_{Am}-\xi_{An} \quad \lambda_{AR}=\xi_{mn}/D_{mn} \\ &\eta_{Ai}=R_{Ai}\mu_{Ai}; \quad \eta_{mn}=\eta_{Am}-\eta_{An}; \quad \mu_{AR}=\eta_{mn}/D_{mn} \\ &\zeta_{Ai}=R_{Ai}\nu_{Ai}; \quad \zeta_{mn}=\zeta_{Am}-\zeta_{An} \quad \nu_{AR}=\zeta_{mn}/D_{mn} \\ &\qquad D^2_{mn}=\xi^2_{mn}+\eta^2_{mn}+\zeta^2_{mn}. \end{aligned} \tag{62}$$

Meteors photographed by stationary cameras

General problems. Either one or both meteor photographs may have been taken with stationary cameras. We shall discuss each case separately; first, however, we may examine a few problems which arise with trailed plates in general.

We shall suppose that the star trails on the undriven plate show "time breaks" caused by a mechanical or hand-operated shutter at certain instants which have been carefully timed. If we refer the meteor and the plate center to one particular set of time breaks on star trails, we do not obtain its true position in the sky, unless the time of appearance of the meteor happened by chance to coincide exactly with the instant of the time breaks. All the declinations we determine in such fashion are correct, but the right ascensions are shifted by an amount $\Delta\theta=\theta_A-\theta'_A$, where θ_A is the sidereal time of the meteor, and θ'_A that of the star breaks, both taken here as observed at Station A. We shall call such a hybrid system of coordinates "relative coordinates," and designate them with a prime (α'_{Ai}, δ'_{Ai}; λ'_{Ai}, μ'_{Ai}, ν'_{Ai}, etc.).

The faintest stars recorded on trailed plates are considerably brighter than those that are normally selected as comparison stars on diverse plates. Thus fewer stars are available and it is almost impossible to find time breaks sufficiently close to the meteor trail to yield satisfactory field correction (Δx, Δy) curves. It is therefore convenient to determine the plate constants from star breaks in a limited

area of the plate rich in star breaks and crossed by the meteor trail—an area sufficiently small to justify the neglect of field corrections within its limits. The "relative" position of the pole (α'_A, δ_A) of the meteor trail must be determined from (x, y) measures confined to this area alone; i. e., in the plot of observed y's in function of x, we must isolate the portion of the diagram that lies within the extreme values of x measured for the star breaks, and draw the best possible straight line through those points only.

If the instant of the meteor is known, or has been computed, relative coordinates can be transformed into true coordinates by the following transformation:

$$\begin{aligned} \lambda_{Ai} &= \lambda'_{Ai} \cos \Delta\theta - \mu'_{Ai} \sin \Delta\theta \\ \mu_{Ai} &= \mu'_{Ai} \cos \Delta\theta + \lambda'_{Ai} \sin \Delta\theta \\ \nu_{Ai} &= \nu'_{Ai}. \end{aligned} \tag{63}$$

The usual checks must be applied to the transformed meteor points

$$\begin{aligned} &\lambda^2_{Ai} + \mu^2_{Ai} + \nu^2_{Ai} = 1 \\ &\lambda_{Ai}\lambda_{Ap} + \mu_{Ai}\mu_{Ap} + \nu_{Ai}\nu_{Ap} = 0 \\ &\lambda_{Ai}\lambda'_{Ai} + \mu_{Ai}\mu'_{Ai} + \nu_{Ai}\nu'_{Ai} = \cos \Delta\theta. \end{aligned} \tag{63a}$$

Once all coordinates (of points on the meteor, of the pole, and of the plate center) have been thus converted, the reduction can proceed in normal fashion, as for driven plates.

When the meteor intersects the star trails at a considerable angle, so that intersection points can be accurately measured, such points can be used to determine the field correction at least in the x coordinate. To avoid interference with the shutter breaks on the meteor trail, we should first measure the y coordinate of the meteor trail at convenient intervals of x (with one of the cross-wires of the measuring engine as nearly parallel to the meteor trail as possible), then plot the observed y's against x and draw a smooth curve through the points. This curve can then be used to *set* the y coordinate of the measuring engine for each intersection to be measured; in this fashion one of the cross-wires replaces the meteor trail, bridging the gaps caused by the rotating shutter.

At the intersection with a star trail, the declination δ_{Mi} of the meteor is equal to the declination of the star. Thus, by feeding the declination of the intersecting star into the equation of the great circle of motion of the meteor in "relative" coordinates:

$$\cos (\alpha'_A - \alpha'_{Mi}) = -\tan \delta_{Ap} \tan \delta_{Mi}, \tag{64}$$

we shall obtain the "relative" right ascension α'_{Mi} of the intersection point. We can do this for all the measured intersections, from the actual beginning to the actual end of the meteor trail; for each intersection we can correct (α'_M, δ'_M) into standard coordinates and compute the corresponding (x, y) coordinates with the help of the plate constants from the time breaks in the small area. A comparison with the measured values of x and y will yield individual residuals Δx and Δy, from which field correction curves can be obtained. While the Δx curve can be considered to be an excellent approximation to the real field distortion relative to the adopted plate constants, the same is not necessarily true of the Δy curve. The reasons for this are two:

(1) We determined the (xy) equation of the trail from a small portion of the trail only, so that the margin of error at the extremes of the trail is rather large.

(2) We assumed, in computing intersections, that the meteor followed a great circle in the sky, and this may not have been rigorously true.

A final word should be said about time breaks. If several time breaks are impressed on star trails during the course of the exposure, breaks belonging to different sets may be used to determine plate constants provided they are all reduced to a common set. On glass plates, the indiscriminate choice of time breaks of different sets should cause no trouble when the timing is accurate. On the other hand, in film photographs taken with conventional cameras some trouble may be caused by progressive film distortion under stress.

Case of one driven and one stationary camera. Suppose the stationary camera is located at Station A. If the instant of the meteor is known, there is no problem. First compute "relative" coordinates of points on the meteor and of the pole of the trail, and then convert them to true coordinates, as described in the preceding section.

If the instant of the meteor is not known, it must first be determined by using flares or

other common points on the two photographic meteor trails. Only when good, sharp common points can be found is a solution worth trying.

Compute first:

$$\begin{aligned}\xi'_{AB}&=\xi'_{ABo}\cos\theta'_A-\eta'_{ABo}\sin\theta'_A\\ \eta'_{AB}&=\eta'_{ABo}\cos\theta'_A+\xi'_{ABo}\sin\theta'_A\\ \zeta'_{AB}&=\zeta'_{ABo}\end{aligned}\qquad(65)$$

Check:

$$\xi'^2_{AB}+\eta'^2_{AB}+\zeta'^2_{AB}=R'^2_{AB}.\qquad(65a)$$

For each flare (relative coordinates λ'_{Af}, μ'_{Af}, ν'_{Af}) compute

$$\begin{aligned}l'_f&=\mu'_{Af}\zeta'_{AB}-\nu'_{Af}\eta'_{AB}\\ m'_f&=\nu'_{Af}\xi'_{AB}-\lambda'_{Af}\zeta'_{AB}\\ n'_f&=\lambda'_{Af}\eta'_{AB}-\mu'_{Af}\xi'_{AB}\end{aligned}\qquad(66)$$

and the coefficients

$$\begin{aligned}A'_f&=\lambda_{Bf}l'_f+\mu_{Bf}m'_f\\ B'_f&=\mu_{Bf}l'_f-\lambda_{Bf}m'_f\\ C'_f&=\nu_{Bf}n'_f.\end{aligned}\qquad(67)$$

Then solve the equation,

$$A'_f\cos\Delta\theta+B'_f\sin\Delta\theta+C'_f=0.\qquad(68)$$

Since $\Delta\theta$ is always relatively small, solve for $\sin\Delta\theta$. If the computation was done for several flares, take a weighted mean of all the resulting values of $\Delta\theta$ and proceed to convert all relative coordinates to true coordinates, as described in the preceding section.

Case of two stationary cameras. If the meteor is photographed with stationary cameras at both stations, the solution is independent of time. By this we mean that correct heights, distances, and velocities will be obtained no matter what instant is assumed for the meteor. Unless, however, we know the instant from observation, the position of the radiant remains indeterminate; i. e., its declination can be computed, but not its right ascension.

If the instant of the meteor is not known, assume for simplicity that the meteor appeared at the time of a given set of time breaks on star trails on plate A. Then the plate constants on plate A can be computed in a straightforward manner by directly correlating the observed (xy) coordinates of star breaks with (ξ, η) coordinates computed from catalog positions for the stars. On plate B, however, the right ascensions of the stars (and of the plate center, as referred to star breaks) must be augmented by $\theta^*_B-\theta'_B$, where θ^*_B is the sidereal time at Station B corresponding to the assumed meteor instant, and θ'_B is the sidereal time, at the same station, of the time breaks.

From here on the solution proceeds as for meteors on driven plates with observed time. One should remember that while the positions of the radiant and of the zenith, as computed, are purely fictitious, their distance Z_R is correct. Since the radiant position is indeterminate, no orbit can be computed.

Plate center from three stars

Estimate the approximate position of the plate center and select three stars S_1, S_2, S_3, as nearly equidistant as possible from the center and at 120° (counted from the center) from each other. We recommend taking a plate of clear glass or a transparent plastic sheet and drawing on it three lines issuing at 120° from a common point, with distances from this point marked on each line. This plate or sheet can then be superimposed on the meteor plate to help select the stars. The three stars should not be too close to the center, but not so far that differential atmospheric refraction might affect the results; also, they should be of the same brightness and rather faint, to avoid excessive coma distortion.

On a measuring engine measure the distance between pairs:

d_1=distance between S_2 and S_3
d_2=distance between S_1 and S_3
d_3=distance between S_1 and S_2

Compute the corresponding angular distances in the sky:

$$\begin{aligned}\cos\gamma_1&=\lambda_2\lambda_3+\mu_2\mu_3+\nu_2\nu_3\\ \cos\gamma_2&=\lambda_1\lambda_3+\mu_1\mu_3+\nu_1\nu_3\\ \cos\gamma_3&=\lambda_1\lambda_2+\mu_1\mu_2+\nu_1\nu_2.\end{aligned}\qquad(69)$$

By successive approximations solve the following equations for $\rho_i(\rho_i^2=f^2+d_i^2$, where f is the focal length of the camera):

$$l_1=\frac{d_1^2-(\rho_2-\rho_3)^2}{2-2\cos\gamma_1};\ \rho_1=\sqrt{\frac{l_2l_3}{l_1}}$$

$$l_2=\frac{d_2^2-(\rho_1-\rho_3)^2}{2-2\cos\gamma_2};\ \rho_2=\sqrt{\frac{l_1l_3}{l_2}}$$

$$l_3=\frac{d_3^2-(\rho_1-\rho_2)^2}{2-2\cos\gamma_3};\ \rho_3=\sqrt{\frac{l_1l_2}{l_3}}.$$

In first approximation it can be assumed that $\rho_2-\rho_3=\rho_1-\rho_3=\rho_1-\rho_2=0$; proceed to further approximations until all three ρ's are stabilized to the nearest micron (0.001 mm). The coordinates of the plate center (λ_c, μ_c, ν_c) are obtained from the equation

$$\lambda_i\lambda_c+\mu_i\mu_c+\nu_i\nu_c=f/\rho_i\ (i=1, 2, 3). \quad (71)$$

Suggested procedure: Solve

$$\lambda_i\rho_i\frac{\lambda_c}{f}+\mu_i\rho_i\frac{\mu_c}{f}+\nu_i\rho_i\frac{\nu_c}{f}=1 \quad (72)$$

for λ_c/f, μ_c/f, ν_c/f; compute f from the obvious relation

$$\left(\frac{\lambda_c}{f}\right)^2+\left(\frac{\mu_c}{f}\right)^2+\left(\frac{\nu_c}{f}\right)^2=\frac{1}{f^2}. \quad (73)$$

Corrections for gravity

The spatial deflection of a meteor from its purely inertial trajectory, due to gravity, at a given point i is

$$G_i=\frac{1}{2}\,g\,t_i^2, \quad (74)$$

where g is the acceleration of gravity (=0.0096 km/sec^2 at average meteor heights) and t_i is the time elapsed from the time origin (i. e., from the instant of the first break, or from any other convenient point on the meteor trail).

The corresponding deflection δy on the photographic plate, in the y direction (perpendicular to the direction of motion of the meteor), is

$$\delta y=\frac{G_i\cos\psi}{R_iS_y}, \quad (75)$$

where R_i is the distance of the meteor from the station, S_y is the scale of the photographic plate in the y direction (see section on photometry, p. 203), and ψ is the zenith distance of the pole of the meteor trail, for Station A (and similarly for Station B), computed from the equation

$$\cos\psi_A=\lambda_A\lambda_{ZA}+\mu_A\mu_{ZA}+\nu_A\nu_{ZA}. \quad (76)$$

As a correction to the observed y's on the trail, δy should be applied with such a sign as to bring the meteor positions closer to the zenith. Ordinarily R_i is computed only at a later stage, but since a very limited accuracy in R_i is needed to obtain δ_i, a rough solution, requiring only a few minutes, is in order.

To correct distances on the trail:

$$D_{corr}=D_i-G_i\cos Z_R. \quad (77)$$

To correct velocities:

$$V_{corr}=V_o-g\,(t_i-t_o)\cos Z_R. \quad (78)$$

Here V_o is the velocity determined for a given instant t_o and Z_R stands for either Z_{AR} or Z_{BR}. A correction to the observed velocities is justified only when it becomes necessary to inter-compare several velocity determinations in the course of a trajectory. For orbital purposes, the correction for zenith attraction (see p. 201) takes into account the effect of gravity from infinity to the point of observation.

To correct accelerations:

$$\dot{V}_{corr}=\dot{V}-g\cos Z_R. \quad (79)$$

This correction is not always negligible in early parts of meteor trajectories.

Corrections for vibrations

A common trouble in the photography of meteors with small cameras provided with frontal rotating shutters arises from vibrations imparted by the shutter to the camera. In Super-Schmidt cameras the shutter is too light to transmit any vibrations to the camera; frequently, however, a modulated flutter is observed in the rotational motion of the shutter. Both of these effects are reflected in a semiperiodic oscillation of the observed position of the meteor in its trajectory. In the first

case, however, the oscillation affects directly the measured (xy) coordinates, while in the second case it affects the computed time of the shutter breaks. We must, therefore, treat the two cases separately.

Camera vibration. In dealing with camera vibrations, we shall assume that the rotating shutter showed no error arising from eccentricity or from asymmetry, or that any such errors have been determined experimentally and corrected for. A true camera oscillation is revealed by its occasional effect on the transverse (y) coordinate of the meteor trail, resulting in a sinuous trajectory. We can easily eliminate this latter effect either by trying to measure the mean rather than the actual y coordinate or by drawing a straight line through the observed oscillations in the (xy) diagram.

In general, the oscillation of a given point on the plate will be along an ellipse, whose shape may be subject to semiperiodic changes. If the oscillation is imparted by the shutter, its period will be either the period of rotation of the shutter, or a submultiple of it. To study the longitudinal component of the oscillations, one should analyze the observed x's; this task, however, is made difficult by the fact that x on the meteor trail is a rather complicated function of time. It is much more convenient to do the analysis when the x's have been reduced to distances D, and then to convert residuals ΔD to Δx by means of simple formulae. When D's have been computed, a retardation diagram must be plotted; if the range of the retardation is large, it is convenient to compute approximate values of the coefficients a_A, b_A, c_A in equation (46) from three points on the retardation curve and compute residuals $\Delta_2 D$ from this equation. These residuals can then be converted to the corresponding residuals in x $(\Delta_2 x)$ by multiplying them by dx/dD $(=V_{mm}/V$; see equation (106)), which can easily be computed to two or three figures even at this stage.

Once the period of oscillation has been established, divide the shutter breaks into as many groups as there are breaks in one cycle of the oscillation, and for each group draw a separate curve of $\Delta_2 x$ against i, the order number of the break. The differences between the curves will supply the systematic corrections to be applied to the observed x of each individual break. Instead of applying this correction to x, one may, of course, multiply it by dD/dx and apply it to D_i.

Shutter flutter. The flutter in the shutter of the Super-Schmidt cameras causes the computed instants of individual shutter breaks to be in error by a visible amount Δt; conversely, if we assume that the computed instants are correct, we shall observe corresponding oscillations $\Delta D = v\Delta t$ in the distances. Since we cannot detect Δt except by analyzing ΔD, it is convenient, once ΔD has been isolated, to apply corrections to the observed distances D_i rather than to the instants t_i.

To isolate the fluctuations ΔD, follow the same procedure as for camera vibrations: construct a retardation diagram and plot residuals $\Delta_2 D$ from equation (46), with coefficients computed from three points, against i. For the Super-Schmidt cameras $\Delta_2 D$ occasionally shows slow, semiperiodic oscillations (most frequent period $= 0^s.23$), superimposed on a slower variation, due to the imperfect fit of equation (46). Draw first a smooth curve through the observed points, following all the oscillations; then draw a smooth curve to bisect all the waves of the oscillations. The difference between the two curves can be taken as the correction to be applied to D_i. If the trail covers only a little more than one cycle of the oscillation, it is convenient to fit a sine term to the observed values of $\Delta_2 D$.

Computation of orbital elements

When the position of the apparent radiant $(\lambda_R, \mu_R, \nu_R)$ and the apparent velocity of the meteor before atmospheric deceleration (V_∞) have been determined, it is possible to compute the orbital elements of the meteor.

If V_∞ is determined separately from two plates, take a weighted mean of the two quantities.

Correction for earth's rotation (aberration). Compute the (negative) velocity components of the velocity:

$$\xi' = \lambda_R V_\infty,\ \eta' = \mu_R V_\infty,\ \zeta' = \nu_R V_\infty. \qquad (80)$$

The corrected velocity and radiant are computed from the equations

$$V_c\lambda_{Rc}=\xi'+\frac{2\pi}{T_s}R_A\cos\phi'_A\sin\theta_A$$

$$V_c\mu_{Rc}=\eta'-\frac{2\pi}{T_s}R_A\cos\phi'_A\cos\theta_A \qquad (81)$$

$$V_c\nu_{Rc}=\zeta'.$$

Here T_s is the sidereal period of rotation of the earth in seconds=86164. Station A is chosen as the observers' point, although no substantial difference is found if Station B is used.

Corrections for zenith attraction. Let us take a central point on the meteor trajectory as photographed from Station A (λ_{Ao}, μ_{Ao}, ν_{Ao}) and compute its distance R_o from the center of the earth and the zenith direction through it (λ_{Zo}, μ_{Zo}, ν_{Zo}):

$$\begin{aligned}R_o\lambda_{Zo}&=R_A\cos\phi'_A\cos\theta_A+R_{Ao}\lambda_{Ao}\\R_o\mu_{Zo}&=R_A\cos\phi'_A\sin\theta_A+R_{Ao}\mu_{Ao}\\R_o\nu_{Zo}&=R_A\sin\phi'_A+R_{Ao}\nu_{Ao}.\end{aligned} \qquad (82)$$

Calculate the direction cosines λ_N, μ_N, ν_N and λ_K, μ_K, ν_K of the normals to the zenith, and the corrected zenith distance Z_{Rc} by the equations

$$\begin{aligned}\lambda_N\sin Z_{Rc}&=\mu_{Rc}\nu_{Zo}-\nu_{Rc}\mu_{Zo}\\\mu_N\sin Z_{Rc}&=\nu_{Rc}\lambda_{Zo}-\lambda_{Rc}\nu_{Zo}\\\nu_N\sin Z_{Rc}&=\lambda_{Rc}\mu_{Zo}-\mu_{Rc}\lambda_{Zo}\end{aligned} \qquad (83)$$

$$\begin{aligned}\lambda_K&=\mu_{Rc}\nu_N-\nu_{Rc}\mu_N\\\mu_K&=\nu_{Rc}\lambda_N-\lambda_{Rc}\nu_N\\\nu_K&=\lambda_{Rc}\mu_N-\mu_{Rc}\lambda_N\end{aligned} \qquad (84)$$

Checks:

$$\begin{aligned}&\lambda_N\lambda_{Zo}+\mu_N\mu_{Zo}+\nu_N\nu_{Zo}=0\\&\lambda_N\lambda_{Rc}+\mu_N\mu_{Rc}+\nu_N\nu_{Rc}=0\\&\cos Z_{Rc}=\lambda_{Rc}\lambda_{Zo}+\mu_{Rc}\mu_{Zo}+\nu_{Rc}\nu_{Zo}\\&\sin Z_{Rc}=\lambda_K\lambda_{Zo}+\mu_K\mu_{Zo}+\nu_K\nu_{Zo}.\end{aligned} \qquad (83a)$$

$$\begin{aligned}&\lambda_K\lambda_N+\mu_K\mu_N+\nu_K\nu_N=0\\&\lambda_K\lambda_{Rc}+\mu_K\mu_{Rc}+\nu_K\nu_{Rc}=0.\end{aligned} \qquad (84a)$$

The velocity V_{cc} corrected for zenith attraction is given by the equation

$$V_{cc}^2=V_c^2-2g_oR_o, \qquad (85)$$

where g_o is the acceleration of gravity corresponding to a distance R_o from the center of the earth. A good approximation for $2g_oR_o$ is given by the equation

$$2g_oR_o=0.79464/R_o\,(\text{in units of 100 km/sec}^2). \qquad (86)$$

The correction ΔZ to the zenith distance is given by the equation

$$\tan\frac{\Delta Z}{2}=\frac{V_c-V_{cc}}{V_c+V_{cc}}\frac{\sin Z_{Rc}}{1+\cos Z_{Rc}} \qquad (87)$$

$$Z_{Rcc}=Z_{Rc}+\Delta Z,$$

in which

$$\sin\Delta Z=\frac{2\tan\frac{\Delta Z}{2}}{1+\tan^2\frac{\Delta Z}{2}};\quad\cos\Delta Z=\frac{1-\tan^2\frac{\Delta Z}{2}}{1+\tan^2\frac{\Delta Z}{2}}. \qquad (88)$$

Compute the direction cosines of the final corrected radiant:

$$\begin{aligned}\lambda_{Rcc}&=\lambda_{Rc}\cos\Delta Z+\lambda_K\sin\Delta Z\\\mu_{Rcc}&=\mu_{Rc}\cos\Delta Z+\mu_K\sin\Delta Z\\\nu_{Rcc}&=\nu_{Rc}\cos\Delta Z+\nu_K\sin\Delta Z\end{aligned} \qquad (89)$$

Checks:

$$\begin{aligned}&\lambda_{Rcc}\lambda_{Zo}+\mu_{Rcc}\mu_{Zo}+\nu_{Rcc}\nu_{Zo}=\cos Z_{Rcc}\\&\lambda_{Rcc}\lambda_{Rc}+\mu_{Rcc}\mu_{Rc}+\nu_{Rcc}\nu_{Rc}=\cos\Delta Z\\&\lambda_{Rcc}\lambda_N+\mu_{Rcc}\mu_N+\nu_{Rcc}\nu_N=0\\&\lambda_{Rcc}\lambda_K+\mu_{Rcc}\mu_K+\nu_{Rcc}\nu_K=\sin\Delta Z.\end{aligned} \qquad (89a)$$

Heliocentric velocity. The geocentric velocity of the meteor in a.u./1/k mean solar days is

$$V_m=3.3595V_{cc} \qquad (90)$$

when V_{cc} is expressed in units of 100 km/sec. In the conversion constant the solar parallax has been assumed to be 8".80. Compute the velocity components,

$$\begin{aligned}X'_m&=-V_m\lambda_{Rcc}\\Y'_m&=-V_m\mu_{Rcc}\\Z'_m&=-V_m\nu_{Rcc}.\end{aligned} \qquad (91)$$

These components are referred to the equinox of the year of the meteor and should now be converted to the standard equinox of 1950.0 by using the same equations and tables as for the precessional rotation of direction cosines.

From an astronomical ephemeris interpolate, for the instant of the meteor, the equatorial rectangular coordinates of the sun for the

standard equinox (1950.0) ($X_\odot$, $Y_\odot$, $Z_\odot$), and their first derivatives ($X'_\odot$, $Y'_\odot$, $Z'_\odot$) with respect to time, expressed in mean solar days. It is convenient to compute the derivatives (using all significant differences) for midpoints between tabulated values for a few days before and after the date of the meteor, and then to interpolate for the exact instant of the meteor.

The interpolated positions and derivatives can be checked against the ephemeris of the radius vector r_T of the earth in its orbit, given elsewhere in the almanac:

$$X_\odot^2+Y_\odot^2+Z_\odot^2=r_T^2$$

$$X_\odot X'_\odot+Y_\odot Y'_\odot+Z_\odot Z'_\odot=-r_T r'_T. \quad (92)$$

To obtain the heliocentric position and velocity components of the earth in the same system and units, we have simply to change sign in the above quantities. The velocities are expressed in a. u. per mean solar day; to add them to the meteor velocity components, we must first multiply them by $1/k$ (=58.132). Neglecting the distance of the meteor from the center of the earth, we can thus compute the heliocentric equatorial coordinates and velocity components of the meteor:

$$X=-X_\odot \qquad X'=X'_m-58.132X'_\odot$$

$$Y=-Y_\odot; \qquad Y'=Y'_m-58.132Y'_\odot$$

$$Z=-Z_\odot \qquad Z'=Z'_m-58.132Z'_\odot \quad (94)$$

$$r^2=X^2+Y^2+Z^2$$

$$rr'=XX'+YY'+ZZ'$$

$$V^2=X'^2+Y'^2+Z'^2. \quad (95)$$

The heliocentric velocity of the meteor in km/sec is 29.767 V.

Orbital elements. The customary symbols used in orbit calculations are given in the following section. Some slight duplication of the previous symbols should not cause confusion.

a=semimajor axis
q=perihelion distance
q'=aphelion distance
p=parameter
e=eccentricity
} in a. u.

i=inclination
ϵ=obliquity of the ecliptic
v=true anomaly
ω=argument of perihelion
Ω=longitude of ascending node
ϖ=longitude of perihelion
} equinox of 1950.0

P=period of revolution (sidereal years)
λ=elongation of the corrected radiant from the apex of the earth's orbital motion.

The elements are derived as follows:

$$\frac{1}{a}=\frac{2}{r}-V^2$$

$$p=r^2V^2-(rr')^2$$

$$e\sin v=r'p^{1/2}$$

$$e\cos v=\frac{p}{r}-1 \quad (96)$$

Check:

$$a=\frac{p}{1-e^2}. \quad (96a)$$

Direction cosines of the major axis:

$$P_X=\frac{1}{e}\left(\frac{1}{r}-\frac{1}{a}\right)X+\left(-\frac{rr'}{e}\right)X'$$

$$P_Y=\frac{1}{e}\left(\frac{1}{r}-\frac{1}{a}\right)Y+\left(-\frac{rr'}{e}\right)Y'$$

$$P_Z=\frac{1}{e}\left(\frac{1}{r}-\frac{1}{a}\right)Z+\left(-\frac{rr'}{e}\right)Z'. \quad (97)$$

Direction cosines of the minor axis:

$$Q_X=\frac{r'}{e\sqrt{p}}X+\frac{p-r}{e\sqrt{p}}X'$$

$$Q_Y=\frac{r'}{e\sqrt{p}}Y+\frac{p-r}{e\sqrt{p}}Y'$$

$$Q_Z=\frac{r'}{e\sqrt{p}}Z+\frac{p-r}{e\sqrt{p}}Z' \quad (98)$$

Checks:

$$P_X^2+P_Y^2+P_Z^2=1$$

$$Q_X^2+Q_Y^2+Q_Z^2=1$$

$$P_XQ_X+P_YQ_Y+P_ZQ_Z=0. \quad (98a)$$

Ecliptic elements:

$$\sin i \cos \omega = Q_Z \cos \epsilon - Q_Y \sin \epsilon$$

$$\sin i \sin \omega = P_Z \cos \epsilon - P_Y \sin \epsilon \qquad (99)$$

$$\cos \Omega = P_X \cos \omega - Q_X \sin \omega$$

$$\sin \Omega = (P_Y \cos \omega - Q_Y \sin \omega) \div \cos \epsilon. \qquad (100)$$

Check:

$$-\cos i \sin \Omega = Q_X \cos \omega + P_X \sin \omega. \qquad (100a)$$

If $Y' \sin \epsilon - Z' \cos \epsilon > 0$, $\omega = 180° - v$ and Ω = Longitude of Sun.
If $Y' \sin \epsilon - Z' \cos \epsilon < 0$, $\omega = 360° - v$ and Ω = Longitude of Sun + 180°.

Additional elements:

$$\varpi = \Omega + \omega$$
$$q' = a(1+e)$$
$$P = a^{3/2} \qquad (101)$$
$$\cos \lambda = -\frac{\lambda_{Rec} X'_\odot + \mu_{Rec} Y'_\odot + \nu_{Rec} Z'_\odot}{(X'^2_\odot + Y'^2_\odot + Z'^2_\odot)^{1/2}}.$$

Photometry

In this section we shall briefly describe the techniques used in the Harvard Meteor Project to measure the apparent brightness of meteors photographed on glass plates (small cameras) and on curved films (Super-Schmidt cameras). We shall start with a few general remarks and useful formulae.

Scale on photographic plates. Apart from relatively small distortions, the scale S (in radians/mm) can be considered to be constant on Super-Schmidt films, and equal to f, the effective focal length of the camera (in mm). We can compute f from the plate constants on the glass copy:

$$f^2 = a^2 + b^2 \text{ (4-constant method)}$$
$$\text{or } f^2 = a_x^2 + b_x^2 \text{ (6-constant method).} \qquad (102)$$

The same formulae can be used to derive the focal length of an ordinary camera using glass plates.

On plates, the scale varies at each point with direction. In the absence of distortions, at a distance d from the projection center (where the optical axis of the camera, or of the copying system, encounters the plate) and in a direction which makes an angle ϕ with the radial direction, the scale of the plate is

$$S_\phi = \frac{\sqrt{f^2 + (d \sin \phi)^2}}{f^2 + d^2}. \qquad (103)$$

In the case of a meteor, in which the x coordinate is measured on the trail, and y is constant, the scale factor S_x in the direction of motion of the meteor, and the scale factor S_y in the perpendicular direction are, respectively:

$$S_x = \frac{\sqrt{\rho^2 - (x - x_c)^2}}{\rho^2}; \quad S_y = \frac{\sqrt{\rho^2 - (y - y_c)^2}}{\rho^2}. \qquad (104)$$

Here x_c, y_c are the coordinates of the projection center; $\rho^2 = f^2 + d^2$; d can be computed from $d^2 = (x - x_c)^2 + (y - y_c)^2$.

Trailing velocity of stars and meteors. On a plate taken with a stationary camera, the trailing velocity of stars (in mm/sec) is

$$v_s = \frac{2\pi}{T_s S_\phi} \cos \delta \qquad (105)$$

where T_s is the sidereal period of rotation of the earth (86164 seconds of mean time).

The trailing velocity of the meteor on the plate, $v_{mm} = dx/dt$, can be determined either by numerical differentiation, from the measured values of x, or from the following formula:

$$v_{mm} = \frac{V_t (x_{At} - x_{AR})^2}{K_A (x_{Ae} - x_{AR})} \left(1 - \frac{d}{dx_A} \Delta x_A\right). \qquad (106)$$

Here the subscript A indicates the plate taken at Station A; with changed subscript, of course, it can be used for Station B. V_t is the instantaneous velocity of the meteor and x_{At}, x_{Ae}, x_{AR} and K_A have the same meaning as in equation (34). Δx_A is read off the field-correction curve in function of x_A; the last factor, which was introduced to account for field distortions, is always very close to 1 and may be disregarded in ordinary cases.

Reciprocity-law failure. If a given star region is successively photographed by a driven camera with different exposure times t_1 and t_2, and the photographic images on the two plates are intercompared for brightness, we find that there is a constant difference between the two sets of

star images, corresponding to a magnitude difference,

$$m_2-m_1=-2.5\log\frac{t_2}{t_1}+f(t_1,t_2), \qquad (107)$$

where $f(t_1, t_2)$ is a term arising from reciprocity-law failure (Mees, 1942). If the reciprocity-law curve, plotted with log I (intensity) as abscissa and log (It) as ordinate, is nearly a straight line in the interval between t_1 and t_2, equation (107) can be written in the form

$$m_2-m_1=-(2.5+F_R)\log\frac{t_2}{t_1}. \qquad (108)$$

In fast emulsions F_R is usually quite large (+0.3 to +0.9) for exposures ranging from 1 minute to a few hours; for short exposures (<1 second) F_R may range from 0.0 to −0.2, according to the type of emulsion. For the Kodak X-Ray emulsion, F_R is nearly zero in the short-exposure branch.

Absolute magnitudes. It is convenient to reduce the apparent (observed) meteor magnitudes to a standard distance of 100 km. If the ranges R_i (i. e., R_{Ai} or R_{Bi}) are expressed in units of 100 km, the reduced, "absolute" magnitudes are, clearly:

$$M_i=m_i-5\log R_i \qquad (109)$$

Photometry on small-camera plates. The brightness of meteors is measured, emulsion against emulsion, with free-trailed star images on comparison plates taken with the same instrument as the driven meteor plate (Jacchia, 1949).

The comparison plates are all taken without rotating shutter and are centered on the equator, in a region rich in bright stars (first choice: Orion; second choice: Aquila); the most suitable exposure seems to be one that gives star trails half millimeter in length. It is useful to take plates with different focal settings, and to have out-of-focus images to compare with fuzzy-looking meteors; also, it is convenient to take several plates of each type, so that plates whose emulsions have been damaged by use can be replaced when necessary. Two standard, driven plates must be taken with rotating shutter, one before and one after the series of comparison plates; the center must be the same as that of all the comparison plates and the exposure equal to that of standard meteor plates. To avoid complications arising from extinction, the whole series of plates must be so timed that its center roughly coincides with the culmination of the selected region. The series can be considered to be acceptable if no difference in brightness can be noticed between the two extreme plates.

Photographic magnitudes in the standard region can be taken from the Henry Draper Catalogue when the following rules are observed:

(1) Take only the stars whose magnitudes are given to two decimal places (the others are simply reduced B. D. magnitudes, too unreliable for our purpose).

(2) Select only stars of spectral types from B5 to F5, for which the color index is reliable, because the photographic magnitudes in the Draper catalog are really visual magnitudes reduced to photographic magnitudes with standard color indices.

When the meteor trail is compared with the comparison star trails, we obtain fictitious magnitudes m_1', which must be corrected for the different trailing velocities of the stars and the meteor on the plate. The correction, according to equation (108) is

$$f(v_{mm})=-(2.5+F_R)\log\frac{v_{mm}}{v_s}. \qquad (110)$$

The effective exposure time for star trails is of the order of 1^s and that for meteor trails of the order of 10^{-3} to 10^{-4} seconds.

Due to the progressive dimming of images with increasing distance r from the center of the plate, a distance correction $f(r)$ must be applied to the observed meteor magnitudes to reduce them to the plate center, where the standard comparison stars are located. This correction must be determined separately for each camera and for each focal setting. A simple way to determine $f(r)$ is to compare the trails on two plates of the same series, on the north-south line through the center, in the northern half of the plate. It is easy to see from equation (105) that on the north-south line v_s is the same for all stars if the plate center is at $\delta=0$; by taking the northern half, which is close to the zenith, extinction problems are

minimized. It appears that $f(r)$ is larger for fainter stars than for brighter stars. The limited number of bright stars available on the plate makes it impossible, however, to determine separate curves of $f(r)$ for different classes of star brightness. A good approximation can be obtained by determining $f(r)$ for stars 1 to 2 magnitudes brighter than the plate limit, and assuming for brighter trails the correction can be expressed as $f(I)f(r)$, where $f(I)$ is a factor dependent on brightness alone, which can be determined by using a few brighter stars.

If we compare stars at the center of the meteor plate with stars of the standard region at the center of the driven comparison plates, we shall find a constant difference between the estimated magnitudes m_e and the catalog magnitudes m_c. When allowance is made for the difference in the exposure times of the meteor plate (t_m) and of the comparison plate (t_o), we obtain a corrected difference,

$$T=m_c-m_e-2.5\log\frac{t_m}{t_o}, \qquad (111)$$

which may be due to any combination of the following factors:

1. Difference in sky transparency.
2. Difference in differential extinction.
3. Difference in the sensitivity of the emulsion.
4. Difference in the development.
5. Clouds on the meteor plate (it is assumed that the comparison plates were taken on a clear night).

The first four factors affect the meteor and the background stars equally; but the fifth does not. Therefore, it is safe to apply the correction to the meteor magnitudes only when there is absolute certainty that no clouds were on the central region during the whole exposure. Otherwise, it is better to ignore the correction and take the risk of introducing an error of a few tenths of a magnitude in the reduction.

To summarize: absolute magnitudes M_i are obtained from "observed" magnitudes m_i' by the equation

$$M_i=m_i'-(2.5+F_R)\log\frac{v_{mm}}{v_s}+f(r)+T-5\log R. \qquad (112)$$

Photometry on Super-Schmidt films. The brightness of meteors photographed with Super-Schmidt cameras is estimated on the original films with the help of free-trailed star images on comparison films. Since the rotating shutter has openings totalling only a quarter of the circumference, the meteor trail is reduced to a succession of widely separated dashes. In most cases these dashes appear diffuse due to the difference in focus between stars and meteor. To avoid systematic errors, it is necessary to compare these dashes with star trails of equal length and equal degree of diffuseness. To this end, comparison films are taken (with stationary cameras without shutter) at various focal settings and with different exposures. Specifically, four focal settings were used in the Harvard Meteor Project and at each focal setting four films taken, with exposures of 3^s, 6^s, 12^s, and 24^s, respectively—a total of 16 films for each camera (actually, the whole series was taken in triplicate, to supply a reserve for replacements).

To enable a direct comparison, emulsion against emulsion, with the meteor films, the comparison films are turned inside out, so that the emulsion is placed on the concave side; the operation can be done with a sharp rap of the hand without injuring the film. As a support for the films, we find that the hemispherical surface of an opalescent glass globe for overhead lighting, with a strong light source inside, provides an almost ideal device. The globes which are available have a radius of 7 inches, one inch less than the radius of curvature of the films, but the difference is well within the tolerable limit. It is actually better to use supporting globes a little more curved than the films; if the curvature is only a small fraction of an inch less than that of the films, these cannot be brought in contact with the supporting surface and the gadget becomes useless.

Stars in Harvard Standard Regions at declination $+15°$ are used for comparison with meteor trails. All comparison films are centered on the celestial equator, so that the center of the standard region is always a little more than halfway from the film center to the edge. No appreciable magnitude correction in function of distance from the film center has been detected.

The trailing velocity of stars on the films, V_s', can be computed from equation (105) with

$S_\phi = 1/f$; the trailing velocity v'_{mm} of the meteor on the film can be obtained from v_{mm} as computed for the glass plate:

$$v'_{mm} = fS_x v_{mm}. \qquad (113)$$

Since compact, small cumulus clouds are frequently present in the New Mexico sky, we deem it safer to do away entirely with the intercomparison of stars on meteor films and driven standard films to determine the correction T. Since the standard exposure for Super-Schmidt films is only 12 minutes, the dimming effect of a passing cloud on field stars can be quite large.

Notation symbols

Sky and plate coordinates.

α, δ—The spherical equatorial coordinates right ascension and declination.
λ, μ, ν—Direction cosines referred to the equatorial astronomical system.
$\bar{\xi}$, $\bar{\eta}$—Standard rectangular coordinates with the origin at the optical plate center.
x, y—Measured rectilinear coordinates on photographic plate.
σ—Angular distance from optical plate center.

Single-letter subscripts:

s—Coordinates of stars.
c—Projection center of plate.
q—Center of rotating shutter.

Double-letter subscripts are used for points on the meteor trail, or related to the trail. The first letter is always A (for Station A) or B (for Station B). A list of second subscript letters follows:

i—A generic point on the trail, in particular any shutter break or segment.
b—Beginning of photographic trail.
e—End of photographic trail.
a—First measured break or segment.
o—Central break or segment.
j—Last measured break or segment.
f—A specific flare.
v—Point of minimum range.
p—Pole of trail, considered as a great circle.
R—Meteor radiant.

Points not on meteor:

ZA, ZB—Zenith at Station A or Station B.

Primes (α'; λ', μ' ν') are used for "relative" celestial coordinates on undriven plates.

Precessional direction cosines:

$$X_x,\ X_y,\ X_z$$
$$Y_x,\ Y_y,\ Y_z$$
$$Z_x,\ Z_y,\ Z_z$$

Rectangular coordinates in space.

$\mathbf{R}$—Range or distance vector, with origin at the observing station.
R—Modulus of $\mathbf{R}$.
ξ, η, ζ—Components of $\mathbf{R}$ in the astronomical equatorial system.

Double-letter subscripts are affixed to these symbols, and they have the same meaning as for sky and plate coordinates.

Additional symbols:

$\mathbf{R}_{AB}$ (ξ_{AB}, η_{AB}, ζ_{AB})—Vector from Station A to Station B.
$\mathbf{R}_{BA}$ (ξ_{BA}, η_{BA}, ζ_{BA})—Vector from Station B to Station A ($=-\mathbf{R}_{AB}$).
$\mathbf{R}_{ABo}$ (ξ_{ABo}, η_{ABo}, ζ_{ABo})—Vector from Station A to Station B at sidereal time $\theta_A = 0$.
$\mathbf{R}_{BAo}$ (ξ_{BAo}, η_{BAo}, ζ_{BAo})—Vector from Station B to Station A at sidereal time $\theta_B = 0$.
R_A, R_B—The single subscripts stand for the distance of the station (A or B) from the center of the earth.
$X_\odot$, $Y_\odot$, $Z_\odot$—Geocentric coordinates of the sun in the astronomical equatorial system (in a. u.).
X, Y, Z—Heliocentric coordinates of the meteor in the astronomical equatorial system (in a. u.).
r_T—Radius vector of the earth in its orbit.
r—Radius vector of the meteor in its orbit.

References

BANACHIEWICZ, T.
1925. Cracow Obs. Circ. No. 17.
1929. Acta Astron., ser. C, vol. 1, p. 63.

BESSEL, W.
1839. Astron. Nachr., vol. 16, p. 323.

BOWER, E. C.
1932. Lick Obs. Bull., vol. 16, p. 34.

JACCHIA, L. G.
1949. Harvard Coll. Obs. and M. I. T. Tech. Rep. No. 3. (Harvard Obs. Repr., ser. 2, No. 31.)

MEES, C. E. K.
1942. The theory of photographic process. Macmillan & Co. (Especially pp. 236–250.)

MILLMAN, P. M., and HOFFLEIT, D.
1936. Ann. Harvard Obs., vol. 105, p. 601.

OLMSTED, M.
1931. Ann. Harvard Obs., vol. 87, p. 221.

SCHAEBERLE, J. M.
1895. Contr. Lick Obs., No. 5, p. 31.

TURNER, H. H.
1907. Monthly Notices Roy. Astron. Soc. London, vol. 67, p. 562.

WHIPPLE, F. L.
1938. Proc. Amer. Philos. Soc., vol. 79, p. 499.

The Method of Reduction of Short-Trail Meteors[1]

By Gerald S. Hawkins [2]

The preceding paper gives a comprehensive account of the reduction of photographic meteor trails and indicates that a great deal of time is spent in evaluating the distortions of the plate, the deceleration of the meteoroid, and the vibrations of the camera and shutter. These three stages of the analysis require a critical assessment by the computer and cannot be handled by existing machines. In the case of short trails, however (angular length $<5°$ on Super-Schmidt plates), distortion, deceleration, and vibration are usually below the limits of measurement, and we may use a simplified method of reduction. This method embodies the minimum requirements for the precise determination of the radiant point, height, and velocity of a meteor when photographed at two separate stations. It is assumed that the cameras are driven to follow the diurnal motion of the sky and that one at least is equipped with an occulting shutter.

Methods of measurements

Plate marking and selection of comparison stars. This method presumes that we are dealing with flat plates which approximate to a gnomonic projection of the sky (loc. cit. Whipple and Jacchia, p. 183).[3] Four stars are selected for comparison purposes and marked on the glass side of a plate. They are labeled 1, 2, 3, and 4 in the direction of motion of the meteor, which is usually given by a visual observation. The direction may also be found by placing the star field of one plate on top of the other and noting the apparent intersection point or radiant of the meteor trails. Two of the stars are used subsequently for determining the plate constants and two are used as checks. The stars are identified in the B. D. catalog and marked together with the meteor trail on B. D. charts (loc. cit., p. 184). Accurate star positions are found from the Yale and A. G. catalogs. In selecting stars for short trail reductions, we should observe certain criteria to obtain the utmost accuracy. These criteria are based on experience with Super-Schmidt plates and a measuring engine which can be read to ± 0.0001 cm.

1. Star positions must be available which are accurate to $0''.5$ of arc.

2. The diameter of the star image should not be greater than $120''$, or 0.012 cm on Super-Schmidt plates.

The above standards severely limit the choice of star images; the Yale and A. G. catalogs do not, in general, give positions for stars fainter than a visual magnitude of 9.2, and stars brighter than magnitude 7.5 produce large

[1] Carried out in part under research contract with the Massachusetts Institute of Technology, Lincoln Laboratory, Contract No. AF19(122)-458, Subcontract No. 57. Reproduction in whole or in part is permitted for any purposes of the U. S. Government.

[2] Harvard College Observatory, Cambridge, Mass.

[3] All references given thus (loc. cit.) refer to the previous paper by F. L. Whipple and L. G. Jacchia on "Reduction Methods For Photographic Meteor Trails."

images. In the ideal case the stars must be close to 9th magnitude visual.

3. The stars should be equally spaced along the trail with not more than 5° between the end stars. They should be not more than ½° from the great circle path of the meteor.

4. Any two of the stars may be chosen for the determination of plate constants, but it is advisable to use a pair with good images which are from 1° to 3° apart and on the same side of the trail.

5. A single star image that is recorded as a double star in the catalogs should be avoided if the separation of the components is greater than 1'.0.

Measurement of the projection center of the plate. In the process of copying Super-Schmidt negatives onto flat plates, the projection center is marked automatically by a white circle. Normally there is sufficient overlap between a pair of plates so that the star fields can be superimposed in the region of the projection centers, and the position of the center can be read from a star chart. An accuracy of ±0°.1 is sufficient and readily obtained.

Measurement of comparison stars and trail. The plate is set, emulsion down, on the machine with the trail parallel to the x axis to within ±20 microns and with x values increasing in the direction of motion of the meteor. Standard precautions, as given in the previous paper (loc. cit., p. 185), are taken in using the machine. In the short trail method it is found expedient to take only one series of measurements, because there are checks at the end of the computing that will detect gross errors such as misreading a vernier or misidentifying a star. Measurements in rectangular coordinates x and y on the plate should be recorded to the nearest micron.

Marked stars: Three readings of x and three readings of y are taken from the center of the star images.

Trail: To obtain a linear equation relating x and y, 10 points on the trail are selected at approximately equal intervals of x. The value of x is measured to the nearest tenth of a mm and three values of y are observed at each point and recorded to within ±0.0001 cm.

Segments of the trail: With an occulting or rotating shutter the meteor trail is divided into bright sigments. With a double-bladed shutter, rotating at 1800 rpm, the segments are short and the vertical crosswire may be set accurately at the midpoint of a segment. Three values of x are obtained for b and e, the first and last segments visible on the plate. These give the beginning and end heights of the trail. (The center and not the end of the dash is measured in these cases, to give additional values of velocity if they should be required. The consequent errors in heights of the beginning and end of the trail are negligible.) The segments are numbered consecutively along the trail with dash b designated zero. Three dashes, a, o, and j, are now selected along the trail, and three values of x are observed for each, with the crosswire set at the center of the dash. It is essential to take great care in selecting a, o, and j as the accuracy of the method depends to a great extent on the quality of the image. Asymmetrical dashes whose image is distorted, for example by a background star, should be avoided. The good quality dashes are selected to make the separation between a–o, and o–j as large as possible. One x value is taken for point f, the point of maximum light. If more than one maximum is present, f refers to the brightest maximum.

To check that the plate has not been disturbed during the series of readings, the x and y values of the first star are measured again.

Finally, one reading is taken of the x and y values of the projection center. The accuracy required in this reading is ±0.01 cm.

Measurement of the magnitude of the meteor and the limiting magnitude of the plate. Photometric estimates are made following the general procedure of the Harvard Meteor Project (loc. cit., p. 205). The brightest segment of the meteor trail is compared with trailed star images which are approximately equal in length to the segment. For this comparison the original Super-Schmidt film is used with the emulsions in contact. The maximum magnitude of the meteor, M_{max}, and the faintest magnitude visible on the comparison plate, M_{lim}, are estimated to ±0.1 mag.

Equations used in the computations

The computing program for short trails is a simplified and abbreviated version of the full treatment described by Whipple and Jacchia (loc. cit.); their notation is used in the equations given here, where possible; new symbols

are listed at the end of this paper. In addition, methods are given for estimating the errors of the observations. Formulae for checking the computing are given in the previous paper.

Reductions are carried out in equatorial rectangular coordinates with the λ axis pointing towards the vernal equinox (R.A. 0^h, Dec. 0°), μ axis pointing towards R.A. 6^h, Dec. 0°, and ν axis pointing towards the north celestial pole.

All measurements are made in "trail coordinates" (x, y), with the x axis along the trail and x increasing in the direction of motion of the meteor. The first stage of the computing is to determine the plate constants which enable one to convert the measured values (x, y) into equatorial direction cosines (λ, μ, ν).

Equatorial coordinates. The direction cosines of a point with R.A.$=\alpha$, Dec.$=\delta$ are given by the formulae,

$$\left.\begin{aligned}\lambda_{T_0}&=\cos\delta\cos\alpha\\ \mu_{T_0}&=\cos\delta\sin\alpha\\ \nu_{T_0}&=\sin\delta.\end{aligned}\right\} \tag{1}$$

In the case of stars a correction has to be made to α and δ for proper motion (loc. cit., p. 185). The direction cosines are computed for the four comparison stars and for the projection centers of each plate. These values apply to the equinox, T_0, of the catalog or chart from which α and δ were obtained.

To convert equatorial direction cosines to R. A. and Dec.,

$$\left.\begin{aligned}\sin\delta&=\nu\\ \tan\alpha&=\frac{\mu}{\lambda}\end{aligned}\right\} \tag{2}$$

where $\sin\alpha$ has the same sign as μ, $\cos\alpha$ has the same sign as λ.

Precession. To convert direction cosines from equinox T_0 to the equinox of the meteor T,

$$\lambda_T=X_x\lambda_{T_0}+X_y\mu_{T_0}+X_z\nu_{T_0}. \tag{3}$$

$$\mu_T=Y_x\lambda_{T_0}+Y_y\mu_{T_0}+Y_z\nu_{T_0}. \tag{4}$$

$$\nu_T=Z_x\lambda_{T_0}+Z_y\mu_{T_0}+Z_z\nu_{T_0}. \tag{5}$$

The values of X_x, X_y, X_z may be found by the Cracovian calculation (loc. cit., p. 186). Values of $(\lambda_T, \mu_T, \nu_T)$ are computed for the projection center and comparison stars of each plate. The equinox T is taken as the beginning of the year which is nearest in time to the date of the meteor.

Standard plate coordinates. The standard plate has the same projection center as the measured plate, but is tangential to a unit sphere. These coordinates are a rectangular, linear system $(\bar\xi, \bar\eta)$ with origin at the projection center and the $\bar\eta$ axis directed northward along a meridian of R. A. The direction cosines of the $\bar\xi$ axis are

$$\left.\begin{aligned}\lambda=p_c&=-\sin\alpha_c\left(=-\frac{\mu_c}{n_c}\right)\\ \mu=q_c&=\cos\alpha_c\left(=\frac{\lambda_c}{n_c}\right)\\ \nu=r_c&=0\end{aligned}\right\} \tag{6}$$

and the direction cosines of the $\bar\eta$ axis are

$$\left.\begin{aligned}\lambda=l_c&=-\sin\delta_c\cos\alpha_c\left(=-\frac{\lambda_c\nu_c}{n_c}\right)\\ \mu=m_c&=-\sin\delta_c\sin\alpha_c\left(=-\frac{\nu_c\mu_c}{n_c}\right)\\ \nu=n_c&=\cos\delta_c\left(=\sqrt{1-\nu_c^2}\right)\end{aligned}\right\} \tag{7}$$

where the subscript c refers to the projection center. These components are computed for both plates. To convert equatorial direction cosines (λ, μ, ν) to standard plate coordinates $(\bar\xi, \bar\eta)$, we may use the equations,

$$\left.\begin{aligned}\bar\xi\cos\sigma&=(\lambda p_c+\mu q_c)\\ \bar\eta\cos\sigma&=(\lambda l_c+\mu m_c+\nu n_c)\end{aligned}\right\} \tag{8}$$

where

$$\cos\sigma=\lambda\lambda_c+\mu\mu_c+\nu\nu_c. \tag{9}$$

To convert standard plate coordinates $(\bar\xi, \bar\eta)$ to equatorial direction cosines (λ, μ, ν), we may use the equations

$$\left.\begin{aligned}\lambda&=(\lambda_c+l_c\bar\eta+p_c\bar\xi)\cos\sigma\\ \mu&=(\mu_c+m_c\bar\eta+q_c\bar\xi)\cos\sigma\\ \nu&=(\nu_c+n_c\bar\eta)\cos\sigma\end{aligned}\right\} \tag{10}$$

where

$$\sec\sigma=+\sqrt{1+\bar\xi^2+\bar\eta^2}. \tag{11}$$

Equations (6)–(11) may be applied to both plates.

Relations between plate and trail coordinates. To convert standard plate coordinates $(\bar{\xi}, \bar{\eta})$ to trail coordinates (x, y) we assume that

$$\left.\begin{aligned} x&=a\bar{\xi}+b\bar{\eta}+c \\ y&=b\bar{\xi}-a\bar{\eta}+d. \end{aligned}\right\} \tag{12}$$

The coefficients a, b, c, and d are called the plate constants.

To convert trail coordinates (x, y) to plate coordinates $(\bar{\xi}, \bar{\eta})$ we use the inverse equations,

$$\left.\begin{aligned} \bar{\xi}&=Ax+By+C \\ \bar{\eta}&=Bx-Ay+D. \end{aligned}\right\} \tag{13}$$

The coefficients A, B, C, and D are called the inverse plate constants.

Determination of plate constants. If the plate constant stars are designated 1 and 2 we have measured values (x_1, y_1), (x_2, y_2), and computed plate coordinates $(\bar{\xi}_1, \bar{\eta}_1)$, $(\bar{\xi}_2, \bar{\eta}_2)$.

Hence

$$a=\frac{(\bar{\xi}_2-\bar{\xi}_1)(x_2-x_1)-(\bar{\eta}_2-\bar{\eta}_1)(y_2-y_1)}{(\bar{\xi}_2-\bar{\xi}_1)^2+(\bar{\eta}_2-\bar{\eta}_1)^2}, \tag{14}$$

$$b=\frac{(\bar{\eta}_2-\bar{\eta}_1)(x_2-x_1)+(\bar{\xi}_2-\bar{\xi}_1)(y_2-y_1)}{(\bar{\xi}_2-\bar{\xi}_1)^2+(\bar{\eta}_2-\bar{\eta}_1)^2}, \tag{15}$$

$$c=x_1-a\bar{\xi}_1-b\bar{\eta}_1, \tag{16}$$

$$d=y_1-b\bar{\xi}_1+a\bar{\eta}_1. \tag{17}$$

As a rough check, c and d should agree with the measured x and y values of the projection center. The inverse plate constants are given by the expressions

$$\left.\begin{aligned} A&=\frac{a}{a^2+b^2}, & C&=-\frac{ac+bd}{a^2+b^2} \\ B&=\frac{b}{a^2+b^2}, & D&=\frac{ad-bc}{a^2+b^2}. \end{aligned}\right\} \tag{18}$$

Eight constants are computed for each plate. To check the distortions of the plate, (x, y) is computed for stars 3 and 4 from equation (12) and the residuals $(\Delta x, \Delta y)$ in the sense "computed minus observed" are found. These should be of the order of the error of measurement.

Determination of the pole of the trail. The equation

$$y=a'+b'x \tag{19}$$

represents the best straight line which may be drawn through the 10 measured points on the meteor trail. Values of y for the beginning, b, and end, e, of the trail are obtained by inserting the observed x values in equation (19). Equatorial direction cosines are then computed from equations (12), (11), and (10). For the pole of the trail we may write

$$\left.\begin{aligned} \lambda_{Ap} \sin 1_A&=\Sigma_{A1} \\ \mu_{Ap} \sin 1_A&=\Sigma_{A2} \\ \nu_{Ap} \sin 1_A&=\Sigma_{A3} \end{aligned}\right\} \tag{20}$$

where

$$\left.\begin{aligned} \Sigma_{A1}&=\mu_{Ab}\nu_{Ae}-\nu_{Ab}\mu_{Ae} \\ \Sigma_{A2}&=\nu_{Ab}\lambda_{Ae}-\lambda_{Ab}\nu_{Ae} \\ \Sigma_{A3}&=\lambda_{Ab}\mu_{Ae}-\mu_{Ab}\lambda_{Ae} \\ \sin^2 1_A&=\Sigma_{A1}^2+\Sigma_{A2}^2+\Sigma_{A3}^2 \end{aligned}\right\} \tag{21}$$

and similarly for trail B.

Determination of the radiant point. The direction cosines of the radiant point are given by the formulae

$$\left.\begin{aligned} \lambda_R \sin Q&=\Sigma_4 \\ \mu_R \sin Q&=\Sigma_5 \\ \nu_R \sin Q&=\Sigma_6 \end{aligned}\right\} \tag{22}$$

where

$$\left.\begin{aligned} \Sigma_4&=\mu_{Ap}\nu_{Bp}-\nu_{Ap}\mu_{Bp} \\ \Sigma_5&=\nu_{Ap}\lambda_{Bp}-\lambda_{Ap}\nu_{Bp} \\ \Sigma_6&=\lambda_{Ap}\mu_{Bp}-\mu_{Ap}\lambda_{Bp} \\ \sin^2 Q&=\Sigma_4^2+\Sigma_5^2+\Sigma_6^2. \end{aligned}\right\} \tag{23}$$

The sign of Q is chosen to orient the radiant above the horizon, and λ_R μ_R, and ν_R are computed for the equinox T and for the equinox of 1950. For later computation we require the quantities $\cos \sigma_R$, x_R, and y_R for both plates. These may be found from equations (9) and (12). We also require E_A and E_B, the elonga-

tions of the trails from the radiant. The elongation is given by the expression

$$\cos E_A=\lambda_R\lambda_{Ao}+\mu_R\mu_{Ao}+\nu_R\nu_{Ao} \qquad (24)$$

where the direction cosines of the approximate center of the trail, o, are found in the manner described for points b and e in section 6.

The third stage is to compute the space trajectory of the meteor.

Hour angle, or sidereal time at the apperance of the meteor. The sidereal time for the instant of the meteor is computed as follows:

$$\left.\begin{aligned}\theta_A&=\theta_o+(\text{U. T.})-L_A+\Delta\theta\\ \theta_B&=\theta_o+(\text{U. T.})-L_B+\Delta\theta\end{aligned}\right\} \qquad (25)$$

where θ_o is the sidereal time at Greenwich for 0^h U. T. on the night of occurrence of the meteor. U. T., the instant of appearance in universal time, is given for New Mexico by the expression

$$\text{U. T.}=\text{Mountain Standard Time}+7^h. \qquad (26)$$

The correction $\Delta\theta$ is given by the expression

$$\Delta\theta^s=236.555\left(\frac{\text{U. T.}^h}{24^h}\right). \qquad (27)$$

The longitudes L_A, L_B of the Harvard stations are

$$\left.\begin{aligned}&\text{Doña Ana: } L_A=7^h7^m11^s.9\\ &\text{Soledad: } L_B=7^h6^m26^s.8.\end{aligned}\right\} \qquad (28)$$

Space vector. The equatorial direction cosines of the vector from Station A to Station B at the instant of the meteor are given by the formulae

$$\left.\begin{aligned}\lambda_{AB}R_{AB}&=\xi_{AB}=\xi_{ABo}\cos\theta_A-\eta_{ABo}\sin\theta_A\\ \mu_{AB}R_{AB}&=\eta_{AB}=\eta_{ABo}\cos\theta_A+\xi_{ABo}\sin\theta_A\\ \nu_{AB}R_{AB}&=\zeta_{AB}=\zeta_{ABo}.\end{aligned}\right\} \qquad (29)$$

The components of the vector from B to A are

$$\left.\begin{aligned}\lambda_{BA}R_{AB}&=\xi_{BA}=\xi_{BAo}\cos\theta_B-\eta_{BAo}\sin\theta_B\\ \mu_{BA}R_{AB}&=\eta_{BA}=\eta_{BAo}\cos\theta_B+\xi_{BAo}\sin\theta_B\\ \nu_{BA}R_{AB}&=\zeta_{BA}=\zeta_{BAo}.\end{aligned}\right\} \qquad (30)$$

The quantities with subscripts *ABo*, *BAo* refer to the components at sidereal time 0^h at Stations A and B, respectively. They are given by equation (16) (loc. cit., p. 189) and for Soledad and Doña Ana are, in units of 100 kms, as follows,

$$\left.\begin{aligned}\xi_{ABo}&=0.12128228 & \xi_{BAo}&=-0.12186172\\ \eta_{ABo}&=0.17695427 & \eta_{BAo}&=-0.17655574\\ \zeta_{ABo}&=-0.188639 & \zeta_{BAo}&=0.188639.\end{aligned}\right\} \qquad (31)$$

Components of the space vector are computed from equations (29) and (30). As a check it may be noted that $\xi_{AB}=-\xi_{BA}$ and $\eta_{AB}=-\eta_{BA}$.

Direction of zenith. The direction of the zenith in equatorial direction cosines is given by the formulae

$$\left.\begin{aligned}\lambda_{ZA}&=\cos\phi_A\cos\theta_A\\ \mu_{ZA}&=\cos\phi_A\sin\theta_A\\ \nu_{ZA}&=\sin\phi_A.\end{aligned}\right\} \qquad (32)$$

Similar formulae give λ_{ZB}, μ_{ZB}, ν_{ZB}, and the directions of both zeniths are calculated.

$$\left.\begin{aligned}&\text{Doña Ana:}\\ &\qquad\cos\phi_A=0.8433343\\ &\qquad\sin\phi_A=0.5373893\\ &\text{Soledad:}\\ &\qquad\cos\phi_B=0.8452266\\ &\qquad\sin\phi_B=0.5344081\end{aligned}\right\} \qquad (33)$$

Range. The range R_{Ai}, in units of 100 km, from Station A to a point i on the trail is given by the expression

$$R_{Ai}=\frac{\xi_{AB}\lambda_{Bi}+\eta_{AB}\mu_{Bi}+\zeta_{AB}\nu_{Bi}}{\lambda_{Ai}\lambda_{Bi}+\mu_{Ai}\mu_{Bi}+\nu_{Ai}\nu_{Bi}}. \qquad (34)$$

Range is calculated for points b, a, o, j, f, and e on trail A. Ranges between Station B and points on trail B are also computed.

Heights. The heights of points A_i, B_i, above the sea level surface of the earth are given by equation (28) of Whipple and Jacchia (loc. cit.). For Doña Ana and Soledad

$$\left.\begin{aligned}H_{Ai}&=h_{Ai}+1.4123+0.7869\left[R_{Ai}^2-\left(\frac{h_{Ai}}{100}\right)^2\right]\\ H_{Bi}&=h_{Bi}+1.5674+0.7869\left[R_{Bi}^2-\left(\frac{h_{Bi}}{100}\right)^2\right]\end{aligned}\right\} \qquad (35)$$

where

$$h_{Ai}=100\,R_{Ai}(\lambda_{ZA}\lambda_{Ai}+\mu_{ZA}\mu_{Ai}+\nu_{ZA}\nu_{Ai}). \qquad (36)$$

A similar equation holds for h_{Bi}. H_{Ai} and H_{Bi} are computed for segments b, f, and e. As a check, heights other than h_{Ab} may be computed from the equation

$$h_{Ai}=h_{Ab}-100\,R_{Ab}\frac{\cos\sigma_{Ab}}{\cos\sigma_{AR}}\frac{(x-x_{Ab})}{(x-x_{AR})}\cos Z_{AR}. \quad (37)$$

A similar equation holds for h_{Bi}. The value of $\cos\sigma_{Ab}$ may be found from equations (11) and (13). Values of h_{Ai} and h_{Bi} are computed for points b, a, o, j, e, and f from equations (36) and (37). Agreement between the values of h found from the two methods shows that there are no errors in the computation of heights and ranges.

Time at segment No. n_i. In the case of Super-Schmidt cameras, a double-bladed shutter rotates in the focal plane about an axis which is aligned with the center of projection of the plate, and the time lapse between dash b and dash n_i is given by the expression

$$t_{Ai}=\frac{30\,n_{Ai}}{|\text{R.P.M.}|}+\frac{30}{(\text{R.P.M.})\pi}(\omega_{Ai}-\omega_{Ab}) \quad (38)$$

where the number of revolutions of the shutter per minute are given first as a modulus and secondly with a sign + or −. If the shutter appears to rotate in a clockwise direction over the sky, the + sign is taken and vice versa. The angle ω is measured clockwise in the sky and is given by the equation,

$$\omega_{Ai}=\tan^{-1}\frac{(x_{Ai}-c_A)}{(a'_A-d_A)}. \quad (39)$$

Similar relations hold for the times on plate B. Values of t_{Ai} and t_{Bi} are computed for a, o, and j.

Velocity of the meteor. The velocity of the meteor determined from segments d_A and o_A is V_{A1}; and the velocity from o_A and j_A is V_{A2}. Equation (35) of Whipple and Jacchia (loc. cit.) gives

$$V_{A1}=\frac{100R_{Ab}}{(t_o-t_a)}\frac{\cos\sigma_{Ab}}{\cos\sigma_{AR}}\left[\frac{(x_{Ao}-x_{Ab})}{(x_{Ao}-x_{AR})}-\frac{(x_{Aa}-x_{Ab})}{(x_{Aa}-x_{AR})}\right]. \quad (40)$$

A similar equation holds for V_{A2}, V_{B1}, V_{B2} and all four velocities are computed.

Correction for deceleration. In the case of a short trail it is usually not possible to measure the deceleration directly (loc. cit. p. 193). It is possible, however, to apply a correction for the drag of the atmosphere based on the measured decelerations from longer trails. We may write

$$V^2_{\infty A1}=V^2_{A1}-31.69\log_e\frac{m_{A1}}{m_{\infty A}}. \quad (41)$$

From the exact reduction of long trails we know that the ratio of the mass at any instant to the mass of the meteoroid outside the atmosphere is given to a good approximation by the assumption that the light curve is formed from two half parabolae joining at n_f. Then before the position of maximum light, when $n'\leq n_f$,

$$\frac{m_{A1}}{m_{\infty A}}=\frac{n_e-n_f}{n_e}+\frac{n_f}{n_e}\left[0.99814+0.09374\left(\frac{0.9598n'\sqrt{\Delta M}}{n_f}-2.2\right)^3\right] \quad (42)$$

and after the position of maximum light, when $n'\geq n_f$

$$\frac{m_{A1}}{m_{\infty A}}=\frac{n_e-n_f}{n_e}-\frac{n_e-n_f}{n_e}\left[0.99814+0.09374\left(\frac{0.9598n'\sqrt{\Delta M}}{n_f}-2.2\right)^3\right] \quad (43)$$

where n' is the difference between the position of maximum light and the mean dash number, hence

$$n'=n_f-\frac{n_u+n_o}{2} \quad (44)$$

and

$$\Delta M=M_{\text{llm}}-M_{\text{max}}. \quad (45)$$

Similar equations hold for $V_{\infty A2}$, $V_{\infty B1}$, $V_{\infty B2}$.

Absolute magnitude. The maximum photographic magnitude, reduced to a range of 100 km, is given for Super-Schmidt plates by the expression

$$M_{\text{pm}}=M_{\text{max}}-9.063-2.5\log_{10}\frac{(x_j-x_a)}{(n_j-n_a)}\left(\frac{R_f}{100}\right)^2-2.5\log_{10}fs_X. \quad (46)$$

Equation (104) of Whipple and Jacchia (loc. cit.) gives fs_X. The last term is a small correction which can be added to M_{max} at the time

the photometric comparison is made. It is a function of the position of the trail on the film, and for Super-Schmidt films with the center of projection at the shutter center, the correction has been tabulated below.

TABLE 1.—*Photometry correction for distance of trail in cms from center of film*

Correction $-2.5 \log_{10} f/x$	Trail parallel to radius	Trail at 45° to radius	Trail perpendicular to radius
	0.0	0.0	0.0
+0.0			
	4.4	5.1	6.2
+0.1			
	7.6	8.8	10.9
+0.2			
	9.9	——	——
+0.3			

In critical cases descend. The absolute visual magnitude is given by the expression

$$M = {}_{vis}M_{pm} + 1.8. \tag{47}$$

Mass of meteoroid. By assuming, as in the section on correction for deceleration (p. 212), that the light curve is a double parabola it can be shown that

$$m_{\infty A} = \left[\frac{1.847\, w}{60 \tau_0}\right] \frac{n_0 e^{-0.9210 M_{pm}}}{V_{A1}^3 \sqrt{\Delta M}} \text{ gms}, \tag{48}$$

where w is visible energy in ergs emitted by a meteor of zero magnitude and τ_0 is the luminous efficiency. In all previous work it has been assumed that the value of the term in brackets is 47.71. If τ_0 is subsequently revised the value of $m_{\infty A}$ must be scaled accordingly. A similar equation holds for $m_{\infty B}$.

The final stage of the computation for radiant and trajectory is to estimate the errors of the computed quantities. This is essential in short trail reductions since only a few measures are available and the accuracy depends on many variable factors.

Probable error in the radiant position. The error in position in radians is given by the expression

$$\delta E = \text{cosec } Q \sqrt{(\sin E_A\, \delta b'_A)^2 + (\sin E_B\, \delta b'_B)^2} \tag{49}$$

where $\delta b'_A$ and $\delta b'_B$ are the estimated errors in the angle of the trail. Usually the largest component of $\delta b'$ is due to plate distortions, and if 1 and 2 are the plate constant stars and 3 and 4 are the check stars, then $\delta b'$ is given by the approximate equation

$$\delta b' = \frac{|\Delta y_4 - \Delta y_3|}{\sqrt{(x_4 - x_3)^2 + (x_2 - x_1)^2}} \tag{50}$$

where Δy_4, Δy_3 are the residuals of the check stars as defined in the section on determination of plate constants (p. 210).

This equation applies to both trails with the appropriate change of values.

Probable error in velocity. The error in individual determinations of velocity is given by the expression

$$\left(\frac{\delta V_{A1}}{V_{A1}}\right)^2 = \left(\frac{\delta(x_0 - x_a)}{(x_0 - x_a)}\right)^2 + \Delta t^2 + (\cot E_A\, \delta E)^2 + \left(\frac{\delta R_A}{R_A}\right)^2 \tag{51}$$

where Δt is the estimated error due to vibration of the shutter. For the Harvard Super-Schmidt cameras, with the original motors and shafts,

$$\Delta t^2 = \frac{3.8 \times 10^{-4}}{(n_0 - n_a)^2} \sin^2\left(2\pi \frac{(n_0 - n_a)}{28}\right) \tag{52}$$

and

$$\frac{1}{R_A} \frac{\delta R_A}{\delta T} = \frac{0.02625\, [\mu_{Bp} \xi_{AB} - \lambda_{Bp} \eta_{AB}]}{\lambda_{Bp} \xi_{AB} + \mu_{Bp} \eta_{AB} + \nu_{Bp} \zeta_{AB}} \tag{53}$$

and δT is the estimated error in the time of appearance of the meteor in units of 6 minutes. In the measurements at Harvard the error in x measurements has been found to be $\delta(x_0 - x_a) = 5 \times 10^{-4}$ cm. Similar equations hold for

$$\frac{\delta V_{A2}}{V_{A2}}, \frac{\delta V_{B1}}{V_{B1}} \text{ and } \frac{\delta V_{B2}}{V_{B2}}.$$

Time of appearance by equalization of velocities. If the time of appearance is not known, but assumed to be at the midtime of the exposure, then the time of appearance is found by adding a correction term ΔT_V where

$$\Delta T_V = \frac{6(V_{\infty A} - V_{\infty B})}{\left(\frac{\delta R_B}{R_B} V_{\infty B} - \frac{\delta R_A}{R_A} V_{\infty A}\right)} \text{ minutes.} \tag{54}$$

The correction should not be applied if $V_{\infty A} - V_{\infty B}$ is less than the error in velocity

estimated from the first three terms of equation (51). It holds for exposure times that are less than 20 minutes from Doña Ana and Soledad stations.

Time of appearance by equalization of heights. The time of appearance may also be calculated by adding a correction ΔT_H to the assumed time. The correction is given by the expression

$$\Delta T_H \simeq \frac{6(H_{Af}-H_{Bf})}{\frac{\delta H_B}{\delta T}-\frac{\delta H_A}{\delta T}} \text{ minutes} \qquad (55)$$

where

$$\frac{\delta H_A}{\delta T} \simeq \frac{\delta h_A}{\delta T} = h_{Af}\frac{\delta R_A}{R_A \delta T} + 2.625\, R_{Af}(\mu_{Af}\lambda_{ZA}-\lambda_{Af}\mu_{ZA}) \qquad (56)$$

and the differential $\delta R_A/R_A\delta T$ is found from equation (53) by putting $\delta T=1$. The correction term ΔT_H should also be evaluated for points b and e on the trail and a mean value taken. However if it is suspected that one camera has not recorded the beginning or end portion of the trail, due to clouds and other causes, then the equalization of heights at that end of the trail should be ignored.

From a weighted mean value of ΔT_V and ΔT_H we may computed the correction to velocity and height. The correction to height is obtained from equation (56); the correction to velocity is obtained from the differential equation

$$\frac{1}{V}\frac{\delta V}{\delta T} = \frac{1}{R}\frac{\delta R}{\delta T}, \qquad (57)$$

Notation symbols additional to those of Whipple and Jacchia (loc. cit., p. 206)

T_o—Equinox of star position or R. A. and Dec. of projection center.

T—Equinox of meteor. This is taken as the beginning of the year nearest in time to the date of the appearance of the meteor.

V_{A1}—Velocity determined from points a, o on trail A.

V_{A2}—Velocity determined from points o, j on trail A.

U. T.—Universal or Greenwich Civil Time.

L_A—Geographical longitude of Station A.

t_{Ai}—Time in seconds for meteoroid to move from middle of segment b to middle of segment i on plate A

R. P. M.—Rotational speed of shutter in revolutions per minute.

$m_{\infty A}$—Mass of meteoroid outside atmosphere as measured on plate A.

m_{Ai}—Mass of meteoroid at any instant, i.

M_{max}—Photographic magnitude of a star which produces a trailed image on a stationary plate equal to the maximum intensity of the meteor trail.

M_{pm}—Photographic magnitude of a star which produces the same intensity as the meteor's maximum photographic intensity when the star is trailed at the angular velocity of the meteor. This magnitude is also corrected for the inverse square law to correspond to a standard range of 100 km.

M_{vis}—Visual magnitude corresponding to M_{pm}.

M_{lim}—The photographic magnitude of the faintest star visible on the comparison plate.

E_A—Angle in the sky between the radiant and point o on trail A.

δE—Probable error in position of radiant in units of circular measure.

$\delta b'_A$—Probable error in the gradient of the trail equation of plate A.

f—The point of maximum light on the trail.

n—The number of the trail segment with segment b numbered 0.

a'_A, b'_A—Constants in the linear equation chosen to represent the meteor trail on plate A.

A Rapid Graphical Method of Meteor Trail Reduction[1]

By Richard E. McCrosky[2]

Since February of 1952 when the Harvard Meteor Project initiated double-station operations with the Baker-Super-Schmidt cameras, more than 4,000 meteor pairs have been photographed. Both the magnitude and the quality of this recent photographic material have made it comparable with visual and radar observations as a basis for statistical analysis. However, a previous method of analysis described by Whipple and Jacchia (in the first paper of this series) is far too time-consuming to be considered practical as a routine reduction method for statistical data. A more rapid method was needed, and is presented here.

When the approximate reduction program was first considered, the criteria for a "satisfactory" method were rather vague. However, from the experience gained in the accurate reduction program one could be certain that data with errors of as little as 1 percent could not be obtained with a small expenditure of time. At the other extreme, one could question the value of statistics derived from data with mean errors as large as 10 to 15 percent. With these limitations on the accuracy, a search for a sufficiently rapid method was made. The general result of this attempt is a method, about to be described, that yields mean errors of about 5 percent and requires 30 minutes for the complete reduction of a meteor pair. The method can be best explained if we first derive the necessary equations, next discuss separately the methods of measurements, and finally, return to the equations and estimate the magnitude of errors due to various simplifying assumptions and to errors of measurement.

Meteor heights

The geometry of the problem can be seen in figure 1, where R_{AB} is the distance between stations A and B; R_A is the distance from Station A to some point on the meteor path C; and R_B is the distance from Station B to the same point in space. This point, on either meteor trail, will be referred to as a *common point* (C). The orientation in space of the triangle (A, B, C) is described by the declination (δ) and the hour angle (t) coordinates. (See figure 1). R_{AB}, δ_{AB} and t_{AB} are constants of the stations. The hour angle, t_{AB}, and declination, δ_{AB}, represent the direction of Station B as seen from Station A.

From the spherical triangle, (Pole, P_{AB}, P_i), we solve for γ_i, the angle between the direction to the meteor and the direction of the line joining the stations. The subscripts i and j may refer to either Station A or Station B.

$$\cos \gamma_i = \sin \delta_i \sin \delta_{AB} + \cos \delta_i \cos \delta_{AB} \cos (t_{AB} - t_i). \quad (1)$$

[1] This paper is based upon research supported by the U. S. Office of Naval Research, Contract N5ori-07647. Reproduction in whole or in part is permitted for any purposes of the U. S. Government.

[2] Harvard College Observatory.

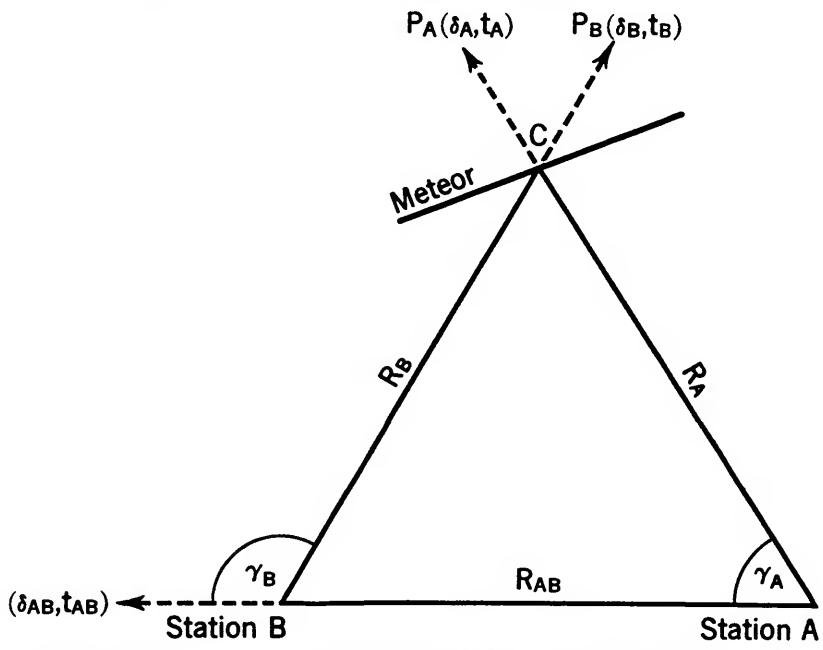

FIGURE 1.—Relationship of geometrical quantities used in determining meteor heights.

With γ determined, the values of the ranges R_A and R_B are found from the equation:

$$R_i = R_{AB} \frac{\sin \gamma_j}{\sin (\gamma_B - \gamma_A)}, \quad i \neq j. \tag{2}$$

The height of the common point above ground, if we assume a flat earth, is then:

$$h_i = R_i \cos Z_i, \tag{3}$$

where Z is the zenith distance of the common point and $\cos Z_i$ is given by the equation,

$$\cos Z_i = \sin \phi \sin \delta_i + \cos \phi \cos \delta_i \cos t_i, \tag{4}$$

where, for the latitude ϕ, we have used the average value of the two stations.

Clearly the same point in space can be described by only one height, and thus $h_A \equiv h_B$. This comparison gives the first check on the computations. The height above sea level, H, is found by assuming h to be measured from an elevation equal to the mean elevation of the two stations.

Solutions for equations (1) and (2) were prepared in graphical form in order to eliminate the tedious and time-consuming task of directly forming such solutions many thousands of times.

Since both γ_i and $\cos Z_i$ are functions of δ_i and t_i, a solution for coz Z was also prepared and superimposed on the graph for γ. These charts will not be reproduced here. They are applicable only to the data acquired at the Soledad Canyon and Doña Ana Stations of the Harvard Meteor Project, and therefore are not of general interest. Table 1 summarizes the information obtained from these graphs and from another to be discussed later.

TABLE 1.—*Graphs utilized in the approximate reductions*

Graph	Enter with—	Read	Accuracy
Ia	$\left\{\begin{matrix}-10° \leq \delta_i \leq 90° \\ -50° \leq t_i \leq 50°\end{matrix}\right\}$	γ_i	0°.1
Ib	{ Same }	$\cos Z_i$	0.01
II	$\left\{\begin{matrix}60° \leq \gamma_A \leq 135° \\ 60° \leq \gamma_B \leq 135°\end{matrix}\right\}$	R_A	1 km
III	{ Same }	R_B	1 km
IV	$\left\{\begin{matrix}.50 \leq E \leq 1.00 \\ 0° \leq \epsilon_{AB} \leq 20°\end{matrix}\right\}$	$\sin \epsilon_i$	.001

Velocities and radiants

The meteor trail is interrupted every 1/10 sec by one of the occulting sections of the rotating shutter. These breaks in the trail allow one to

measure the apparent angular velocity of the meteor at some point along its trajectory. This measure is referred to as the *apparent* angular velocity, since only the component normal to the line of sight is measured. In general, such measures are made on both photographs of the meteor at the position of the common points.

Figure 2 shows the relationships between the apparent angular velocity, ω'; the angular velocity, ω; and the radiant. We see that:

$$\omega_i=\frac{\omega_i'}{\sin \epsilon_i} \tag{5}$$

where ϵ_i is the angular distance from the radiant to the common point. The space velocity, V, is then given by the equation:

$$V_i=\frac{\omega_i' R_i}{\sin \epsilon_i} \tag{6}$$

where R_i is the range found in the solution for heights. As in the case of the heights, the velocities obtained from the two photographs should agree.

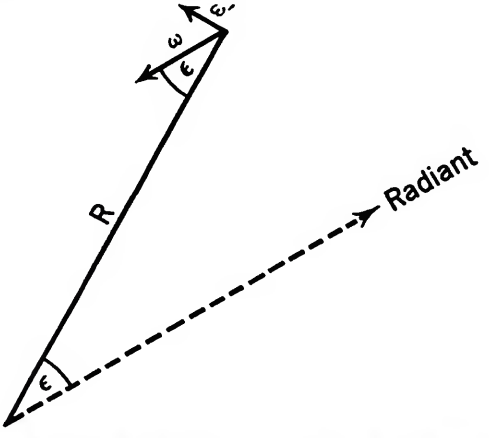

FIGURE 2.—Relationships of geometrical quantities used in determining meteor velocities.

For equation (6) to be applicable, we must have determined the position of the radiant. When the two meteor trails intersect at a small angle, Q, it is difficult to find an accurate radiant point. In such cases another approach to determine the velocity is desirable. From equation (6) we have:

$$V_A=V_B=\frac{\omega_A' R_A}{\sin \epsilon_A}=\frac{\omega_B' R_B}{\sin \epsilon_B} \tag{7}$$

or

$$\frac{\sin \epsilon_A}{\sin \epsilon_B}=\frac{\omega_A' R_A}{\omega_B' R_B}\equiv E, \text{ by definition.} \tag{8}$$

If the apparent angular velocity is measurable on both trails of a meteor pair, E may be computed. This gives one relationship between ϵ_A and ϵ_B. For meteors with a small Q, it is possible to measure $\epsilon_A-\epsilon_B$ (or $\epsilon_A+\epsilon_B$) with good accuracy. That this is true can be most easily seen by considering the extreme case of a meteor pair intersecting at $Q=0°$ (or $Q=180°$); i. e., both trails lie on the same great circle. Then the distance between the two common points will be exactly:

$$\epsilon_A-\epsilon_B=\epsilon_{AB} \text{ (or } \epsilon_A+\epsilon_B=\epsilon_{AB}\text{), by definition.} \tag{9}$$

The simultaneous equations (8) and (9) may be solved for sin ϵ_A and sin ϵ_B. This solution was prepared in graphical form. (See table 1, graph IV.) With these values of ϵ_i, V_i is found from (6). We have called velocities determined in such a fashion "indirect velocities," as distinct from the velocities obtained from meteors where a direct measure of the radiant is possible (direct velocities). It will be noted from equation (7) that we have forced the indirect velocities determined from each trail to agree. The comparison of these velocities offers a check on the computations.

The position of the radiant may be obtained by finding the intersection of two small circles, with radii of ϵ_A and ϵ_B with centers at P_A and P_B, respectively. In general such circles will intersect twice, but a quick inspection of the trails is sufficient to distinguish the spurious radiant point.

Reduction procedure

In this section we shall carry through the complete reduction of an imaginary meteor pair. Our purpose is not primarily to instruct in technique but to present, in logical sequence, the various difficulties and approximations that are present so that the reader may acquire a realization of the limitations of the method.

A separate computing form is used for each meteor. Certain data necessary for each meteor

are copied from the card catalog maintained for all Harvard meteors. These include:

(a) Meteor serial number for each trail.
(b) Camera designation (SS, ST, SK, SL) and plate number for each film.
(c) Region of the plate center, given by δ and α.
(d) Astronomical date of the exposure.
(e) Time of meteor occurrence, to 0.01 minute if the meteor was observed visually; or the mean time of the exposure if no visual observation was available.

The local sidereal time, in degrees, of the nearest midnight is obtained for the date. To this is added a correction to obtain the local sidereal time of the meteor instant.

The preceding section makes it clear that the entire method depends heavily on our ability to locate on each film a point on the meteor trails that represents the same point in space, the common points. If the meteor shows a burst or some other discontinuity in the light curve, a common point is obvious. However, the faint meteors, with which we are primarily concerned here, usually have smooth light curves. In these cases a more subtle technique is necessary. The number of dashes visible on each trail is counted and, if it is the same, we assume that dashes with the same ordinal number are common points.

Such an assumption fails in three minor respects. Firstly, the shutters are not synchronized; i. e., we do not know the orientation of one shutter with respect to the other at any given instant. Consequently the common point can be in error by as much as half the distance between dashes. Secondly, the focal plane shutter interrupts the same position of the *film* at constant time intervals. The rate at which the meteor is interrupted depends on its direction of motion and its apparent velocity on the film. In the extreme case of a meteor trail passing through the film center, an error of one dash can be made. But since the two trails of a meteor pair are usually similar in their direction of travel on the film, and since their apparent velocities on the film are small compared to the shutter velocity, the error will generally be only a small fraction of a dash. Thirdly, in assuming that breaks with the same ordinal number are common points, we assume that both cameras have photographed the meteor to the same limiting absolute magnitude or, alternatively, that the differential distance correction from the beginning to the end of the meteor is small or the same for both trails. Since most of our trails are short, the differential distance correction is small.

We can conclude that the common points chosen on trails showing the same number of breaks will be accurate to within one dash. However, the two cameras often do not record the same number of breaks for the following reasons:

1. The sensitivities of the cameras are not equal. With increasing experience in figuring the correcting plate, the manufacturer has been able to improve the quality of each succeeding camera. The effect is most noticeable when we compare trails obtained on the first (SS) and second (ST) Super-Schmidts.

2. The apparent magnitude of the meteor as seen from the two stations may differ by several tenths of a magnitude because of distance corrections. Effects 1 and 2 often compensate one another in part, since the earlier camera, at Soledad Station, is directed more nearly toward the zenith than is the mate camera at the Doña Ana Station.

3. The effective exposure time per dash is proportional to ω_i'. Thus, the trail nearer the radiant is photographed as a brighter image and the plate limit is reached at a fainter absolute magnitude.

Effects 1 and 2 combined are usually minor compared to effect 3. By noting the general shape of the meteor light curve of the brighter trail one can obtain an acceptable common point by estimating the number of dashes that failed to be recorded at the beginning and at the end of the fainter meteor trail. In only a very few cases does the combination of the factors of effective sensitivity of the camera, and the apparent velocity of the meteor, differ so much that no acceptable common point can be found. For each common point, we record under "Quality" an estimate of the number of dashes by which the common point may be in error. This never exceeds three for an acceptable meteor and rarely exceeds two.

To mark the common points, a small piece of Scotch tape is placed on the reverse side of the film at the location of the trail. Ink dots placed on this tape indicate the common point. For longer meteors (20 dashes or more) two common points are chosen in order to make a check on the entire reduction. The common point is recorded as the ordinal number of the dash, the dash nearest the radiant being

The transparent plotting globe. The declination scale pivots about the horizontal rod which passes through the globe at the celestial poles. The computer is positioning the curved rules to be coincident with the meteor image on each film. The juncture of the rulers (under the right hand) represents the meteor's radiant.

called "1." The duration of the meteor is measured in terms of the total number of visible dashes, N.

To measure the celestial coordinates of the common points and radiant, we utilize a transparent Plexiglass hemisphere of 8-inch radius, calibrated in hour angle and declination. The scale of these calibrations and the radius of the globe correspond to the scale and radius of the Super-Schmidt films. To read the coordinates of the common point, we need only to position the film properly on the globe. We accomplish this by choosing three or four bright stars which appear on one of the films, determining the declination and hour angle of these stars at the time of the meteor, and plotting these star positions on the globe. The film is then placed on the globe so that the star images and their plotted positions coincide. Since the regions of the two mate films overlap in an area of approximately one-quarter of the film, we can position the second film by superimposing stars in this region. The hour angle and declination of the common points are then read from the globe scales.

We determine the radiant and radiant distances, ϵ_A and ϵ_B, with the aid of a pair of curved rulers of 8-inch radius and 90° length, attached to one another by a hinge. They are calibrated in degrees, the pivot point of the hinge being zero degrees. When each rule lies parallel to one of the meteor trails, the zero point represents the radiant. The radiant distances are read from the rules and the coordinates of the radiant point are read from the hemisphere (see pl. 1). The cosine of the zenith distance of the radiant (cos Z_R) is determined from graph Ib of table 1.

The quantity Q is the angle of intersection of the two trails. An estimate of this quantity, accurate to about 10 per cent, is made when the radiant is found. The value of this angle is not used in the reductions but it serves as a measure of quality of the directly determined radiant.

The apparent angular velocity, or distance per break, is measured on the Harvard Coast and Geodetic measuring machine. This has been equipped with a section of an 8-inch radius Plexiglass sphere for the support of the film. The spherical section is large enough to permit all measurements to be made with the optical axis perpendicular to the image when the trail occurs at the edge of the film. This reduces the focusing problem and also allows us to neglect any correction for the projection effect which would be necessary if the curved film rested on the flat carriage of the measuring engine.

The number of breaks measured depends on the apparent angular velocity of the trail. In general, we attempt to measure a distance of from 1 to 3 mm, which may represent 2 to 8 breaks. The measurements are usually made from the end of one dash to the end of another; that is, an integral number of dashes is measured. Corrections, by eye, are made for the photographic spreading of the image if the two terminal dashes of the measured trail section do not appear to be of about the same intensity. The dashes to be measured are chosen in such a way that the common point lies in the center of the measured section.

The trails are inspected for any wake, terminal blending, or marked abnormalities in the distribution of light over the trail. The position and apparent magnitude of the brightest dash may be measured.

This completes the measurements made on a meteor pair. We then determine, from the equations given earlier, cos Z_i, γ_i, R_i, h_i H, E, and V_i, in that order.

To complete this outline of the method, we will add a description of an earlier approach to the problem of finding common points. The argument, due to C. P. Olivier,[3] proceeds as follows: Consider the plane defined by the two stations and a point on the meteor. The lines R_A, R_B, and R_{AB} lie in this plane which intersects the celestial sphere on a great circle. Then the position of the meteor point as seen from each station must lie on a great circle which also includes the celestial position of one station as seen from the other. Conversely, if the two meteors are located properly on the globe, we can draw a great circle through the point defining the direction between the stations. Then, by the argument above, the intersections of this great circle with the meteor

[3] Meteors, 276 pp., 1925. Williams and Wilkins Co., Baltimore. (Esp. pp. 156–157.)

trails must represent common points. This technique was tried and discarded as being too insensitive for most cases. In practice, we employed a movable great circle which was attached to the measuring globe and pivoted at the points (δ_{AB}, t_{AB}) and ($-\delta_{AB}$, $t_{AB}-180°$). When the meteor trails formed a moderately small angle with this circle, the common points could be varied by several dashes with only a slight shift of the films. If the time of the meteor occurrence is lacking, the precise position of the film on the celestial sphere is unknown.

Single-station shower meteors and the approximate method

The program of meteor astronomy at the Harvard College Observatory includes the investigation of the origin and histories of the shower meteors by study of the distribution of the radiants over the period of the shower. Single-station meteors are used in a least-squares solution to determine the radiant, if they appear to belong to the shower—that is, if an extension of the trail passes through (or near) the assumed radiant point for the time of the meteor, and if visual inspection determines that the apparent angular velocity of the meteor is reasonable for the shower velocity and the radiant distance. A small amount of work with the globe used in the approximate method removes the guesswork from this visual determination. By assuming that the meteor belongs to the shower, we can estimate a height that corresponds to that of meteors of the shower velocity. The apparent angular velocity (ω'_i), cos Z_i, and the distance from the assumed radiant (ϵ_i), are measured for some point on the trail. From equations (3) and (6), we have:

$$V=\frac{\omega'_i h_i}{\cos Z_i \sin \epsilon_i}. \qquad (10)$$

If the meteor belongs to the shower, the measured values should yield the shower velocity. We may be deceived occasionally by meteors whose true radiants and velocities are not those of the shower but combine, by chance, in such a way that

$$(V \sin \epsilon_i)_{\text{shower}}=(V \sin \epsilon_i)_{\text{nonshower}}. \qquad (11)$$

Such cases must be far more rare than the 10 percent of single-station meteors which we have been able to eliminate from those meteors thought to belong to the shower.

It is obvious that the usual approximate method may also be used to eliminate those double-station meteors that have the proper radiant but a nonshower velocity.

Height errors

The problem of errors in our data reduction includes two major questions, neither of which has yet been finally answered. First, the velocities and radiants determined by the direct and indirect methods are, in general, at variance with one another. We need some quantitative criteria for making a choice between the two results. Second, we desire a more exact knowledge of the mean errors as a function of the various parameters of the solution. The final answers to these questions will be found only after the completion of the reduction project. Eventually we intend to acquire approximate data on 2000 meteors, including about 300 faint meteors that have been reduced by the method described by Hawkins in the preceding paper. An intercomparison of results should supply the information we want. Comparison can be made with several hundred brighter meteors already reduced by Jacchia. However, the accuracy we can obtain in determining the radiant of these long meteors will seldom be approached for fainter meteors. On the other hand, common points are often more difficult to obtain on long meteors. All in all, we do not consider bright meteors to be comparable to faint ones with regard to our system of measuring. A comparison of velocities obtained by accurate methods and by the present method has been made for some 25 bright meteors. Our average error in velocity was about 3 percent.

With respect to the order-of-magnitude estimate we can study the results of measuring errors of probable amounts. We may also compare our velocity results for shower meteors with their known values.

Let us begin with the errors in height introduced by our assumption that the earth is a plane surface. The correction for this was

ignored as being small compared with the intrinsic errors of measurement. This is true if the meteors are in the vicinity of the zenith. It is easily shown that:

$$\Delta h = h - h' = \frac{R^2 - h'^2}{D} \tag{12}$$

where h is the computed height above the station level, h' is the true height above the station level, R is the range from meteor to station, and D is earth's diameter. With the assumption that

$$\Delta h \ll 2h \tag{13}$$

we obtain

$$\Delta h \doteq \frac{R^2 - h^2}{D + 2h}. \tag{14}$$

Employing equation (3), we may write

$$\Delta h \doteq \frac{h^2(\sec^2 Z - 1)}{D + 2h}. \tag{15}$$

For meteors of 100 km altitude, the correction factor reaches 0.5 km at a zenith distance of 37°.7. Essentially none of the meteors reduced exceed this value. The average zenith distance is of the order of 20°.

If the common point is improperly chosen or measured, or if the two films are not correctly positioned on the globe, the two range lines, as defined by (δ_A, t_A) and (δ_B, t_B) will either not intersect in space or will not intersect at a point on the meteor trail. Whether the intersection occurs for any given set of measures or not, our computations still lead to a complete description of *some* triangle which represents, to some degree of approximation, the true triangle defined by the two stations and a point on the meteor. We are interested in knowing how good an approximation our measures probably give. We will discuss the errors involved in one particular case. Computations for other cases show that the total errors will be similar in other parts of the sky where meteors have been photographed.

It is a bit difficult to estimate a reasonable amount for the errors in the common point, positioning, or measuring which combine to give the total errors, $\Delta\delta$ and Δt. The error involved in reading the globe scale should not exceed 0°.2. For fast meteors with a high apparent angular velocity and with a common point of only moderate quality, say two, the common point error would be about 1°. We believe this to be considerably greater, perhaps by a factor of two, than the common point error for the average meteor.

Positioning errors can occur in two ways. First, the two films may not be properly superimposed. Because the globe is not perfectly spherical and because its mean radius is not exactly that of the films, we can not always superimpose the entire star field common to both films. The attempt is always made to carry out the superposition in the vicinity of the meteors and an error of about 0°.5 would probably be large. The second positioning error, resulting from an unknown time of the meteor occurrence, is a special case and will be treated separately.

From the preceding extreme figures, we may estimate that the average error, in δ_i or t_i, will almost certainly not exceed 1°. It is unfortunate that this figure cannot be verified by more rigorous methods than those used. However, another check on our errors, to follow later, will supply additional information tending to confirm this as being an extreme value.

Let us assume that the common point at Station B has been properly located, positioned and measured, and that, for any of the aforementioned reasons, a 1°.0 error exists in the measures of the common point at Station A. The percentage errors for this case have been computed from the differentials of equations 1, 2, 3, and 4 and are listed in table 2. The quantity t'_i is defined by the equation

$$\Delta t'_i = \Delta t_i \cos \delta_i.$$

TABLE 2.—*Errors resulting from a 1°.0 error in the common point*

Percentage error in:	$\Delta\delta_A = 1°.0$	$\Delta t'_A = 1.0$
$R_A =$	3.7	3.6
$R_B =$	3.7	3.7
$h_A =$	3.5	3.7
$h_B =$	3.8	3.7

The similarity of values within either column should be expected. The similarity between the two columns is the result of chance and indicates that the maximum error for the

meteor will occur for departures in a direction roughly half way between the directions of the δ and the t axes.

When the instant of the meteor is unknown, we choose the instant of the middle of the exposure for reduction purposes. Thus, with 12-minute exposures our maximum error is Δt_i=6 minutes=1°.5. However, in this case the common points do not suffer a shift relative to one another and the resulting errors in the ranges will be the algebraic sums of the errors caused by the displacement of both common points. Since these are of opposite sign and of about the same magnitude, the final errors will be small. Table 3 shows the percentage errors resulting from a 1°.5 shift in t_i of both films. We can see that the timing error will be negligible even in those cases where the maximum possible error results from a displacement along the t-axis.

TABLE 3.—*Errors resulting from a displacement of* Δt_i *1°.5 of both films*

Quantity	R_A	R_B	h_A	h_B
Error (km)	+0.34	−0.14	+0.20	−0.17
Percentage error	0.4	0.2	0.2	0.2

Velocity errors

Errors in velocity may result from errors in any of the measures. Errors in the apparent angular velocity, ω_i', are probably small compared to any other type and we will neglect these. From differentials of equation (6) we see that the percentage errors due to range and radiant errors are, respectively:

$$\left(\frac{\Delta V}{V}\right)_{\omega',\epsilon} = \frac{\Delta R}{R} \tag{16}$$

$$\left(\frac{\Delta V}{V}\right)_{\omega',R} = -\cot \epsilon \Delta\epsilon. \tag{17}$$

Thus the error in velocity cannot be less than the range error, which we found to be about 4 percent with the assumption of a common point error of 1°.0. The function $\Delta\epsilon$ is itself a function of ϵ as one can understand by visualizing the extreme cases when the meteor appears *at* the radiant (ϵ=0°, $\Delta\epsilon$=0°), and when the meteor appears at a great distance from the radiant (say, ϵ=90°, $\Delta\epsilon$=?≠0°). We might estimate this unknown $\Delta\epsilon$ to be of the order of 5° or 10° in the worst cases. We may say that certainly $\Delta\epsilon$ varies less rapidly than tan ϵ. This leads to the apparently contradictory result that, in general, meteors must have a badly determined radiant to allow us to produce an accurate velocity. However, another independent error in ϵ, that imposed by our scale reading accuracy, 0°.2, weighs more heavily against meteors of small ϵ. These two errors may combine in such a way that meteors at some intermediate ϵ give the best velocities.

We have no method of determining a satisfactory relationship between ϵ and $\Delta\epsilon$ and we must therefore approach this problem from another side. Among the meteors reduced, there are 36 Orionid and 45 Geminid shower meteors for which we know velocities. These groups will determine our velocities errors. Furthermore, since most meteors in these showers were reduced by both the direct and indirect methods, we can find some estimate of a criterion for choosing between the results of the two methods.

In general, the direct velocities from the two films of a given meteor do not agree with one another to within several percent. The direct velocity chosen is usually the average of the two. However, in some examples, the radiant distance of one common point greatly exceeds that of the mate photograph and, in these instances, the velocity derived from the more distant trail is used or weighted more heavily in the average. Average velocities, mean errors, and percentage errors were found for both sets of shower meteors for the following cases:

(a) Direct velocity used for all meteors.
(b) Indirect velocity used for all meteors.
(c) Indirect velocities used when $|\epsilon_{AB}| \geq 10°.0$, direct when $|\epsilon_{AB}| < 10°.0$.
(d) Same as (c), with division made at $|\epsilon_{AB}| = 9°.0$.
(e) Same as (c), with division made at $|\epsilon_{AB}| = 8°.0$.

Table 4 gives the average values, mean deviations, and percentage errors for each of these velocity criteria and for both groups of shower meteors. The letters refer to the categories outlined above.

We should qualify the character of these data before discussing the results. First, the Geminids were somewhat brighter meteors than

normal and, hence, easier to measure. Furthermore, the radiant of this shower is not far distant from α Geminii, a star that appears on most of the Geminid meteor photographs. Since these meteors were reduced specifically to check for errors, it was necessary for the measurer to "forget" the position of the radiant for each measure, a difficult task with a radiant so clearly marked. Still, we believe this was accomplished.

TABLE 4.—*Errors in velocity for two sets of shower meteors*

	Number of meteors	Number of indirect determinations used	$V\left(\frac{\text{km}}{\text{sec}}\right)$	$\sigma\left(\frac{\text{km}}{\text{sec}}\right)$	Percentage error
Geminids:					
(a)	44	0	35.7	1.42	4.0
(b)	38	38	35.7	1.74	4.9
(c)	45	16	36.3	0.92	2.5
(d)	45	21	36.1	1.05	2.9
(e)	45	26	36.0	1.13	3.1
Orionids:					
(a)	34	0	68.3	3.01	4.4
(b)	34	34	67.2	2.52	3.8
(c)	36	18	68.2	2.59	3.8
(d)	36	24	67.7	2.17	3.2
(e)	36	28	67.6	2.05	3.0

In the case of the Orionids, the situation is quite different. The radiant was not present on the region being photographed and, more important, we did not realize we were reducing shower meteors until after the measures had been made. Also, these meteors did not produce such bright trails as the Geminids. Perhaps, then, the Orionids should be regarded as giving the best test, although, as can be seen in table 4, the errors for both showers are comparable.

In regard to the indirectly determined velocities, our measured quantities are E and ϵ_{AB} as defined by equations (8) and (9). It may easily be shown that if the radiant is properly chosen and there are no measuring errors,

$$\Delta\epsilon_A=\Delta\epsilon_B=\frac{(\Delta E+\Delta\epsilon_{AB})\sin\epsilon_i^2}{\sin\epsilon_{AB}} \tag{18}$$

where ϵ_i, in this case, is the angle from the radiant to the common point of the trail most distant from the radiant. A poorly determined common point has little effect on E, since this quantity is determined from a ratio of the ranges, R. A reasonable error in the common point results in comparable changes, of the same sign, in the two ranges. We may write

$$E\propto\frac{R_A}{R_B} \tag{19}$$

Then:

$$\Delta E=\frac{R_B\Delta R_A-R_A\Delta R_B}{R_B^2}. \tag{20}$$

Thus, the errors in the range tend to compensate one another in the determination of E. However, since we must still apply the velocity equation (6) in its original form after determining ϵ_i, any error in range will affect the velocity in the usual fashion.

One can see that an error in the common point will directly affect ϵ_{AB}, which is essentially the distance between common points. It is also clear from the $\frac{1}{\sin\epsilon_{AB}}$ factor in equation (18) that the indirect method will be more powerful when ϵ_{AB} is sufficiently large. From the shower meteors we can obtain an idea of how large.

Table 4 indicates that the deviation from the mean velocities of the showers is of the order of 3 to 4 percent, but we have yet to show that these mean velocities actually correspond to those expected for these showers. Our velocities are those at some point in the atmosphere, uncorrected for deceleration and therefore somewhat lower than the velocity outside the atmosphere which is usually quoted for a shower. In general, we choose common points as near the beginning of the trail as possible to minimize the deceleration correction. From Orionid and Geminid meteors reduced by Jacchia, we have obtained the velocities at the beginning point of the meteor (V_e). These results, as well as Jacchia's values for the no-atmosphere velocity (V_∞) are given in table 5. They are compared with the average velocity we obtained for the method which yielded the smallest σ in table 4. The agreement is excellent and there is no evidence of a systematic error with velocity. We may conclude that our velocity errors, for these cases, are about 3 percent and that the

TABLE 5.—*Average velocities obtained by accurate reductions of shower meteors (by Jacchia)*

	Number of meteors	V_∞	V_e	V_{RBM}
Geminids	17	36.6	36.3	36.3
Orionids	7	67.5	67.4	67.6

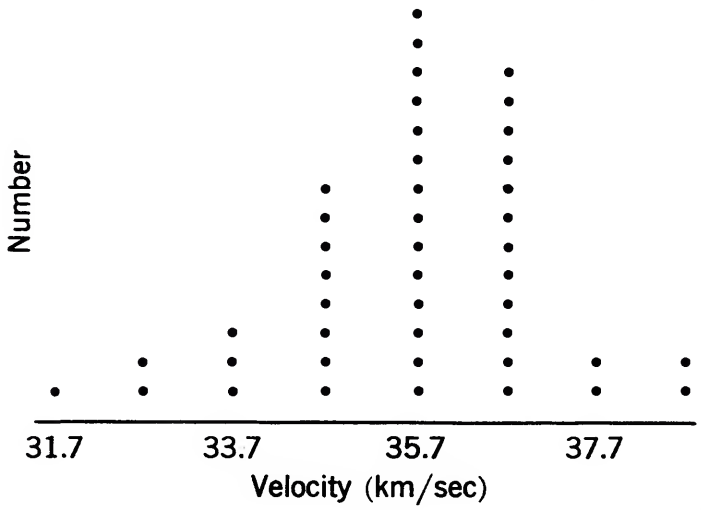

FIGURE 3.—Velocity distribution of Geminid shower meteors, approximate reductions.

optimum minimum value of ϵ_{AB} for the indirect reductions is about 8° to 10°. It seems unlikely that measures on somewhat shorter and fainter nonshower meteors would yield errors that exceed 5 percent. When this result is compared with the errors *expected* for ranges and heights, we see that we must have overestimated the probable error in the common point, for, as was pointed out earlier, the velocity error cannot be less than the range error, which was of the order of 4 percent on the assumption of a 1°.0 error in common point.

There still remains the possibility that in selecting the shower meteors, we passed over some cases which were so badly determined that they were unrecognizable as members of the shower. A study of the frequency diagram of the velocities of the individual meteors makes such a hypothesis unlikely if, on the basis of such a diagram, one is willing to grant that the scatter may be represented to a fair degree of approximation by the usual error curve. We have reproduced in figure 3 the frequency diagram for the directly determined velocities of our Geminid meteors.

A Reduction Method for the Motions of Persistent Meteor Trains[1]

By Allan F. Cook[2] and Robert F. Hughes[2]

Two Baker Super-Schmidt cameras, located 35 kilometers apart, at Mayhill and at Sacramento Peak, New Mexico, operate continuously to obtain multiple exposures of persistent meteor trains. The method of operation of the cameras and the general process of obtaining wind velocities normal to such meteor trains have been described by F. L. Whipple (1953). Further results from the program have been presented by Liller and Whipple (1954). No details of the reduction methods have been published, however, nor have the methods been previously extended to include determination of the air motion parallel to the direction of the meteor. Hence we present, in considerable detail, the procedures of measurement and reduction that we have found to be useful in determining atmospheric motions from multiply-photographed persistent meteor trains.

For measurement the spherical Super-Schmidt films undergo an approximate gnomonic projection to a flat glass-plate emulsion by means of a copying camera. With the Mann measuring engine, train positions are measured with respect to the infinitely distant reference system provided by the stars. The loci of the multiple trains are readily converted to linear plate displacements from the trail in the reduction system of the concurrent meteor photographs, which provide complete geometric and time coordinates of the meteor's flight. From the length of the exposures, as determined by photometric measures and clock records, the velocity components of the train motion on the plate are calculated and transformed to two components in space. One component of the train motion is normal to both the meteor trail and the line of sight, and the second is parallel to the projection of the meteor trail on the plane normal to the line of sight. If the former component is observed at both stations, the air motion is determined as a composite of a mean wind field plus a superimposed turbulent field. Given the train motion component parallel to the projected trail at even one station, one may investigate the existence of any systematic motion of the train along the actual meteor trail.

Selection of train films

The Super-Schmidt cameras used by the Harvard Meteor Expedition for photographing meteor trains are triggered photoelectrically or manually. The exposure durations of roughly $1/2^s$, 2^s, 2^s, etc., are separated by $0.^\circ3$ shifts of the camera in declination, and are programmed automatically with a special long exposure added manually at the end. On the train film, the various star exposures appear in a line at angular separations of about $1/3°$, or 1 mm linearly, where the fainter end exposure is the first exposure. Plate 1 is an example of

[1] This paper is based upon research supported by the U. S. Air Force under Contract No. AF19(122)-482. Reproduction in whole or in part is permitted for any purposes of the U. S. Government.

[2] Harvard College Observatory, Cambridge, Mass.

such a photograph. The observers generally use a greased crayon to indicate the trains, which may be continuous, diffuse, or varying in intensity and amount of distortion from a straight line. The possible appearance of the meteor trail on the train film, or alignment with the concurrent meteor film, confirms the identification. Trail films marked SS (Sacramento Peak) or ST (Mayhill) have concurrent meteor films SL and SK, respectively. The initial "processing" of the train films may be outlined as follows:

1. Standards for selection:

(a) Concurrent meteor films are successful.

(b) Train film is in good focus.

(c) At least four train exposures or 3 trains and a trail are observable

2. Copying:

(a) The train and concurrent meteor films are both copied.

(b) If the meteor or the train occurs very near the film edge, an offset position of the desired projection center is indicated so that the containing rim of the camera will not eclipse the image.

(c) The plates of the films are inspected in order to see that all detail observed on the train film has been reproduced. Several copying attempts are sometimes necessary to insure optimum results.

3. Marking:

(a) Reference stars are marked on the train and meteor plates during the reduction for the meteor's trajectory, velocity, and deceleration. At Harvard this is done by the Meteor Analysis Laboratory.

(b) If the number of train exposures is greater than four, the first and last images of the fainter stars are indicated.

(c) Stars, lettered A to Z in the direction of meteor flight, are placed every 5–10 mm, as near the train as possible, and extending slightly beyond the extremities of the trains.

4. Photometric reduction:

(a) After the films are successfully copied, they are subjected to photometric analysis. Magnitude differences between successive images are determined by eye intercomparison of the images of a selected standard star sequence (Payne-Gaposchkin, 1937).

(b) The film center is indicated from record sheets to aid in the identification of the star field.

Measuring procedures

Careful application of the parallax test is necessary to adjust the focus of the measuring engine properly. To measure a diffuse line with poorly defined edges which are susceptible to distortions from grain structure in the emulsion requires an eye integration along nearly 1 mm of the cross-hair. Any one position is best defined with the aid of neighboring points, which tend to average out the small irregularities of the train shapes. Train images are measured to the limit of visibility. The horizontal cross-hair, which is parallel to the engine carriage, is the X-axis; the vertical cross-hair is the Y-axis. The procedure for measurement is as follows:

1. Plate alignment:

(a) The plate is secured in the frame with the emulsion down.

(b) The lighting is adjusted for maximum train visibility.

(c) The train is placed (similar to trail) parallel to the X-axis and the frame locked securely in position.

(d) The four verniers are read as accurately as possible (to 10″ on the Mann engine).

2. Stars and trains:

(a) Stars. For each exposure one reading is made in X and Y to the nearest micron (0.001 mm) in the region of the respective train image. The reading is repeated after the train measurements to obtain averaged star readings and to check for the possibility that a plate movement has occurred during the train measurement. Two fiducial marks (sharp images of faint stars, emulsion defects, etc.) are chosen and their positions read before and after the measurements as a further protection against disturbance of the plate during the measures.

(b) Trains. For convenience in making the reduction, the Y coordinate of the train is measured at equal intervals of X along the train. X intervals need only be small enough to define and confirm the varying shape of the train. Generally 0.5 to 1.0 mm is adequate for earlier images. This is sometimes diminished to 0.1 to 0.25 mm for later images where

distortions occur and difficulty in measurement increases. Regions about singular points in the trains are specially defined in each image.

(c) Elimination of personal equation. The systematic error, due to personal equation, in centering the cross-hairs on the train images is averaged out by taking two sets of readings measured from opposite directions. After the plate has been rotated 180°, the measurements described in section 2–b are repeated. Comparison of the vernier readings with the first position allows a very close approximation to 180° rotation. A shift in the Y scale is often necessary to make the train region observable.

Reduction to a single train system

The transformation of the two sets of train readings into a common train system consists of a rotation and translation, where the angle of rotation may be expressed as $180°+\epsilon$. Then,

$$\begin{pmatrix} X-a \\ Y-b \end{pmatrix}_2 = -\begin{pmatrix} 1 & \epsilon \\ -\epsilon & 1 \end{pmatrix}\begin{pmatrix} X \\ Y \end{pmatrix}_1, \qquad (1)$$

where the constants of rotation (ϵ) and translation (a, b) are found from the star measurements as follows:

1. Averaging. The star readings of each of the two sets of measurements are averaged.

2. Conversion from one system to the other. Three stars in good focus are selected, two of which have a long base line in X. The third is taken near the midpoint as a check. If (X_1+X_2) and (Y_1+Y_2) are constant for these stars, $\epsilon=0$, and the average sums are taken as a and b, respectively. A nonzero ϵ will introduce in (Y_1+Y_2) a marked linear change in proportion to X. In this case, a larger number of points (Y_1+Y_2, X_1) is plotted to determine the slope ϵ. The X and Y sums are corrected for ϵ, and then a, b determined from the average values of $(X_1+X_2+\epsilon Y_1)$ and $(Y_1+Y_2-\epsilon X_1)$, respectively.

3. Choice of adopted system. The single train system is taken as that in which the X coordinate of stars A, B, to Z increases positively. Finally all star and train readings are transformed by equation (1).

Reduction to the concurrent meteor system

The precise reduction of the concurrent meteor plates (see Whipple and Jacchia in the first paper of this group) provides accurate geometric and time coordinates of the meteor's flight in space and as projected on the tangent plane of the sky at the plate center. In order to relate the train positions to the original trail position and to the time of train formation, measurements in the common train system are transformed to the concurrent computed meteor system, the coordinates of which are equal to the original plate measure plus field corrections. The coordinates of identical stars in the computed meteor system and in the train system define the transformation of X and Y coordinates for each train image. The difference in the coordinate values for the image (i), $(X-X_i, Y-Y_i)$ will be a nonlinear function in X_i, with a possible additional linear term in the Y transformation, proportional to the distance of the star from the meteor trail. Although a least-squares solution is possible, a graphical representation is sufficient and much easier, since $(X-X_i)$ can readily be found graphically to 0.01 mm and $(Y-Y_i)$ to 0.003 mm. The detailed procedure of this transformation is as follows.

1. Transformation plots. Averages for the two sets of star positions in the common system are formed. For each image the differences $(X-X_i)$ and $(Y-Y_i)$ are formed and plotted against X_i. It is preferable to plot these on the same graph by using one abscissa scale and introducing various ordinate scales, because the X and Y transformations for all images have the same general variation; this aids in the curve drawing, especially when one or two star positions are found to be inconsistent. The X transformation function is well defined (to 0.01 mm by the above difference plots). In other words, the scatter of points about a freehand curve smoothed by a French curve is small. If the scatter in $(Y-Y_i)$ is too large to define a function to 0.003 mm, a linear correspondence of the residuals from a first approximation function to the star's displacement from the trail may be noted. Introduction of a linear term in displacement from the trail should reduce the scatter enough to allow a determination of the transformation to within 0.003 mm.

2. The X, Y coordinates. The X, Y coordinates for both sets of train measurements are next transformed individually according to

the above difference functions. The transformed X is expressed to the nearest 0.01 mm and Y to the nearest 0.001 mm.

Train displacements

The systematic error in the train measurements due to personal equation depending on intensity of the train image is now averaged out by freehand curves drawn through the plots of the train images in the meteor system. This elimination is possible since points from both the direct and reversed measurements will have been plotted. Since the equation of the trail is known, displacements of train images from the trail at any position along the trail (X) are readily computed. A more detailed description follows.

1. Plotting. Abscissa scales (X) for all images should allow estimation of X coordinate to 0.01 mm. Ordinate scales (Y) for earlier images (1–3) should allow estimation to 0.001 mm, but in later images the Y scale must be compressed to facilitate curve drawing, because the magnitude of the scatter in train measures increases in the later exposures. However, the percentage (scatter) generally remains rather constant (10 percent).

2. Averaging. The two sets of train measures will differ systematically from each other with an increased separation in the later images, if this separation has not already been eliminated by the large scatter that results from the extreme difficulty of measurement. A freehand curve averaging the two sets of readings is drawn to represent the most likely train position. All curve variations consistent with the two independent sets of measurements are drawn regardless of the scales adopted in the plotting. At this stage no attempt should be made to correct for distortion introduced by the emulsion and varying scales.

3. Displacement computation. The displacement of train image (i) from the meteor trail, at a point X along the trail, may be defined as $\Delta_i Y = Y_i - Y_T$, where the subscript T denotes the trail. Since Y_T is a very slowly varying linear function of X, $\Delta_i Y$ may be tabulated directly by reading the smoothed plots of the train images at appropriate intervals of X and subtracting Y_T. Again, the X interval need only be small enough to define the freehand curve.

Epochs of exposure

Photometric measures of star exposures give the relative exposure times for different images. The total time of shutter opening during the automatic program is indicated by the clock record, and thus determines the actual duration of the exposure. Clock readings and the observations provide consistency checks. If reasonable assumptions are made for the decay function of train luminosity, the effective epoch of exposure for a train image will not deviate significantly from a simple average of the times at the beginning and end of the exposure. Since the time interval required to shift the camera from one exposure to another is negligible compared with the duration of all exposures after the first, the effective time of exposure of image (i) with respect to the beginning of the first exposure is the sum of the durations of the preceding exposures plus one-half the duration of image (i). In order to determine the time since formation of the train, the time interval (τ_0) between the beginning point ($t=0$) on the meteor's trail and the beginning of the first exposure must be known. The reduction of the photometric data, consistency checks, and the determination of τ_0 are carried out as follows:

1. Photometric determination of exposure duration:

(a) Given the magnitude differences between successive images, the magnitude difference (Δm_i) between image (i) and the first image is obtained. Negative differences are taken conventionally to indicate greater brightness of image (i) with respect to the first image.

(b) Relative exposure durations. If the exposure duration (d_i) is proportional to I_i, then the exposure time of image (i) relative to the total exposure (program plus special exposure) is given by the expressions $(I_i/I_1)/(\Sigma_i I_i/I_1)$, where the summation is over all exposures.

(c) As a rough check, the ratio of program time to special exposure time from photometric analysis and clock record should agree to better than 40 percent.

(d) The relative time of exposure of image (i) to the program time (P) is given by the expres-

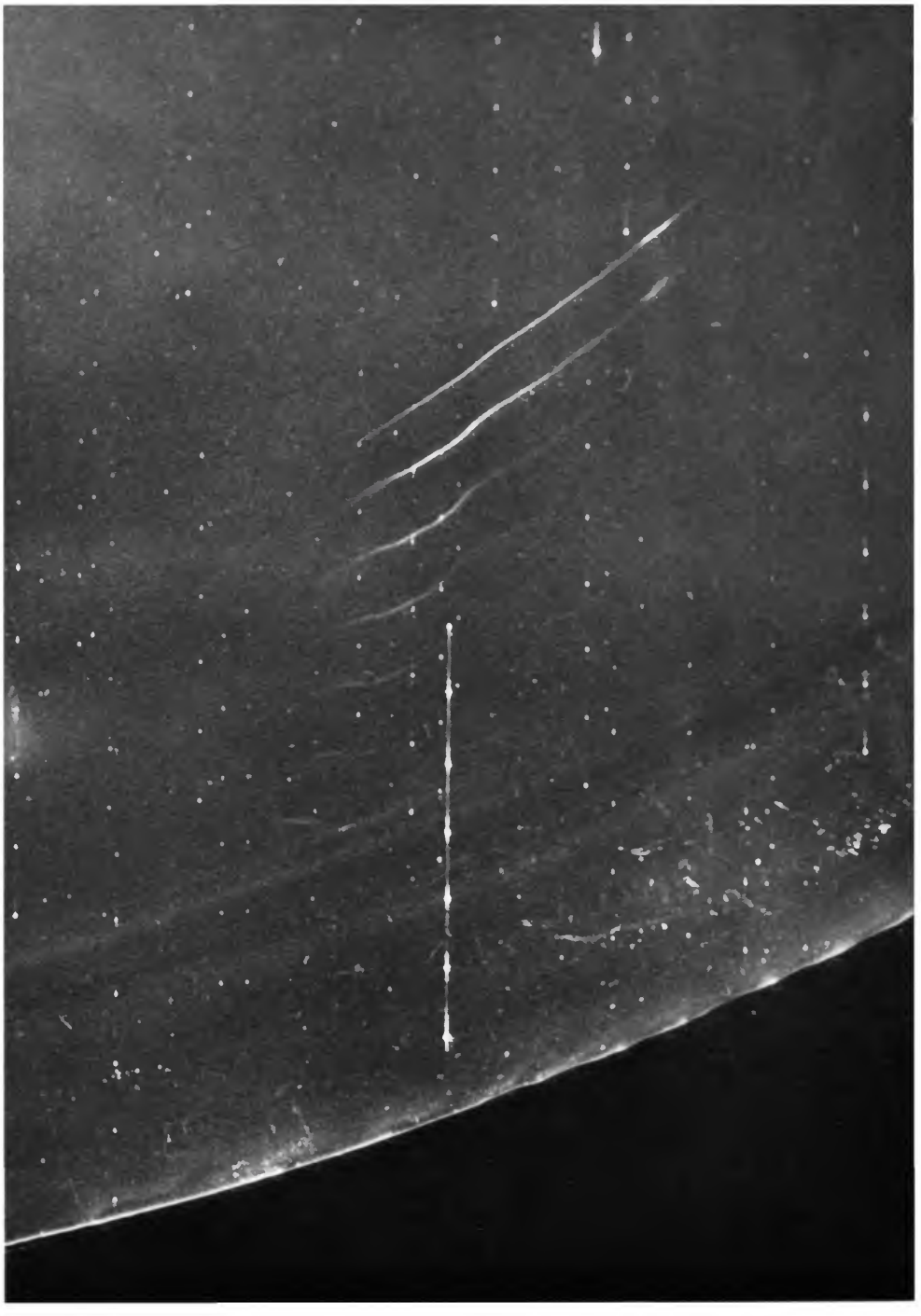

Multiple photograph of meteor train of June 29-30, 1954, on film No. ST 5488 from Doña Ana, N. Mex., by J. R. Coultis.

sion: $(I_i/I_1)/(\Sigma_i I_i/I_1)$, where the summation is only over the automatically programmed exposures.

(e) The program time (P) is read directly from the clock record; the exposure duration is the product of P and the expression for the relative times given above. The exposure duration for the last exposure (special) is taken directly from the clock record. The duration times (d_i) should be expressed to three significant figures, which generally means to 0^s01 for the early images.

2. *Clock check for consistency.* Time readings as given on the clock tape (0.01 min.) are about one order of magnitude less precise than desired, but nevertheless they provide limits to the possible range in the exposure durations determined photometrically. If $\pm 0^m004$ maximum error is allowed in each clock tape-reading for beginning and ending of exposures, the allowable values of d_i may be determined, and checked with the photometry for consistency. If disagreement occurs, the photometric values must be adjusted to fit those of the clock in the following manner:

(a) A d_i and a beginning or ending time of an exposure which are well substantiated by the clock and by photometry should be sought. As an example, if the clock records the time exactly midway between successive hundredths of a minute, both digits will be observed on the tape straddling the proper position; i. e., the dial for 0.01 minute intervals moves continuously. This increases the accuracy of the clock so that it becomes comparable to that of the photometry. If agreement for these durations is good, the exposure time is well substantiated.

(b) Small magnitude differences given photometrically are more accurate than large differences ($>0^m6$). Successive exposures with small magnitude differences ($<0^m25$) are used as much as possible; d_{i+1} then may be computed from $\delta d = -0.92\ d_i\ \delta m$ where δd and δm denote small increments in duration and magnitude respectively. This procedure allows simulation of the clock tape record of beginning and ending times. If d_i was well chosen, successive exposure times computed from the small difference equation should be consistent with the clock readings.

(c) For a large magnitude difference, d_{i+1} is computed from the expression,

$$\log_{10} \frac{d_{i\pm1}}{d_i} = -0.4\Delta m.$$

If a computed end or beginning time of an exposure is not consistent with that of the clock, the allowable clock time nearest to the photometric value is the best to assume.

(d) All program exposures can be adjusted except possibly the first exposure. The magnitude differences between the first and second image may be as large as 2^m and consequently subject to large errors. In this case, the clock will generally be of no aid in fixing a lower limit on d_1, so one usually has no choice but to assume the photometric value. If photometry is also done on the train images the decay law for its radiation may be found and the epochs of exposure corrected accordingly.

(e) The validity of the adjusted durations can be checked by comparison of the final magnitude difference for the adopted times with the original photometric values. Errors of about 0^m5 are possible in large differences, especially when star images are extremely distorted, or when one star is excessively faint.

(f) The epoch of exposure with respect to the beginning of the first exposure (τ'_i) is given by the expression $(d_1+d_2+\ \ldots\ +d_{i-1}+1/2\ d_i)$.

3. Observational test for consistency of adopted durations. Assume that the train displacements from the trail at a given value of X are directly proportional to the time elapsed since the train was formed for all time intervals. In the meteor system, $t=0$ is taken as the time at the first measurable dash on the trail; the time of meteor passage at all other points is given by $t(X)$. If τ_0 is the time between $t=0$ and the beginning of the first exposure, then for an image (i) at point X, the time elapsed since the train was formed (time of meteor passage) is given by $\tau_0+\tau'_i-t(X)$, and consequently

$$\frac{\Delta_i Y}{\Delta_j Y - \Delta_i Y} = \frac{\tau_0+\tau'_i}{\tau'_j-\tau'_i} - \frac{t(X)}{\tau'_j-\tau'_i}. \qquad (2)$$

The ratio $\Delta_i Y/(\Delta_j Y-\Delta_i Y)$ is a linear function of $t(X)$. The determination of the slope provides an observational check on the exposure epochs which, if successful, leads immediately

to an evaluation of τ_0 from the intercept. Details of the observational test follow:

(a) Generally, only the first and second train images are long enough to provide a sufficient time base for a slope determination. A plot of $\Delta_1 Y/(\Delta_2 Y - \Delta_1 Y)$ against $t(X)$ is required.

(b) The instability of the displacement ratio due to the small values of $\Delta_i Y$ necessitates an estimate of the ordinate error originating from the scatter in the train measurements. If the root mean-square scatter in Y_i from the smoothed train position for image (i) at X is given by ϵ_i, then the corresponding root mean-square scatter in the ratio $\Delta_i Y/(\Delta_2 Y - \Delta_1 Y)$ is:

$$\epsilon = \frac{[(\Delta_2 Y \times \epsilon_1)^2 + (\Delta_1 Y \times \epsilon_2)^2]^{1/2}}{(\Delta_2 Y - \Delta_1 Y)^2}. \qquad (3)$$

When the distribution of the scatter magnitude has been noted, the most reasonable slope for the above linear function may be drawn. The slope $-(\tau_2' - \tau_1')^{-1}$ gives $d_1 + d_2$. If the observational estimate is consistent (20 percent), the clock-photometric durations are adopted as the final values.

4. Epoch of exposure with respect to first break on trail. In order to decrease the percentage errors in $\tau_j' - \tau_i'$ and $\Delta_i Y/(\Delta_j Y - \Delta_i Y)$, two widely separated images are chosen to determine a point on the linear function as follows:

(a) For i and j, the first and last images respectively are usually used.

(b) A small range of $t(X)$ in a region of well-defined train images giving $\Delta_i Y/(\Delta_j Y - \Delta_i Y)$ is selected and its scatter computed. An averaged point $\Delta_1 Y/(\Delta_j Y - \Delta_i Y)$, $t(X_0)$ may be estimated graphically.

(c) If the adopted epochs are taken, then τ_0 is given by the equation

$$\tau_0 = (\tau_j' - \tau_i') \frac{\Delta_i Y}{\Delta_j Y - \Delta_i Y}\Big|_{X=X_0} + t(X_0). \qquad (4)$$

(d) For a rough check, τ_0 may be computed from the $(\Delta_1 Y/\Delta_2 Y - \Delta_1 Y,\ t)$ plot by use of the slope from the adopted times. If many images are observed, several pairings of first and later images may be employed to find a weighted average of τ_0.

(e) The epoch of exposure with respect to $t=0$ for image (i) is given by $\tau_i = \tau_0 + \tau_i'$.

(f) If the trail is present on the train film, then τ_0 is equal to the time of meteor passage at the point along the trail where the train ends and the trail begins.

Linear plate velocity and correction for rotation

The displacement of the train normal to the meteor trail $\Delta_i Y$ and the times since formation $[\tau_i - t(X)]$ determine the velocity on the plate normal to the projected trail. Because the stars are used as a reference system, a spurious train motion is introduced corresponding to the westward diurnal motion of the stars. The correction to the normal velocity is generally large enough to be considered. Corrections to the X coordinate of the measurement of $\Delta_i Y$ may be neglected if three or fewer images exist, but they are otherwise required. Details of plotting the corrected normal velocities are as follows:

1. Normal velocities. The normal train velocities (V_{Ni}) for each image should be tabulated:

$$\frac{\partial Y}{\partial t} = V_{Ni}(X) = \Delta_i Y/[\tau_i - t(X)]. \qquad (5)$$

2. Correction for diurnal rotation. The detailed equations may be found in Appendix III. Note that the time rates of change of the plate coordinates X and Y are proportional to the time rate of change of the right ascension of the corresponding spatial point of the train. A westward motion of the reference system increases the right ascension of the train point spuriously, and hence its X and Y points also. The time during which a train point has been tracking is simply the time elapsed since its formation, namely $\tau_i - t(X)$. Let the rate of change of X, Y due to rotation of the reference system be $\dot{X}_r(X)$ and $\dot{Y}_r(X)$ respectively in mm $\sec^{-1}$. Then the correction procedure is as follows (the formulae are derived and given in Appendix III):

(a) The correction to X_i is $-\dot{X}_r(X)[\tau_i - t(X)]$.

(b) The correction to Y_i is $-\dot{Y}_r(X)[\tau_i - t(X)]$.

Since V_{Ni} is proportional to $[\tau_i - t(X)]^{-1}$, the correction to the normal velocity is simply $-\dot{Y}_r(X)$, a constant for all images.

(c) The magnitude of $\dot{Y}_r$ is about 0.007 mm and varies linearly but slowly with X. The magnitude of $\dot{X}_r$ is about 0.01 mm and varies quadratically in X.

(d) The tabulated correction of the normal velocity is applied and the abscissa X corrected and plotted in a single operation. Velocity points for each image are plotted on one graph with an indication of the scatter in V_{Ni} given by $\epsilon_i/[\tau_i - t(X)]$.

Train motion components

Inspection of the plots of velocity on the plate determines semiquantitatively whether one or two components are defined. If the V_{Ni} agree within the scatter of the measurements, a single component of train motion is defined; namely, that which is normal to the projected meteor trail. In this case a freehand curve may immediately be drawn through the points, weighted inversely proportional to the scatter in velocity for each train image. If the plots of the train velocities have similar shapes and show a systematic shift parallel to the trail, then the train motion component that is parallel to the projected meteor trail may be found. Measurement of a normal displacement of a train over a small range in X adequately defines the displacement in Y at the given X, but a given displacement in Y defines X poorly. Consequently, detection of a motion parallel to the trail requires a large relative shift in X (0.5 to 3 mm) over several images that form distinctive shapes. Large relative shifts become increasingly apparent, the greater the time since formation of the train; hence, a large number of images (more than five) is required for a solution for velocity parallel to the trail. No parallel motion will be apparent from the scatter of the normal velocity component for two-image to four-image trains. The procedure for defining the parallel component $V_P(X)$ is as follows:

1. Displacements parallel to trail. Displacements in X between images widely separated in time are measured from the normal velocity plots at those velocities for which the normal curve has a non-zero slope.

2. Determination of parallel velocity. The parallel plate velocity component (V_P) at a given normal velocity (V_N) is computed from the X displacement between images j and k ($k>j$) by the equation:

$$V_P(V_N) = (X_k - X_j)/(\tau'_k - \tau'_j). \qquad (6)$$

The determinations of V_P from various image pairings are plotted against V_N, and a freehand smooth curve is drawn through the points which are weighted roughly in proportion to the time base $(\tau'_k - \tau'_j)$. The scatter will be considerably larger than for the normal velocity component, but a general agreement on the shape of the function must exist in order to establish V_P. No systematic deviations should be observed from any highly weighted image pairings.

3. Correction of normal velocity for parallel displacement. A normal velocity, $V_{Ni}(X)$, is now plotted on a separate graph at the abscissae $\{X - V_P(V_N)[(\tau_i - t(X)]\}$. Enough points in V_N should be used to prevent introduction of any systematic error in the definition of the transposed curves other than the abscissa correction.

4. Final normal velocity component. After the parallel velocity correction, all train images occur at the point in X along the trail where the train was originally formed. A smooth curve is drawn as in the case of a single component solution to define $V_N(X)$.

5. Plot of parallel velocity component. The normal velocity as a function of X, $V_N(X)$, is defined by the smoothed curve in section 4, which in turn defines V_P from section 2 above. The tabulation of (X, V_P) is plotted with X as the independent variable.

6. The accuracy of the results. Steps 1–5 may be considered as the first step in successive approximations for $V_N(X)$ and $V_P(X)$, since the times used to compute V_{Ni} were taken at points along the trail where the train image was observed rather than at the points where the train was actually formed. But $t(X)$ enters as $\tau_k - t(X)$, where X here is the point at which the train was observed. Since

$$|t(X) - t(X - V_P(X)[\tau_k - t(X)])| \ll \tau_k, \qquad (7)$$

the first approximation to the normal and parallel velocity components is entirely satisfactory.

Coordination of velocity components from two stations

Double-station observation of the train motion requires the matching of the X coordinates in the two meteor systems according to a common

height above sea level (H) in the following manner:

Let subscripts A and B refer to the Mayhill and Sacramento Peak Stations respectively.

The distance (D) along the trail from the first measurable dash at one station, say Mayhill, must be computed from the equation,

$$D_A=100K_A(X-X_{Aa})/(X-X_{AR}), \qquad (8)$$

where K_A, X_{Aa}, X_{AR} are constants provided in the meteor reduction. At Harvard these appear on the reduction sheets of the Meteor Analysis Project. See the notation list in Appendix V for more detailed definitions.

The height of the point X_A above the plane tangent to the earth at one station, e. g., Mayhill, is given by the equation,

$$h_A=h(D_A=0)-D_A.\cos Z_A, \qquad (9)$$

where $h(D_A=0)$ and the zenith angle Z_A are given quantities.

From the Δh_A versus h_A graph, the height above sea level (H_A) is given by $h_A+\Delta h_A$

The mated meteor systems are arranged so that points with the same D have the same height; therefore the X_B corresponding to X_A is given by the equation

$$X_B=\frac{D(X_A)\,X_{BR}-100\,K_B\,X_{Ba}}{D(X_A)-100\,K_B}, \qquad (10)$$

where the subscript B denotes the second station, e. g., Sacramento Peak.

Intervals in height should be small enough to define the projected velocity curves. A table of D, X_A, X_B, and the respective normal and parallel velocity components versus H as independent variable may then be prepared.

Spatial components of train motion

The plate velocities normal and parallel to the trail are readily transformed to two spatial components normal and parallel to the meteor trail as projected on a plane perpendicular to the line of sight. These velocities in turn may be expressed in terms of the three components of velocity of the train. These components are taken parallel to the east, north, and zenith directions from the midpoint of the observed train region. Since the X axis is parallel to the projected meteor trail, a systematic motion of the train along the trail will not influence the component normal to the meteor trail in space. Thus this normal component is indicative only of air motion flowing transversely to the meteor trail. When the component normal to the projection of the meteor trail is plotted against distance along the trail, large variations in amplitude occur over ranges in distance along the trail of the order of 10 kilometers. Smaller variations in amplitude over a considerably smaller distance scale are superimposed on these. A smooth curve is drawn through the large-scale fluctuations and the smaller fluctuations are smoothed out. This curve defines the component of the mean wind field normal to the projected trail. The difference between the two curves represents the component of turbulent motion. Because the parallel velocity component is much less accurately measured than the normal component, only the latter can be used to define the small-scale velocity variations.

Observation of the two normal and parallel velocity components at both stations defines three linear equations in terms of the unknown train motion components (T_E, T_N, T_Z). The solution of the simultaneous equations for T is not singularly significant for several reasons. First, the combining of the less accurate parallel function with the more accurate normal function decreases the accuracy of all the train components. Second, the relatively small base of triangulation makes the determinant of the coefficients of (T_E, T_N, T_Z) nearly zero. This results in a solution in which the errors inherent in the train measurements are noticeable fractions of the derived train-velocity components. Third, in the first double-station train reduction attempted, an observed systematic motion of the train along the trail had a vertical component six times the maximum value ($\sim 5 ms^{-1}$) allowable for vertical air transport in the thermally stable region above about 80 kilometers. The theory of the persistence of meteoric luminescence and the momentum exchanges from meteor to air particles can explain such a coasting train-velocity, but has not been developed to a degree of accuracy such that the parallel component functions can be corrected to represent only the mean wind projection.

The analysis is therefore aimed at investigating the existence of a coasting train-velocity from the solutions for **T** after the mean wind field has been defined by the normal components alone.

The reasonable assumption is made that the vertical component of the mean wind (**W**) is very small compared to the horizontal component, or $W_Z=0$. The horizontal mean-wind components, W_E and W_N, are computed from the smoothed spatial component normal to the projected trail as observed at both stations. It is to be noted that, under certain geometrical conditions, some small variations on the plate will become greatly enlarged when projected on the horizontal plane. The reduction of **T** by the mean-wind solution leaves the train components (T_E-W_E, T_N-W_N, T_Z) independent of any mean air motion. The only remaining wind contribution is a fluctuating component due to turbulence. Since the random component fluctuates about a zero point, each component is smoothed as in the procedure of separating the mean wind component from the normal wind component. If the resulting smooth curves actually can be regarded as representing a coasting velocity along the meteor trail, then the direction cosines of the velocity vector will coincide with the direction of meteor flight at all heights.

Derivation of normal and parallel spatial velocity components

1. Basic linear equations. For a general point at a distance R from the observing station and with direction cosines (l, m, n), equation (11) gives the components of the point with respect to axes parallel to those of the meteor system (see Appendix I):

$$\begin{aligned}\xi&=Rl\\ \eta&=Rm\\ \zeta&=Rn.\end{aligned}\qquad(11)$$

Because the train velocity components $\mathbf{T}(H)$ (ms^{-1}), are very small (10^{-3}) compared to R, the time rates of change in the coordinates of a train point may be represented as the projection of $\mathbf{T}(H)$ on the respective axes of the meteor system:

$$\dot{\xi}=R\dot{l}+l\dot{R}=T_El_E+T_Nl_N+T_Zl_Z \qquad (12a)$$
$$\dot{\eta}=R\dot{m}+m\dot{R}=T_Em_E+T_Nm_N+T_Zm_Z \qquad (12b)$$
$$\dot{\zeta}=R\dot{n}+n\dot{R}=T_En_E+T_Nn_N+T_Zn_Z \qquad (12c)$$

where $(l, m, n)_{E, N, Z}$ are direction cosines of the train coordinate axes in the meteor system (see Appendix II).

2. Linear expression for rate of change of distance. The distance by equations (11) is,

$$R=(\xi^2+\eta^2+\zeta^2)^{1/2},$$

and by equations (11), $\dot{R}=l\dot{\xi}+m\dot{\eta}+n\dot{\zeta}$, or,

$$\begin{aligned}\dot{R}=&l(T_El_E+T_Nl_N+T_Zl_Z)+\\ &m(T_Em_E+T_Nm_N+T_Zm_Z)+\\ &n(T_En_E+T_Nn_N+T_Zn_Z).\end{aligned}\qquad(13)$$

3. Distance as a function of position on the plate. If R_ϵ is the minimum distance to the trail, R_ϵ/R is the cosine of the included angle, or the scalar product of the direction cosines of $\mathbf{R}_\epsilon$ and $\mathbf{R}$ expressed in any system. In the local system (see Appendix I) R_ϵ/R is given by equation (14) where the subscript (ϵ) denotes the point of minimum distance:

$$R_\epsilon/R=\bar{\xi}'\bar{\xi}_\epsilon'+\bar{\eta}'\bar{\eta}_\epsilon'+\bar{\zeta}'\bar{\zeta}_\epsilon', \qquad (14)$$

and

$$R_\epsilon/R=\bar{\zeta}'\bar{\zeta}_\epsilon'(1+\bar{\xi}\bar{\xi}_\epsilon+\bar{\eta}\bar{\eta}_\epsilon)$$

from equation A(2)[3] (Appendix I). From equation A(9), $xx_\epsilon+yy_\epsilon=\bar{\xi}\bar{\xi}_\epsilon+\bar{\eta}\bar{\eta}_\epsilon$ where x, y are dimensionless as defined in Appendix I. Y may be taken as the same value used in the rotation correction formulae; X_ϵ is defined by formulae (8) and (10) for $D=D_\epsilon$ (see Appendix IV). Also,

$$\bar{\xi}'^2+\bar{\eta}'^2+\bar{\zeta}'^2=1.$$

By equations A(2) (Appendix I),

$$\bar{\zeta}'=(1+\bar{\xi}^2+\bar{\eta}^2)^{-1/2}, \qquad (15)$$

and from equation A(9) (Appendix I),

$$\bar{\zeta}'=(1+x^2+y^2)^{-1/2}.$$

Substitution of these expressions in equation (14) gives:

$$R_\epsilon/R=\frac{1+xx_\epsilon+yy_\epsilon}{(1+x_\epsilon^2+y_\epsilon^2)^{1/2}(1+x^2+y^2)^{1/2}}. \qquad (16)$$

4. Rates of change of direction cosines as functions of position on the plate. From Appendix

[3] Equation numbers preceded by the letter "A" indicate formulae appearing in the appendices.

I, $x=l/n$, $y=m/n$, and $n=\overline{\zeta}'=(1+x^2+y^2)^{-\frac{1}{2}}$ by equation (15). Straightforward differentiation with time gives:

$$\left.\begin{aligned}\dot{l}&=n[(1-n^2x^2)\dot{x}-n^2xy\dot{y}],\\ \dot{m}&=n[-n^2xy\dot{x}+(1-n^2y^2)\dot{y}],\\ \dot{n}&=-n^3[x\dot{x}+y\dot{y}].\end{aligned}\right\}\quad(17)$$

5. Equations for velocities on the plate as functions of components of velocities of the train. Direct substitution into equation (12) of $\dot{R}$ from equation (13), R from equation (16), and $(\dot{l}, \dot{m}, \dot{n})$ from equation (17) gives three non-independent equations for $\mathbf{T}(H)$. Multiplication of expression (12c) by x and subtraction from expression (12a), and multiplication of expression (12c) by y and subtraction from expression (12b) reduces the three expressions to equations (18a) and (18b), respectively:

$$(l_E-n_Ex)T_E+(l_N-n_Nx)T_N+(l_Z-n_Zx)T_Z=\frac{R_\epsilon(1+x_\epsilon^2+y_\epsilon^2)^{\frac{1}{2}}}{(1+xx_\epsilon+yy_\epsilon)}\dot{x},\quad(18a)$$

$$(m_E-n_Ey)T_E+(m_N-n_Ny)T_N+(m_Z-n_Zy)T_Z=\frac{R_\epsilon(1+x_\epsilon^2+y_\epsilon^2)^{\frac{1}{2}}}{(1+xx_\epsilon+yy_\epsilon)}\dot{y}.\quad(18b)$$

Here $\dot{x}=V_P/f$ and $\dot{y}=V_N/f$ have units of inverse seconds; if R_ϵ is in units of meters, the train velocities are expressed in meters per second. The left-hand sides of expressions (18a) and (18b) are similar to the scalar products of $\mathbf{T}(H)$ and the vector parallel and normal to the projected trail, respectively. Hence, normalization of the vectors in equation (18a) by the factor $(1+x^2)^{-\frac{1}{2}}$ and of the vector in equation (18b) by the factor $(1+y^2)^{-\frac{1}{2}}$ represents the spatial components $P(H)$ and $N(H)$ corresponding to the plate components V_P and V_N, respectively, or

$$\left.\begin{aligned}P(H)&=\psi^*(1+x^2)^{-\frac{1}{2}}V_P,\\ \text{and}\quad N(H)&=\psi^*(1+y^2)^{-\frac{1}{2}}V_N,\\ \text{where}\quad \psi^*&=(R_\epsilon/f)(1+x_\epsilon^2+y_\epsilon^2)^{\frac{1}{2}}(1+xx_\epsilon+yy_\epsilon)^{-1}.\end{aligned}\right\}\quad(19)$$

$N(H)$ and $P(H)$ are directly proportional to V_N and V_P, R_ϵ, and a slowly varying function $\psi^*(x(H))$.

6. Formulae for components of velocity of train. The normal component expressions (18b) from both stations are combined with one parallel component of the form of expression (18a) to give three simultaneous equations in three unknowns. Two solutions for $\mathbf{T}(H)$ are obtained by taking the parallel component from each of the two stations individually. As an example, for Station A,

$$\left.\begin{aligned}\left[\frac{l_E-n_Ex}{(1+x^2)^{\frac{1}{2}}}\right]_A T_E+\left[\frac{l_N-n_Nx}{(1+x^2)^{\frac{1}{2}}}\right]_A T_N+\left[\frac{l_Z-n_Zx}{(1+x^2)^{\frac{1}{2}}}\right]_A T_Z&=P_A(H)\\ \left[\frac{m_E-n_Ey}{(1+y^2)^{\frac{1}{2}}}\right]_A T_E+\left[\frac{m_N-n_Ny}{(1+y^2)^{\frac{1}{2}}}\right]_A T_N+\left[\frac{m_Z-n_Zy}{(1+y^2)^{\frac{1}{2}}}\right]_A T_Z&=N_A(H)\\ \left[\frac{m_E-n_Ey}{(1+y^2)^{\frac{1}{2}}}\right]_B T_E+\left[\frac{m_N-n_Ny}{(1+y^2)^{\frac{1}{2}}}\right]_B T_N+\left[\frac{m_Z-n_Zy}{(1+y^2)^{\frac{1}{2}}}\right]_B T_Z&=N_B(H).\end{aligned}\right\}\quad(20)$$

7. Formulae for mean horizontal wind. If $W_Z=0$ is assumed, then the simultaneous solution of expressions for the normal train component defines the mean wind, where the smoothed normal components $(\overline{N})$ of the mean wind motion are used:

$$\left.\begin{aligned}\left[\frac{m_E-n_Ey}{(1+y^2)^{\frac{1}{2}}}\right]_A W_E+\left[\frac{m_N-n_Ny}{(1+y^2)^{\frac{1}{2}}}\right]_A W_N&=\overline{N}_A(H),\\ \left[\frac{m_E-n_Ey}{(1+y^2)^{\frac{1}{2}}}\right]_B W_E+\left[\frac{m_N-n_Ny}{(1+y^2)^{\frac{1}{2}}}\right]_B W_N&=\overline{N}_B(H).\end{aligned}\right\}\quad(21)$$

8. Formulae for investigation of coasting velocity. As functions of height, the train meteor components corrected for the mean air motion are: (T_E-W_E, T_N-W_N, T_Z). The magnitude and direction cosines of the motion are readily determined. If $(\lambda_R, \mu_R, \nu_R)$ are the direction cosines of the meteor radiant, then the velocity component is truly a coasting train motion if the condition (22) is satisfied at all heights, where V_C is the magnitude of the above vector:

$$\left.\begin{aligned}\overline{T_E-W_E}&=-V_C(\lambda_R\lambda_E+\mu_R\mu_E+\nu_R\nu_E),\\ \overline{T_N-W_N}&=-V_C(\lambda_R\lambda_N+\mu_R\mu_N+\nu_R\nu_N),\\ \overline{T_Z}&=-V_C(\lambda_R\lambda_Z+\mu_R\mu_Z+\nu_R\nu_Z).\end{aligned}\right\}\quad(22)$$

The bar denotes smoothed expressions; λ_E, etc., are the equatorial direction cosines of the east, north, and zenith points at the midpoint of the observed train region.

Outline of computational steps with formulae

Following is a convenient outline of the steps in reducing a meteor train with the numbers of the appropriate formulae.

1. Transformation constants: A(1).
2. Direction cosines of train system in meteor system: A(11), A(12), A(13), A(14), A(15), A(1), A(10).
3. Plate coordinates, x, y, x_c, y_c in dimensionless form: A(20), A(6), (8), (10).
4. Minimum distance between trail and station: A(20), A(21).
5. Tabulation of velocity components relative to trail at H: (19).
6. Tabulation of coefficients in solution for T: (20).
7. Computation of total train motion components: (20).
8. Computation of mean wind components: (21).
9. Analysis of coasting velocity: (22).

Appendix I: Coordinate transformation formulae

1. Equatorial system. Direction cosines are given by (λ, μ, ν).

2. Local system. The equatorial system is transformed so that the vertical axis is parallel to the direction of the plate center and the other axes are directed towards the east and north points. Direction cosines (λ, μ, ν) are transformed to $(\bar{\xi}', \bar{\eta}', \bar{\zeta}')$ by equation A(1), where the subscript $(_c)$ denotes the plate center.

$$\begin{pmatrix}\bar{\xi}'\\ \bar{\eta}'\\ \bar{\zeta}'\end{pmatrix}=\begin{pmatrix}-\mu/\gamma & +\lambda/\gamma & 0\\ -(\lambda/\gamma)\nu & -(\mu/\gamma)\nu+\gamma & \\ +\lambda & +\mu & +\nu\end{pmatrix}_c\begin{pmatrix}\lambda\\ \mu\\ \nu\end{pmatrix}, \qquad \text{A(1)}$$

where $\gamma_c^2+\nu_c^2=1$.

3. Meteor system. The spherical Super-Schmidt film is projected on the tangent plane of the sky at the point of the plate center. The $\bar{\xi}'$, $\bar{\eta}'$ axes, toward the east and north points respectively, become the standard coordinate axes $\bar{\xi}$, $\bar{\eta}$ as given by equations A(2).

$$\left.\begin{aligned}\bar{\xi}&=\bar{\xi}'/\bar{\zeta}',\\ \bar{\eta}&=\bar{\eta}'/\bar{\zeta}'.\end{aligned}\right\} \qquad \text{A(2)}$$

The X, Y axes in the tangent plane are taken so that the X axis is parallel to the projected meteor trail; they represent a rotation and translation from the $\bar{\xi}$, $\bar{\eta}$ axes except for additional plate distortion effects. The plate constants a_x, a_y, etc., are given at Harvard on the reduction sheets for the meteor.

$$\left.\begin{aligned}X&=a_x\bar{\xi}+b_x\bar{\eta}+c_x,\\ Y&=a_y\bar{\xi}+b_y\bar{\eta}+c_y,\end{aligned}\right\} \qquad \text{A(3)}$$

or sufficiently,

$$\left.\begin{aligned}X&=a'\bar{\xi}+b'\bar{\eta}+c_x,\\ Y&=b'\bar{\xi}-a'\bar{\eta}+c_y,\end{aligned}\right\} \qquad \text{A(4)}$$

where,

$$\left.\begin{aligned}a'&=\frac{1}{2}(a_x-b_y),\\ b'&=\frac{1}{2}(b_x+a_y).\end{aligned}\right\} \qquad \text{A(5)}$$

Let the nondimensional quantities x, y be defined as follows:

$$\left.\begin{aligned}x&=\frac{X-c_x}{f},\\ y&=\frac{Y-c_y}{f}.\end{aligned}\right\} \qquad \text{A(6)}$$

Here f denotes the focal length of the camera and is given by

$$f=(a'^2+b'^2)^{1/2}. \qquad \text{A(7)}$$

The corresponding nondimensional plate constants are

$$a=a'/f,\ b=b'/f. \qquad \text{A(8)}$$

Substitution into equation A(4) simplifies the form as shown in equation A(9),

$$\begin{pmatrix}x\\ y\end{pmatrix}=\begin{pmatrix}a & b\\ b & -a\end{pmatrix}\begin{pmatrix}\bar{\xi}\\ \bar{\eta}\end{pmatrix}, \qquad \text{A(9)}$$

where $a^2+b^2=1$. If (l, m, n) are the direction cosines of a point in the meteor system, then the dimensionless x, y, are equal to l/n and m/n respectively. Substitution of the expressions for x, y, and $\bar{\xi}$, $\bar{\eta}$ into equation A(9) gives the direction cosines in the meteor system:

$$\left.\begin{aligned}\begin{pmatrix}l\\ m\end{pmatrix}&=\begin{pmatrix}a & b\\ b & -a\end{pmatrix}\begin{pmatrix}\bar{\xi}'\\ \bar{\eta}'\end{pmatrix},\\ n&=\bar{\zeta}'.\end{aligned}\right\} \qquad \text{A(10)}$$

The vertical component (n) is invariant under a rotation about the vertical axis.

Appendix II: Direction cosines of train coordinate axes in the meteor system

The train coordinate system has its origin near the midpoint of the train region with axes directed toward the east, north, and zenith points at the midpoint. Let $(l, m, n)_{E, N, Z}$ respectively represent the direction cosines of these vectors in the meteor system. Computational formulae are outlined below.

1. Equatorial direction cosines of the zenith.

(a) Given the equatorial direction $(\lambda_m, \mu_m, \nu_m)$ of the midpoint of the train, and its distance R_m from a station, the rectangular coordinates from the station are:

$$\left.\begin{aligned}\xi_m&=R_m\lambda_m,\\ \eta_m&=R_m\mu_m,\\ \zeta_m&=R_m\nu_m.\end{aligned}\right\} \qquad \text{A(11)}$$

(b) Referred to a geocentric system, equations A(11) become:

$$\left.\begin{aligned}\gamma&=(\rho_s\cos\phi_s)\cos\theta_z+\xi_m,\\ \delta&=(\rho_z\cos\phi_s)\sin\theta_z+\eta_m,\\ \epsilon&=\rho_s\sin\phi_s+\zeta_m,\end{aligned}\right\} \qquad \text{A(12)}$$

where ρ_z is the geocentric distance of the station, ϕ_s is its geocentric latitude and θ_s is the local sidereal time. Equations A(13) represent the equatorial direction cosines corresponding to $(\gamma, \delta, \epsilon)$.

$$\left.\begin{aligned}\lambda_{zm}&=\gamma/\rho_m,\\ \mu_{zm}&=\delta/\rho_m,\\ \nu_{zm}&=\epsilon/\rho_m,\end{aligned}\right\} \qquad \text{A(13)}$$

where $\rho_m=(\gamma^2+\delta^2+\epsilon^2)^{1/2}$ is the geocentric distance of the midpoint.

2. Equatorial direction cosines of east and north points.

(a) Given the equatorial coordinates of the zenith at the midpoint of the train as $(\alpha_{zm}, \delta_{zm})$, the east and north points are in the directions toward $(\alpha_{zm}+\pi/2, 0)$ and $(\alpha_{zm}\pm\pi, \pi/2-\delta_{zm})$, respectively.

(b) Let $\gamma_{zm}=\cos\delta_{zm}$, whence $\gamma_{zm}^2+\nu_{zm}^2=1$. Then, for the east point:

$$\left.\begin{aligned}\lambda_E&=-\mu_{zm}/\gamma_{zm},\\ \mu_E&=+\lambda_{zm}/\gamma_{zm},\\ \nu_E&=0,\end{aligned}\right\} \qquad \text{A(14)}$$

and for the north point,

$$\left.\begin{aligned}\lambda_N&=-\nu_{zm}\lambda_{zm}/\gamma_{zm},\\ \mu_N&=-\nu_{zm}\mu_{zm}/\gamma_{zm},\\ \nu_N&=\gamma_{zm}.\end{aligned}\right\} \qquad \text{A(15)}$$

(c) As a check, $\lambda_i\lambda_j+\mu_i\mu_j+\nu_i\nu_j=\delta_j^i$, where $\delta_j^i=0$ for $i\neq j$ and $\delta_j^i=1$ for $i=j$.

3. Direction cosines on the meteor system. The equatorial coordinates of the east, north, and zenith points of the train system are transformed by equations A(1) and A(10) to $(l, m, n)_{E,N,Z}$. As a check:

$$l_il_j+m_im_j+n_in_j=\delta_j^i. \qquad \text{A(16)}$$

Appendix III: Correction for rotation

For a given point on the train with plate coordinates (X, Y) and equatorial coordinates (α, δ), $(\dot{X}_r, \dot{Y}_r)$, the change in (X, Y) from the increase in the right ascension, due to the westward motion of the reference system, is desired. The X, Y coordinates are dimensional [mm] as measured. From equation A(3),

$$\left.\begin{aligned}\dot{X}_r&=a_x\dot{\bar{\xi}}+b_x\dot{\bar{\eta}},\\ \dot{Y}_r&=a_y\dot{\bar{\xi}}+b_y\dot{\bar{\eta}}.\end{aligned}\right\} \qquad \text{A(17)}$$

$\dot{\bar{\xi}}$, $\dot{\bar{\eta}}$ are functions of $\dot{\bar{\xi}}'$, $\dot{\bar{\eta}}'$ and $\dot{\bar{\zeta}}'$ by equations A(2). Differentiation of equation A(1) with respect to time for the point $\lambda=\cos\delta\cos\alpha$, $\mu=\cos\delta\sin\alpha$, $\nu=\sin\delta$ and straightforward substitution into the expressions for $\dot{X}_r$, $\dot{Y}_r$ define the spurious plate velocities by equations A(18),

$$\left.\begin{aligned}\dot{X}_r&=\dot{\alpha}[a_x\gamma_c+\nu_c(-a_x\bar{\eta}+b_x\bar{\xi})+\gamma_c\bar{\xi}(X-c_x)],\\ \dot{Y}_r&=\dot{\alpha}[a_y\gamma_c+\nu_c(-a_y\bar{\eta}+b_y\bar{\xi})+\gamma_c\bar{\xi}(Y-c_y)],\\ \dot{\alpha}&=7.272\times10^{-5}[\mathrm{s}^{-1}]\end{aligned}\right\} \qquad \text{A(18)}$$

where $\bar{\xi}$, $\bar{\eta}$, derived from the inverse of equation A(3), are given by

$$\left.\begin{aligned}\bar{\xi}(x)&=A_\xi X+B_\xi Y+C_\xi,\\ \bar{\eta}(x)&=A_\eta X+B_\eta Y+C_\eta.\end{aligned}\right\} \quad \text{A(19)}$$

The inverse plate constants A_ξ, B_ξ, etc., are given at Harvard on the reduction sheets. Y may be taken as a constant equal to a mean position of the observed train images. The differential expression of $\dot{Y}_\tau$ for a change in Y indicates that $\dot{X}_\tau$ and $\dot{Y}_\tau$ are insensitive to a change in Y of about one half millimeter. One may even choose $Y=Y_T$, the trail ordinate.

Appendix IV: Minimum distance to meteor trail from station

On the reduction sheets of the meteor as observed from Station A, the direction cosines of the point $t=0$ are given by λ_{Aa}, μ_{Aa}, ν_{Aa}. Let the direction of the radiant be λ_R, μ_R, ν_R; then the distance along the trail from $t=0$ to the point of minimum distance is given by the equation,

$$D_{A\epsilon}=100\,R_{Aa}(\lambda_R\lambda_{Aa}+\mu_R\mu_{Aa}+\nu_R\nu_{Aa}) \quad \text{A(20)}$$

where R_{Aa} is the distance in units of 100 km from Station A to the point for $t=0$. Then

$$R^2_{A\epsilon}=R^2_{Aa}-\left(\frac{D_{A\epsilon}}{100}\right)^2 \quad \text{A(21)}$$

where $R_{A\epsilon}$ is in units of 100 km. Similar formulae hold for Station B.

Appendix V: Notation

The following symbols and units have been arranged in an order roughly corresponding to their use in train analysis. It is understood that each symbol is applicable at either station and may carry a subscript (for the Harvard Meteor Expedition, A=Mayhill, B=Sacramento Peak) when distinction is necessary. A and B are carefully indicated on the meteor reduction sheets.

X, Y—Meteor plate system coordinates [mm].
Y_T—Ordinate of meteor trail in meteor plate system [mm].
$\Delta_i Y$—Train displacement of image i from trail [mm].
d_i—Duration of exposure i [s].
τ'_i—Epoch of exposure (i) with respect to beginning of the first train exposure [s].
τ_0—Time interval between $t=0$ and the beginning of the first train exposure [s].
τ_i—Epoch of exposure (i) with respect to $t=0$ [s].
$t(X)$—Time of meteor passage at a general point on the trail [s].
a_x, b_x, c_x—Plate constants for transformation of standard coordinates to X, Y system [mm].
$\bar{\xi}$, $\bar{\eta}$—Standard coordinates.
$\bar{\xi}'$, $\bar{\eta}'$, $\bar{\zeta}'$—Direction cosines in local system.
λ, μ, ν—Direction cosines in equatorial system.
λ_c, μ_c, ν_c—Direction cosines of plate center.
λ_R, μ_R, ν_R—Direction cosines of radiant.
$\dot{\alpha}$—Time rate of change of hour angle due to the earth's rotation [s^{-1}].
V_i—Normal train velocity component from image (i) [mms^{-1}].
V_P—Plate velocity component of train parallel to the trail [mms^{-1}].
V_N—Plate velocity component of train normal to the trail and corrected for V_P [mm^{-1}].
X_a—Position of $t=0$ in meteor system [mm].
X_R—Position of the radiant in the meteor system [mm].
Z_R—Zenith distance of radiant.
D—Distance along the trail from $t=0$ [km].
h—Height above tangent plate [km].
H—Height above sea level [km].
R—Distance to trail from station [km].
a—Subscript denotes first measurable dash.
ϵ—Subscript denotes point of minimum distance from station.
m—Subscript denotes midpoint of train region.
R—Subscript denotes meteor radiant.
l, m, n—Direction cosines in the meteor system for a general point.
$(l, m, n)_{E, N, Z}$—Direction consines in the meteor system for east, north and zenith axes of the train system respectively.
x, y—Dimensionless plate coordinates.
T_E, T_N, T_Z—Train velocity components in the train system [ms^{-1}].
W_E, W_N—Horizontal components of the mean wind field [ms^{-1}].
$N(H)$—Spatial component of $\mathbf{T}(H)$ normal to the projected meteor trail [ms^{-1}].
$P(H)$—Spatial component of $\mathbf{T}$ parallel to the projected meteor trail [ms^{-1}].
$\overline{N}$—Smoothed functions are denoted by a bar.
v—Coasting velocity [ms^{-1}].

References

LILLER, WILLIAM, AND WHIPPLE, F. L.
1954. *In* Boyd and Seaton, eds. Rocket exploration of the upper atmosphere, pp. 112–130. Pergamon Press.

PAYNE-GAPOSCHKIN, C.
1937. Ann. Harvard Obs., vol. 89, No. 8.

WHIPPLE, F. L.
1953. Journ. Meteor., vol. 10, p. 390.

Methods for the Study of Shower Radiants from Photographic Meteor Trails[1]

Fred L. Whipple[2] and Frances W. Wright[3]

The techniques described here were developed for the rapid analysis of single-station photographic meteor trails used in determining the nature of shower radiants. The measurements are made graphically on Durchmusterung star charts; the reductions have been simplified as far as possible without sacrifice of significant accuracy. Continued application of the methods to many of the trails photographed by the Baker-Super-Schmidt meteor cameras has led to improvement and elaboration of the techniques described earlier (Whipple, Proc. Amer. Philos. Soc., vol. 91, No. 2, p. 189, 1947). We present the method in some detail.

Measurement

To measure single-station meteors, we plot each photographic meteor trail carefully, with the aid of a magnifying glass, on a large-scale Bonn, Cordoba, or Cape Photographic Durchmusterung chart, according to the region of the meteor's occurrence. Through the observed points, with as much care as possible, we pass a smooth curve which represents closely a great circle; the chart scale is approximately 1° to 2 cm. For convenience and greater accuracy we select five points that are nearly equally spaced on the smooth trail, at intersections of the trail with hour or declination circles. After making visual measurements, under a magnifier, of distances on the chart, we determine the equatorial coordinates of these five points. Then, using formulae of analytic geometry, we derive the direction cosines, given below, of the pole of the great circle through four of the points selected above (the mean for points 1–4 and 2–5); the fifth central point is used for a check. The probable error of the independently measured point from the great circle through the plotted points is approximately 30 seconds of arc. The precision of plotting and measurement exceeds the intrinsic accuracy with which shower meteors usually emanate from the mean radiant at a given instant of time. Hence no greater precision is required in practice.

Reduction of measurement of meteor trail

The direction cosines, λ, μ, ν, for each of the above points are given by the formulae,

$$\left.\begin{aligned}\lambda &= \cos\alpha\cos\delta\\ \mu &= \sin\alpha\cos\delta\\ \nu &= \sin\delta.\end{aligned}\right\} \qquad (1)$$

[1] Carried out in part under research contracts with the U. S. Naval Bureau of Ordnance (Task I of NOrd 10449) and the U. S. Office of Naval Research (Contract No. N5ori-07647). Reproduction in whole or in part is permitted for any purposes of the U. S. Government.

[2] Smithsonian Astrophysical Observatory.

[3] Harvard College Observatory.

The direction cosines λ_p, μ_p, ν_p of the pole of the great circle through any two points a and b follow from the expressions:

$$\left.\begin{aligned} \lambda_p \sin C_{ab} &= \mu_a\nu_b - \nu_a\mu_b \\ \mu_p \sin C_{ab} &= \nu_a\lambda_b - \lambda_a\nu_b \\ \nu_p \sin C_{ab} &= \lambda_a\mu_b - \mu_a\lambda_b \end{aligned}\right\}, \qquad (2)$$

where C_{ab} is the great circle distance between the points a and b. The square of sin C_{ab} is obtained from the sum of the squares of the right-hand members of equations (2).

Analysis of a meteor shower

When we begin the identification and analysis of shower meteors we use, when possible, a "skeleton" path of the radiant from the photographic double-station meteors with accurate radiants, velocities, and orbital elements. These positions, elements, and velocities—all of which are similar for any one shower—then furnish criteria for membership in any particular shower.

First, we eliminate as possible members of the stream all extended meteor trails more than 10 degrees from the appropriate point along the skeleton path of the moving radiant. This elimination is easily made by quick plotting on a large globe, or by calculation in case the trail is short and distant from the assumed radiant. Second, the apparent velocity of these accurate double-station meteors fixes the mean velocity in any one shower, a second criterion of membership. To find velocities of other double-station meteors, we use the extremely rapid approximation developed by McCrosky (in the third paper of this group)—the so-called "whirl-wind" reduction technique. This same technique may also be used to determine approximate velocities for single-station trails with shutter breaks. We derive the velocity from quick measurement of breaks in the trail on the basis of an assumed radiant. If the approximate velocity of a possible member of a shower differs by more than 15 percent from the mean velocity determined by the precise techniques, we then eliminate the suspected member. When trails of double-station meteors have not been measured and reduced precisely, we measure and reduce them by the rapid techniques used for a single-station meteor. Even though such reductions may lead to fairly accurate radiants, we usually prefer to treat the two trails of these doubles as two single trails in the final least-squares solution.

Assumed radiant and pole of radiant motion. The direction cosines of all radiants or poles of trial trails must be reduced to a common equinox. We recommend the method presented by Bower (Lick Obs. Bull., vol. 16, No. 445, p. 34, 1932). We then adopt an assumed preliminary radiant, usually the corrected radiant, α_R, δ_R, of the accurate double-station meteor nearest to the mean position of the radiant as shown by these accurate radiants. The direction cosines λ_{PM}, μ_{PM}, ν_{PM} of the preliminary pole of radiant motion can be obtained by choosing for a second point along the great circle of radiant motion one of the earlier (or later) accurate radiants. When the circle of radiant motion has a small inclination to the celestial equator we often take, for convenience, the second point at the same declination as δ_R.

Next, we establish a rectangular coordinate system with origin at α_R, δ_R and x-axis coincident with the great circle of motion of the radiant, x increasing with α and y with δ.

Formulae for distance. The position of a single trail j can be specified conveniently by the intersection point X_j of the extended trail with the x-axis, and by the intersection angle ψ_j which is taken from 0° to 180° as indicated in figure 1. For each single trail j, where λ_{Pj}, μ_{Pj}, ν_{Pj} denote the direction cosines of the pole of the trail, we calculate these positional quantities from the equations

$$X_j \sin \psi_j = \lambda_{Pj}\lambda_R + \mu_{Pj}\mu_R + \nu_{Pj}\nu_R, \qquad (3)$$

$$\cos \psi_j = \lambda_{Pj}\lambda_{PM} + \mu_{Pj}\mu_{PM} + \nu_{Pj}\nu_{PM}, \qquad (4)$$

$$\sin \psi_j \text{ (from trigonometric tables)}, \qquad (5)$$

$X'_j \sin \psi_j$ (in minutes of arc) follows from (3) and X'_j (in minutes of arc) and ψ from (5) and (4) respectively.

Signs and the quadrant of ψ are determined from the geometry of the situation for each case.

Zenith corrections. $X_j \sin \psi_j$ gives the nearest point of each trail j to the assumed radiant of the shower, and corrections for both diurnal

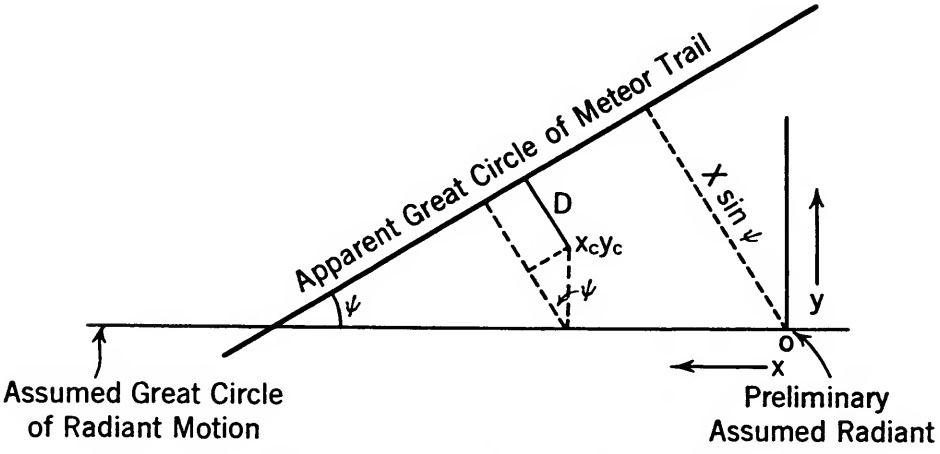

FIGURE 1.—Geometry of single trail and radiant.

motion and zenith attractions must be applied to correct the position of this point. When we have approximately 30 or more members of a meteor shower, we make up tables and graphical curves of corrections which we can then enter to find the proper corrections for an individual meteor. If the shower has fewer members, we usually apply each correction separately, without making tables. The basic formulae used for zenith correction are

$$V_G^2 = V_C^2 - 2g\rho, \tag{6}$$

and

$$\tan 1/2\ \Delta Z_R = \frac{V_C - V_G}{V_C + V_G} \frac{\sin Z_R}{1+\cos Z_R}, \tag{7}$$

where

V_∞ = Velocity of meteor outside the atmosphere.
$V_C = V_\infty$ corrected for rotational motion.
$V_G = V_C$ corrected for zenith attraction.
g = Attraction of gravity (the term introduced by the rotation of the earth is subtracted) at the station.
ρ = Radius of the earth.
Z_R = Zenith distance of an assumed radiant that approximates the mean value of the apparent radiant.

If there is no correlation between time and velocity, we adopt the mean V_∞ and the mean V_G of the accurate double-station meteors. We find the mean V_C from equation (6).

The zenith distance, Z_R, may be obtained quickly from the navigation tables of the U. S. Hydrographic Office, H. O. 214. In these tables declination arguments in whole and half degrees head the main columns of each page, while hour-angle arguments in whole degrees appear at the side; we enter the tables, therefore, with different values of hour angle and with a declination as close to the radiant as possible. Then with the interpolation tables of H. O. 214, we find the altitude of the radiant and hence the zenith distance Z_R for any hour angle of the radiant at any specific station. The interpolation tables are convenient when the latitude of the station is not a whole number of degrees.

A third formula determines, by means of the sine law, the sine of the angle ν at the "radiant vertex" in the pole-zenith-radiant triangle:

$$\sin \nu = \cos L \times \sin (\text{H. A.}) / \sin Z_R. \tag{8}$$

From formulas (7) and (8), the relations

$$\Delta\alpha \cos\delta = \Delta Z_R \sin \nu \tag{9}$$

and

$$\Delta\delta = \Delta Z_R \cos \nu \tag{10}$$

give the zenith corrections in Δx and Δy for any one trail. The signs of these corrections appear from the geometry of the situation in each case.

Diurnal-motion corrections. The diurnal-motion corrections require a knowledge of the station's rotational velocity V_S, given by the equation

$$V_S = \frac{2\pi}{86{,}164} \rho \cos \phi'. \tag{11}$$

where ρ and ϕ' are, respectively, the radius of the earth and the geocentric latitude of the station; time is measured in seconds of mean solar time. We have used the following specific values of V_S for various Harvard Meteor Stations:

Station	V_s(km/sec)
Cambridge, Mass. Agassiz Station, Mass.	0. 344
Arequipa, South America	0. 447
Bloemfontein, South Africa	0. 406
Doña Ana, N. Mex. Soledad, N. Mex.	0. 392

The following equations in Δx and Δy suffice for the diurnal-motion correction:

$$\Delta\alpha \cos\delta = A_\alpha \sin\theta + B_\alpha \cos\theta, \quad (12)$$

$$\Delta\delta = A_\delta \sin\theta + B_\delta \cos\theta, \quad (13)$$

where θ is the local sidereal time and the coefficients are functions of the velocity V_∞ and of the position of the radiant α_R and δ_R (which can be the assumed mean radiant for single-station meteors). The above coefficients are given by the formulae

$$\begin{aligned} A_\alpha &= -(V_S/V_\infty)\sin\alpha_R, \\ B_\alpha &= -(V_S/V_\infty)\cos\alpha_R, \\ A_\delta &= -(V_S/V_\infty)\cos\alpha_R \sin\delta_R, \\ B_\delta &= +(V_S/V_\infty)\sin\alpha_R \sin\delta_R. \end{aligned} \quad (14)$$

Finally, the sums of (9) and (12) and of (10) and (13), respectively, provide the total corrections for zenith correction and diurnal motion. The corrections may range from only a minute of arc to several degrees, depending largely upon the velocities of the meteors and the altitudes of the radiants for the respective showers.

Corrected ($X_j \sin\psi_j$). The corrected quantity, $X_j \sin\psi_j$, designated by Δ_j, is given by the formula

$$\Delta_j = (X_j \sin\psi_j) + \Delta x_j \sin\psi_j + \Delta y_j \cos\psi_j. \quad (15)$$

If the path of radiant motion roughly parallels the celestial equator, Δx_j = total $\Delta\alpha_j \cos\delta_j$; and Δy_j = total $\Delta\delta_j$ with sufficient accuracy.

General formulae for Δx_j and Δy_j. When, on the other hand, the inclination (smallest angle) β of the path of radiant motion to the celestial equator is large over a long time interval, more accurate formulae are

$$\Delta x_j = |\Delta\alpha_j| \cos\delta_j \cos\beta \pm |\Delta\delta_j| \sin\beta, \quad (16)$$

and

$$\Delta y_j = \mp |\Delta\alpha_j| \cos\delta_j \sin\beta + |\Delta\delta_j| \cos\beta. \quad (17)$$

Formulae for double-station meteors. The date of the meteor is taken as t_i for a double-station, or as t_j for a single-station meteor, and is measured in degrees of true longitude of the sun at the time of observation and referred to a fixed equinox. The daily motion of the radiant can now be determined for double-station meteors from the observational equations

$$A_x + B_x t_i = x_i + \Delta x_i \text{ and } A_y + B_y t_i = y_i + \Delta y_i, \quad (18)$$

where the coefficients A_x, B_x, A_y, and B_y are to be found by least squares.

For any radiant R_i, x_i and y_i can be computed from the formulae

$$\sin y_i = \lambda_{PM}\lambda_{Ri} + \mu_{PM}\mu_{Ri} + \nu_{PM}\nu_{Ri} \quad (19)$$

and

$$\sin x_i = \lambda_{Px}\lambda_{Ri} + \mu_{Px}\mu_{Ri} + \nu_{Px}\nu_{Ri}, \quad (20)$$

where P_x is the pole of a great circle though the assumed radiant orthogonal to the great circle of radiant motion. When the path of radiant motion is nearly parallel to the celestial equator, we take, for convenience, $\alpha_{Px} = \alpha_R + 90°$ and $\delta_{Px} = 0$, with sufficient accuracy.

For single-station meteors, the distance D of the calculated radiant x_{cj}, y_{cj} from the great circle of the meteor trail is to be minimized by a least-squares solution; i. e., D_j is to be considered as a final residual. As seen from figure 1, D_j is given by the equation,

$$D_j = (x_{cj} - X_j)\sin\psi_j + y_{cj}\cos\psi_j. \quad (21)$$

A substitution of the corrected x_i and y_i from equations (18) into equation (21) leads to the following equations of condition for a least-squares solution to determine the six constants and to minimize D_j:

$$\begin{aligned} A_x \sin\psi_j + A_y \cos\psi_j + B_x t_j \sin\psi_j + B_y t_j \cos\psi_j \\ = X_j \sin\psi_j + \Delta x_j \sin\psi_j + \Delta y_j \cos\psi_j. \end{aligned} \quad (22)$$

Least-squares equations of condition. The coefficients A_x and A_y, after the least-squares solution, provide corrections to be applied to the assumed radiant, while B_x and B_y provide the daily motion of the best radiant path through the calculated radiant, with minimized distances of extended meteor trails to the mean radiant of the corresponding instant.

Terms to include possible secular changes in the radiant motions over many years can easily be introduced into the least-squares solution. No such effect has yet become detectable because of the limited span of precise photographic observations. When such secular effects become measurable, most investigators would probably prefer to divide the material into groups of about two or more epochs and investigate each group separately.